Identification of Voltage Stability Condition of a Power System Using Bus Measurements

A THESIS SUBMITTED TO GAUHATI UNIVERSITY
FOR THE AWARD OF DEGREE OF

DOCTOR OF PHILOSOPHY

In the Faculty of Engineering

By,
Brajesh Mohan Gupta

Under the guidance of,
Prof. Durlav Hazarika
Electrical Engineering Department

Assam Engineering College
Department of Electrical Engineering, Assam Engineering College,
Jalukbari, Guwahati-781013

2018

ABILITY ANALYSIS CERTIFICATE

This is to certify that the thesis entitled "**Identification of voltage stability condition of a power system using bus measurements**" submitted by Mr. **Brajesh Mohan Gupta,** who got his name registered on 08-04-2014 in the Department of Electrical Engineering of Assam Engineering College for the award of the degree of **Doctor of Philosophy in the Faculty of Engineering** is absolutely based upon his own work under my supervision and that neither his thesis nor any part of the thesis has been submitted for any degree/diploma or any other academic award anywhere before.

Date: 19/01/19

Place: Guwahati

Dr. Durlav Hazarika
Research Guide
Electrical Engineering Department
Assam Engineering College
Guwahati -781013

DECLARATION

I hereby declared that the thesis entitled “Identification of voltage stability condition of a power system using bus measurements ” submitted to Gauhati University for the award of the degree of Doctor of Philosophy in the Faculty of Engineering is absolutely based upon my own work under the supervision Dr. D. Hazarika, Professor, Department of Electrical Engineering, Assam Engineering College, Guwahati. I also declared that neither this thesis nor any part of the thesis has been submitted for any degree/diploma or any other academic award any where before.

Dated: 19/01/2019

Place: Guwahati

Brajesh Mohan Gupta
Enrolment no.(Engg.-23/14)
Department of Electrical Engineering
Assam Engineering College
Guwahati-781013
Assam

ACKNOWLEDGEMENT

I would like to show immense gratitude to my supervisor, **Dr. Durlav Hazarika**, Professor, Department of Electrical & Instrumentation Engineering, Assam Engineering College. I sincerely thank him for his exemplary guidance and encouragement, without whose guidance and persistent help, this project would not have been materialized.

I am indebted to the Department of Electrical & Instrumentation Engineering, **Prof. Damodar Agarwal**, Head of the Department and all the faculty of which provided enthusiastic support and assisted towards the completion of the project.

I am especially thankful to **Prof. Bani Kanta Talukdar**. He has given me valuable supports and encouragements during the time I am doing the thesis.

I am indebted to my friends for their help and moral support all throughout the project.

Finally I would like to thank my Parents, family members , In laws and wife Dr. Nilay Sharma for their moral support and encouragement.

Dated: 19/01/2019
Place: Guwahati

Brajesh Mohan Gupta
Department of Electrical Engineering
Assam Engineering College
Guwahati-781013
Assam

ABSTRACT

In recent years, power system has been forced to operate at its threshold of operating limit(s) owing to economic and operational factors. As a result, voltage instability in power system has become a major concern in power system operation and planning. Under such situation, the problem of voltage instability is receiving more and more attention. Voltage instability may create voltage collapse, if the issue is not attended properly. A voltage collapse in large system or subsystem may have far reaching consequences, such as system black out. During voltage collapse situation, the phenomenon of change in voltage is very rapid and therefore, the voltage control devices may not be able to undertake appropriate corrective actions/measures to prevent cascading voltage collapses of a power system leading to blackouts. Therefore, it is necessary for operators and planners to know the measure of voltage stability/instability of a power system under steady operating condition of the system. Voltage collapse is characterized by a slow variation in the system operating point due to increase in load in such a way that the voltage magnitude gradually decreases until a steep fall take place. It has been found that voltage magnitude does not give a good indication of proximity of voltage stability condition. Several computational based Voltage Stability Indices (VSIs) were proposed to indicate voltage stability condition of a power system. These VSIs a have their own threshold values to indicate the proximity of voltage collapse. Therefore, it is necessary to determine the VSI of all the buses of a power system and busses having VSI values near to the threshold value are to be treated as vulnerable buses to voltage collapse and when a VSI of a single bus exceeds the threshold value, the system collapse occurs.

Recently, bus measurements based methods are developed to investigate the voltage stability problem of a power system. It has found that for voltage and current phasors of a bus contain sufficient information to develop mathematical model(s) for

analyzing its characteristic behavior or respond to the load change at the bus. Vu et al. proposed the first voltage stability index that uses the local voltage and current phasor measurements at a load bus. The method requires two consecutive measurement of voltage and current phasors of a load bus is used to calculate the Thevenin's equivalent parameters of the system. Phasor Measurement Unit (PMU) is to be used to read voltage and current phasors of a bus. A PMU is a device which measures the electrical waves on an electricity grid, using a common time source for synchronization. Time synchronization allows for synchronized real-time measurement of multiple remote measurement points on the grid. The on-line monitoring of voltage instability of a power system based on the PMU's local measurements has drawn wide attentions in the field of power system research. Most of these works use Thevenin's equivalent source impedance as the basis for monitoring voltage stability condition of a power system using PMU measurements. However, PMU is a costly device, for example a low cost PMU such as; SEL-487E PUM cost $5750.00. In addition to this, time synchronization of the phasor variables invites continuous operating cost and somehow dependent on remote measurement. Therefore, the objective of this research work is to find out alternative measurement based method for identification of voltage stability condition of a power system bus. The work reported in this thesis, proposed a method for online monitoring of voltage stability condition of a bus of a power system using two consecutive measurements of bus variables namely – (i) real power (ii) reactive power and (iii) bus voltage magnitude of a bus. A new voltage stability index is proposed based on these measurements. The advantage of the method is that necessary bus measurements required to determine the voltage stability index of the bus are non-phasor (scalar) quantities of a bus and they could be extracted by a smart energy meter. Therefore financial involvement for implementation of the proposed method would be significantly low compared to the PMU based methods. Continuation power flow analysis is used to examine the performance and behavior of the index along the PV curve and around the proximity of voltage collapse of the bus.

CONTENTS

LIST OF FIGURES

LIST OF FIGURES

LIST OF TABLES

Abbreviations

Abbreviations

VSI	Voltage Stability Index
NVSI	Node Voltage Stability Index
ENVCI	Equivalent Node Voltage collapse Index
ESM	Equivalent System Model
ELNM	Equivalent Local Network Model
PMU	Phasor Measurement Unit
TEC	Thevenin's Equivalent Circuit
TBEC	Two Bus Equivalent Circuit
LFA	Load Flow Analysis
PLM	Percentage of Load Margin

Nomenclature

List of symbol

P_i	Net injected active power at bus-i.
P_{Gi}	Active power output of a generator at bus-i
P_{Di}	Active power component of a load at bus-i
Q_i	Net injected reactive power at bus-i.
Q_{Gi}	Reactive power output of a generator at bus-i
Q_{Di}	Reactive power component of a load at bus-i
V_i	Bus voltage at bus-i.
δ_i	Voltage phase angle of bus-i.
Y_{ij}	Bus admittance matrix of bus i and j
G_{ij}	Conductance of admittance matrix of bus i and j
B_{ij}	Susceptance of admittance matrix of bus i and j
θ_{ij}	Angle between G_{ij} and B_{ij}
λ	Load parameter
σ	Step size
P_{Dok}	Original active power demand
Q_{Dok}	Original reactive power demand

L	Rate of load change at bus k
e_k	Appropriate row vector with all elements equal to zero except the k^{th} element equals 1
x_k	State variable
$\acute{\eta}$	Predicted value of the state variable
E_{TEC}	Source voltage of TEC
R_{TEC}	Source resistance of TEC
X_{TEC}	Source reactance of TEC
V_k	Voltage at K^{th} bus
I_k	Current in K^{th} bus
E_{TBEC}	Source voltage of TBEC
R_{TBEC}	Source resistance of TBEC
X_{TBEC}	Source reactance of TBEC
P_{DK}	Change in load at bus k
P_{Dk}^{crt}	Critical load at bus k

Chapter- 1

1.1 Introduction

A modern human is believed to have been originated around 200,000 years ago or earlier. The level intelligence possessed by a human is phenomenal. Human learned to live in society. They started involving themselves in activates like - arts & culture and it helped them in the development of their scientific temper. It contributed tremendously in the rapid growth of Human Civilization. The fundamentals of Western Civilization were largely shaped in Ancient Greece, with the world's first democratic government and the era of modern philosophy, science, and engineering took shape for the future world. European Civilization began to change from around 1500AD, which finally, ignited the process of scientific and industrial revolutions. The industrial houses started the use of fossil fuel for production of energy to operate the industrial production purposes. Scientists began their investigations to develop an energy source that could be easily used to transfer power form source to the consumer site. This resulted in development of Electrical Energy System components for production and utilization of electrical energy. However, production of Electrical Energy for commercial purpose began during 1880AD, when Thomas Edison started generating of electricity. Immediately, people accepted electrical energy as a clean source of energy for domestic and industrial utilizations. Therefore, electricity became an essential commodity for development of industries and growth of a Nation is measured in terms of per capita electrical consumption. Electric power demand increased exponentially and as a result, expansion process of electrical system in generation, transmission and distribution had been accelerated. To meet this ever growing power demand, high power generating stations, such as supper thermal power stations, nuclear power stations and mega hydropower stations were installed. Power system becomes the largest man made system in the Globe at present.

Owing to the ever increasing size of the power system, predictive analysis of the system for operational purpose becomes a challenging task for the power system operators and planners.

Initially, physical network simulations were used, but they were limited to small systems. In due course of time, with the advent of digital computers, attempts were made to model the power system network suitable for analysis. Eventually better techniques for the purpose of predictive analysis of power system were developed. Knowing the network of a power system, comprising of generators, transformers, lines, compensating devices and loads, it is possible to model a power system to compute the power flows in all system elements and know the voltage magnitudes and the corresponding voltage angles with respect to a reference bus using suitable mathematical techniques.

Power system in recent times has been forced to operate at its threshold of operating limit(s) owing to economic and operational factors. As a result, voltage instability in power system has become a major concern in power system operation and planning. Under such situation, the problem of voltage instability is receiving more and more attention. Voltage instability may create voltage collapse, if the issue is not attended properly. A voltage collapse in large system or subsystem may have far reaching consequences, such as system black out.

The phenomenon of voltage collapse has been observed in many countries and has been analysed extensively. During the last decade, voltage collapse phenomenon has attracted more and more attention throughout the world and several studied have been presented which relate to this problem.

1.2 Basic problem of power system stability and voltage stability[1]

Power system stability has been recognized as an important problem for its secure operation since 1920s . Traditionally, the problem of stability has been treated as maintaining the synchronous operation of generators, operated under parallel condition; this analysis aims at knowing the rotor angle stability. The problem of rotor angle stability is well understood and documented. With continuous disproportional increase in power demand and power system infrastructure (such as, deficiency in the growth of generation and limited expansion of transmission systems), modern power system networks are being operated under highly

stressed conditions. This has imposed the threat of maintaining the required bus voltages and thus, the systems have been facing voltage instability problem.

Voltage stability is the ability of a power system to maintain voltage magnitudes at all the buses in the system within acceptable operating limits after being subjected to a disturbance for a given initial operating condition . It depends on the ability to maintain/restore equilibrium between load demand and power supply of a power system. A system is considered to suffer voltage instability, if (for at least one bus) the bus voltage magnitude decreases rapidly for small increased in reactive/active power injection to the bus.

Even though, the voltage stability is generally considered as the local problem, however, the consequences of voltage instability may have a widespread impact on the operation of a power system. The result of such impact may lead to voltage collapse, which results from a sequence of contingencies rather than from one particular disturbance. It creates low voltage profile in a major part of a power system.

The main factors causing voltage instability are

• The inability of the power system to meet demands of reactive power in the heavily stressed system to keep voltage in the desired limits.

• Characteristics of the device that compensates the reactive power of a power system.

• Coordination and activation of the voltage control devices of a power system.

• Generator reactive power limits.

• Load characteristics.

• Parameters of transmission network.

1.3 Classification of power system stability and voltage stability problem[1,2]

To understand the issues related to the power system stability problem, power system stability issues are classified into – (i) rotor angle stability, (ii) frequency stability and (iii) voltage stability as depicted in figure-1.1. The subsequent classifications are based on time scale and criteria that is responsible for it. Time scale is divided into short-term and long-term durations and the driving forces for instability are generator-driven and load-driven.

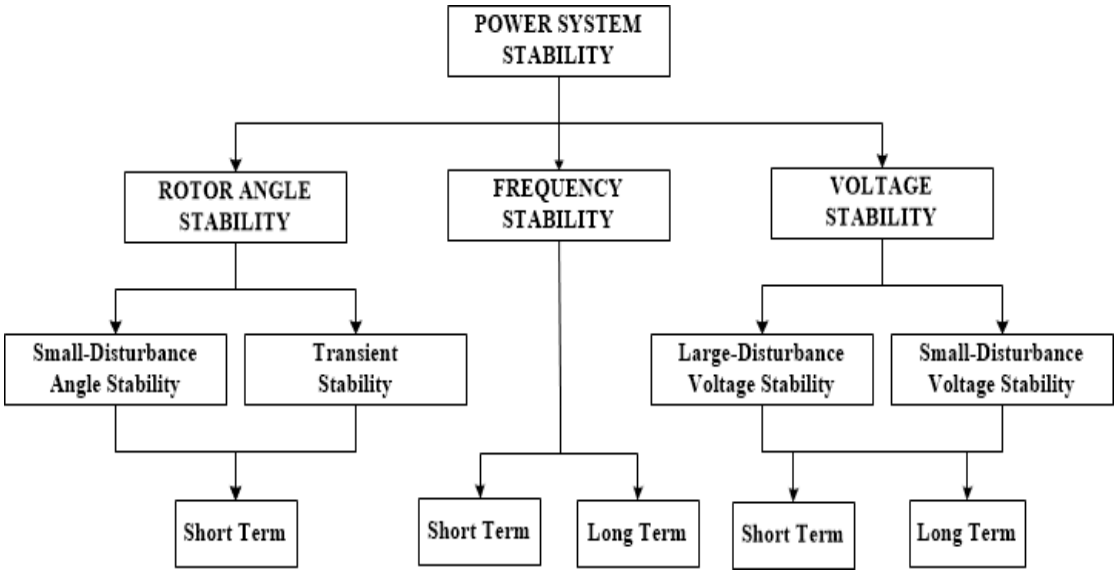

Figure 1.1 Classification of power system stability

The rotor angle stability is divided into small signal and transient stability and is considered to be generator-driven. Small signal stability is the ability of power system to maintain the synchronism under small disturbances in the form of un-damped electromechanical oscillations. Such disturbances occur continually on the power system because of small variation in load and generation. The transient stability is related to synchronizing torque of the generation system and it is caused by a large disturbance, such as, three phase fault, loss of line etc. During such situation, the system experiences large swings of generator rotor angles and which is governed by a non-linear power-angle relationship. The time frame of rotor angle stability is called short- term time scale, because the dynamics typically last for a few milliseconds.

The voltage stability is divided into short-term and long-term voltage stability and it is considered to be load-driven. The distinction between long and short-term voltage stability is according to the time scale of load component dynamics. Short term voltage stability is characterized by components like induction motors, excitation of synchronous generators and devices like high voltage direct current (HVDC) or static VAR compensators. The time scale of short-term voltage stability is similar to that of rotor-angle stability. Sometimes, it is not easy to distinguish between these two phenomena, because voltage stability does not always occur in its pure form and it may contribute to introduction of rotor-angle stability problem of a power system. However, the distinction between these two stabilities is necessary for understanding of the underlying causes of the problem in order to develop appropriate analytical methods and operating procedures.

The duration of long-term dynamics is considered up to several minutes. For long-term consideration, the stability problem is classified into two types as shown in figure 1.1. The frequency stability caused due to a major disturbance and it may create islanding of a power system. The major cause of such instability is mainly due to a disturbance that introduces significant imbalance active power between generators and loads.

The long-term voltage stability is categorized into small-disturbance and large-disturbance voltage stability problems. Large-disturbance voltage stability problem is analyzed to understand the response of the power system to large disturbances like- faults, loss of load or loss of generation etc. The ability to maintain voltages of a power system following large disturbance depends on system load characteristic and the interactions of continuous or discrete controls and protective devices.

Small-disturbance voltage stability problem is considered as ability of a power system to maintain bus voltages after small disturbances like - changes in load. It is also determined by load characteristics and continuous/discrete controls of power system devices. The analysis of small-disturbance voltage stability is carried out under steady state operation of a power system.

1.4 Voltage instability and voltage collapse

A power system operating condition should be stable at any point of time. During the operation of a power system, it is necessary that operational criteria of all the devices and equipments should be stratified. In addition to this, it is to be ensured that it should remain secure in the event of any credible contingency (like line outage contingency, generation outage contingency, load outage contingency etc) . Present day power systems are being operated closer to their stability limits due to economic and load demand. Maintaining a stable and secure operation of a power system is therefore a very important and challenging issue. Voltage instability has been given much attention by power system researchers and planners in recent years and it considered as one of a major cause of power system insecurity.

A power system is considered to have influenced by voltage instability problem when a disturbance results in a progressive and uncontrollable decline in voltage profile of the system buses. The voltage instability of a power system may cause voltage collapse of the system, if the post disturbance equilibrium voltages of the load buses are below acceptable limits. Voltage collapse of a power system [3] may be defined as a process that causes very low voltage profile in a significant part of a power system. In fact, voltage collapse may cause total or partial blackout of a power system. The main cause of voltage collapse may be due to the inability of the power system to supply the reactive power or an excessive absorption of the reactive power by the system itself.

The information about the Load Margin (LM) of a bus of a power system with respect to its collapse point is helpful for a power system planner and operator to operate the system under stressed condition. LM of a bus is the amount of additional load when picked-up that causes a voltage collapse of a power system. The PV curve shown in figure-1.2 is used to represent the load margin of a bus of a power system. A PV curve of a bus of a power system is derived by increasing load at the bus gradually and for each incremental load, power flow solution is obtained to determine the bus voltage of the corresponding load bus. The process of increment of load is ended when the point of voltage collapse is arrived.

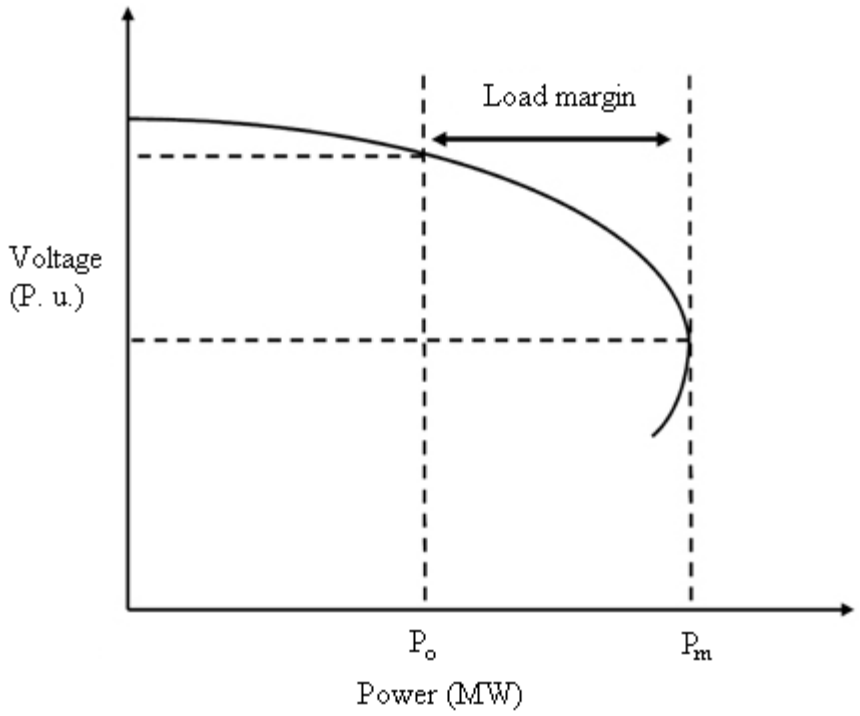

Fig. 1.2 Power Voltage (P-V) curve of a power system bus.

As shown in figure-1.2, P_0 is the load power at the given operating point, and P_m is the maximum active power that the load can consume from the system. Therefore, the load margin of the bus with respect to the given operating point is = P_m - P_0

1.5 Literature survey

Different methods are available in the literature for carrying out a steady state voltage stability analysis of a power system. These methods can be broadly classified into the following types.

- Methods based on voltage stability index (VSI)
- Eigen value based methods
- Continuation load flow methods.

- Measurement based methods

During voltage collapse situation, the phenomenon of change in voltage is very rapid and therefore, the voltage control devices may not be able to undertake appropriate corrective actions/measures to prevent cascading voltage collapses of a power system leading to blackouts. Therefore, it is necessary for operators and planners to know the measure of voltage stability/instability of a power system under steady operating condition of the system. The problem of voltage collapse may be attributing to the inability of power system to supply the reactive power or by an excessive absorption of reactive power by the system itself [4]. Voltage collapse is characterized by a slow variation in the system operating point due to increase in load in such a way that the voltage magnitude gradually decreases until a steep fall take place. It has been found that voltage magnitude does not give a good indication of proximity of voltage stability condition [5]. From the point of view of load flow equations, voltage collapse is characterized by the singularity of the Jacobian matrix and this has been the base line concept of many researches. [6,7,8,9]. If the system is operating in the stable region, the determinant of Jacobian matrix is positive. On the other hand, if it is operating in the unstable region, the determinant is negative [10].

Several voltage stability indices (VSIs) were proposed to indicate voltage stability condition of a power system [5, 6,11,12,13]. Voltage stability indices of the buses of a power system can provide the measures of voltage stability/instability condition of a power system under steady operating condition in terms of their threshold values. The index L [5] is derived using the solution of load flow analysis and it is reliable in indicating the proximity of voltage collapse of a power system load bus. The index L provides a scalar number that varies in the range 0 to 1. The bus with L-index value near 1 is the most vulnerable one to voltage collapse. Therefore, the threshold value of index L is given as "1". Similarly, other VSIs also have their own threshold values to indicate the proximity of voltage collapse. Therefore, it is necessary to determine the VSI of all the buses of a power system and busses having VSI values near to the threshold value are to be treated as vulnerable buses to voltage collapse and when a VSI of a single bus exceeds the threshold value, the system collapse occurs. Under such situation reactive power control

approach is suggested for reducing the voltage stability of a power system [14,15]. The possibility of reactive power supply from a doubly fed induction generator to improve voltage stability problem of a bus of an interconnected power system has been investigated [16]. Again, basis of singularity condition of load flow Jacobian matrix is also used for voltage stability analysis and singular value decomposition [1,17,18,19,20,21,22,23,24] are used as standard tools for the assessment of voltage stability condition of a power system.

The continuation power flow [25] uses a predictor corrector method to determine the point of voltage collapse when the load is increased gradually. The power flow equations are reformulated to include a load parameter in order to find the solution path and to avoid the singularity of the load flow Jacobian matrix near the point of collapse. Several other aspects of continuation power flow and its application in power system voltage stability were addressed by researchers [26,27,28,29,30.31,32]. Information of load margin of a bus with respect to its voltage collapse limit is essential for a power system operation. Attempts were made by several researchers to address this issue of determining load margin of bus for a given operating point of a power system [33, 34]. This Information of load margin of a bus constitutes an important criterion for load pick-up step during power system restoration planning and operation. The bus having highest load margin appears to be the best choice [35] for load pick-up and magnitude of load to be picked-up must be less than the load margin for a bus.

Voltage and current phasors of a bus contain sufficient information to develop mathematical model(s) for analyzing its characteristic behavior or respond to the load change at the bus [36]. Vu et al. proposed a stability index that uses the local voltage and current phasor measurements at a load bus [37]. A simple, computationally very fast local voltage-stability index has been proposed using Tellegen's theorem [38]. Both the methods require two consecutive measurements of voltage and current phasors of a load bus to calculate the Thevenin's equivalent parameters of the system. A voltage stability index called ENVI (Equivalent Node Voltage Collapse Index) has been proposed in [39], which is based on "Equivalent System Model" (ESM) of a load bus of a power system. The ESM is represented using the effect of the system buses on the load bus under consideration. An Equivalent Local Network Model (ELNM) has been used for this purpose. The ELNM requires the parameters of the transmission lines connected to the selected

load bus and voltage phasors of the system buses that are connected to the selected load bus. Therefore, the major disadvantage of this method is that PMUs are required in all the connecting buses and at the selected node. The on-line monitoring of voltage instability of a power system based on the PMU's local measurements has drawn wide attentions [40-56] in the field of power system research. All these works use Thevenin's equivalent source impedance as the basis for monitoring voltage stability condition of a power system using PMU measurements.

1.6 Main contribution of the research

In recent years, the on-line monitoring of voltage instability of a power system based on the PMU local measurements has been used for power system voltage stability analysis. It has drawn wide attention in the field of power system research. A PMU is a device which measures the electrical waves on an electricity grid, using a common time source for synchronization [57]. Time synchronization allows for synchronized real-time measurement of multiple remote measurement points on the grid. Most of these proposed methods use two consecutive measurements of the local voltage and current phasor of a load bus to derive Thevenin equivalent circuit of the bus. However, PMU is a costly device, for example a low cost PMU such as; SEL-487E PUM cost $5750.00. In addition to this, time synchronization of the phasor variables invites continuous operating cost and somehow dependent on remote measurement. Therefore, the objective of research work is to find out an alternative measurement based method for identification of voltage stability condition of a power system bus.

1.7 Organization of this thesis

The thesis is organized into five chapters and a bibliography.

Chapter 1: This chapter presents a brief review of the work done by other researchers in the field of voltage stability analysis of a power system, the problem statement and the objectives of the research work.

Chapter 2: This chapter presents an approach for determination of bus measurements variables for two consecutive time steps using a continuation power flow analysis. The chapter provides detailed formulation of the continuation power flow model and its solution algorithm that enables determination of bus measurements variables for two consecutive time steps.

Chapter 3: This chapter presents two established methods proposed for indicating voltage stability condition of a bus using two consecutive measurements of voltage and current phasors of the bus. PMU is used for the measurements of voltage and current phasors of the bus. Continuation power flow analysis described in chapter-2 is used to examine the performance and behavior of the indices along the PV curve and around the proximity of voltage collapse of the bus.

Chapter 4: This chapter presents a method for online monitoring of voltage stability condition of a bus using two consecutive measurements of bus variables namely – (i) real power, (ii) reactive power and (iii) bus voltage magnitude of a bus. A new voltage stability index is proposed based on these measurements. The advantage of the method is that necessary bus measurements required to determine the voltage stability index of the bus could be extracted by a smart energy meter. Therefore financial involvement for implementation of the proposed method would be significantly low compared to the PMU based methods. Continuation power flow analysis described in chapter-2 is used to examine the performance and behavior of the indices along the PV curve and around the proximity of voltage collapse of the bus.

Chapter 5: This chapter presents the summary of the research work in the light of its contribution and future scope.

Chapter- 2

Continuation load flow: A tool for voltage stability analysis

2. 1 Introduction

Several voltage stability indices were proposed to indicate the voltage stability condition of a power system based on power flow analysis. In recent years, bus measurements based voltage stability indices are proposed to provide information about the condition of the bus. These methods need continuous measurements of voltage and current phasors of a bus to determine Thevenin's equivalent of the bus. The Thevenin's equivalent representation of the bus is used to derive voltage stability index of the bus. It is essential to know the behaviour and nature of change of a voltage stability index as it approaches the proximity of voltage collapse. Continuation load flow provides facility to vary load of a power system load bus along the "Power Voltage" curve (PV curve) using a continuation parameter. These steps can be utilized to generate continuous variation of voltage and current phasors of a bus due to change in load in it and can be used to verify the performance of the measurement based voltage stability indices.

Normally, a power flow analysis is used for planning and operation of a power system. A power flow analysis determines the operating condition of a power system variables (bus voltage magnitude and phase angle) using the system network parameters and power injections at the buses. NR based power flow analysis is extensively used by the power system analyzer, as the Jacobian matrix of a load flow model could be used to derive operating condition of a power system. The Jacobian matrix of power flow model becomes singular at the point of voltage collapse. Therefore, it is numerically not possible to obtain a power flow solution near the point of voltage collapse. Continuation power flow has been developed to overcome this problem. The continuation power flow uses a predictor corrector steps to determine the load at the bus along PV curve. For this purpose, the power flow equations are reformulated to include a continuation perimeter for a load bus in order to find the solution path along the PV curve. The reformulation

helps in avoiding the singularity of the Jacobian at the point of voltage collapse and ensures solution of power flow analysis all along the PV curve. From a known base solution, a tangent predictor is used so as to estimate next solution for a specified pattern of load increase. The corrector step then determines the exact solution using Newton-Raphson technique employed by a conventional power flow. After that a new prediction is made for a specified increase in load based upon the new tangent vector. Then corrector step is applied. This process goes until critical point is reached. The critical point is the point where the tangent vector is zero. The illustration of predictor-corrector scheme is depicted in Figure 2.1.

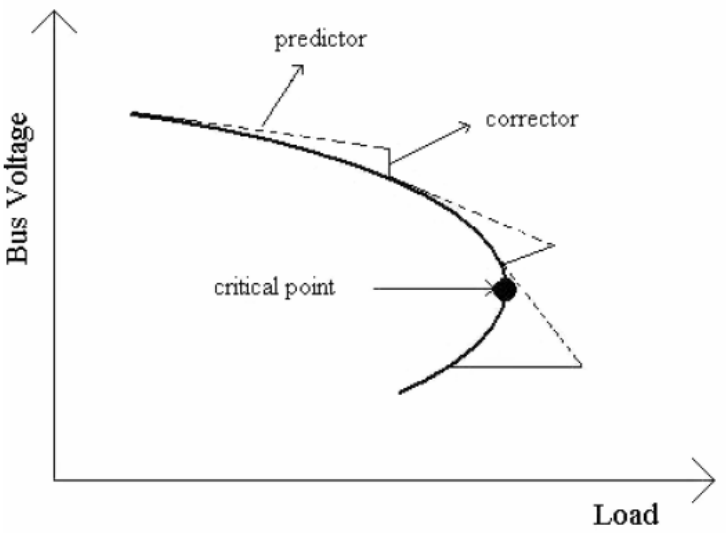

Figure 2.1: Illustration of prediction-correction steps

Therefore, to constitute a continuation load flow model, a continuation parameter λ is introduced in a normal NR based load flow model to find the solution path along the PV curve and λ is used to predict or determine the increment of load along PV curve. As, this prediction is based on linearized NR based load flow model, the over prediction occurs as shown in figure 2.1. Therefore, in a continuation load flow analysis the predicted load is normalized using a step size **σ** and a corrective load flow is carry out to track the PV curve.

2.2 Load Flow Analysis in a NR Load Flow Model

Load Flow Analysis (LFA) of a power system aims at determining the operating state of the system for the given power injection at its nodes. Therefore, for the formulation of the model for LFA, the network topology and the parameters and system bus injections must be known. Mathematically, for a N bus power system, load flow model is represented by 2N sets equations with 2N state vector. Bus voltage magnitude and phase angle constitute the state vector for a conventional power flow problem. In other words, one must find the bus voltage magnitude and their respective phase angle relative to the chosen reference phasor.

2.2.1 Classification of Buses

In an interconnected power system, the buses are connected with one device or a combination of devices like generators, loads and voltage control equipment. Variables are specified depending upon the equipment connected to the bus. Buses are classified into four types as:

1. PQ or load bus
2. PV or generator bus
3. Slack or swing or reference bus
4. Voltage controlled bus

2.2.2 PQ or load bus: A majority of the buses in a power system are of this type (about 85% of total buses). At this bus, active and reactive powers injected are specified, and the voltage magnitude and phase angles are unspecified. At each PQ bus, the generated power values P_{Gi} and Q_{Gi} are fixed or specified and the local power demand P_{Di} and Q_{Di} are known from measurements or by load forecasting. Knowing generation and demand, the net injected powers at the bus can be calculated as

$$P_i = P_{Gi} - P_{Di} \tag{2.1}$$

$$Q_i = Q_{Gi} - Q_{Di} \tag{2.2}$$

2.2.3 PV bus or Generator bus: A bus can be designated as a PV bus only when a generator is connected to it. At this bus, the injected active power P_i and the magnitude of the bus voltage $|V_i|$ are specified. About 15% of the buses in a power system are PV bus.

Basis for specifying P_i and $|V_i|$: P_{Gi} value can be set to a desired value based on the requirements of active power at the generating buses within the permissible control action of the generator. This type of bus is generally term as generating bus. Within the permissible control action of the exciter, the voltage magnitude can be controlled at this bus. However, as excitation has its limits, the generator at this bus cannot generate reactive power less than $Q_{Gi_{min}}$ or more than$Q_{Gi_{max}}$. Knowledge of these reactive power limits is necessary. As long as the Q_i value is within the limits, this generator bus can be continued to be treated as the voltage controlled PV bus. However, if in any of the iteration Q_i violates the limits, the bus can no longer be treated as a PV bus, and the power flow solution should again be initiated by re-designating this bus as a PQ bus. When it is re-designated, the value of Q_{Gi} is set to either $Q_{Gi_{min}}$ or $Q_{Gi_{max}}$ as the case may be.

2.2.4 Voltage controlled bus: Because of its capabilities in maintaining bus voltage to the specified value, a PV bus/ generator bus may be designated as a voltage controlled bus. However, a pure voltage controlled bus has a basic distinction in that it is connected with only voltage controlled equipment like SVCs and not generators. Hence at this bus, the following values are known:

$$P_{Gi} = Q_{Gi} = 0;\ P_i = -P_{Di};\ Q_i = -Q_{Di};\ |V_i| = specified\ value$$

$\delta_i$is the only unknown variable.

2.2.5 Slack bus/ Swing bus/ Reference bus: In a power system, if one bus is connected to a generator with high generation capacities (both P and Q), it is designated as the slack bus. At this bus, $|V_i|$ and δ_i are specified, and P and Q are unknown parameters.

Justification for specifying $|V_i|$ and δ_i : To find the phase angle difference δ amongst n-bus voltage vectors, one of the voltage vectors is taken as the reference vectors. Since slack bus voltage is chosen as the 'reference vector', its phase angle difference δ value is always zero and hence is known to us. As the bus is equipped with a generator, specifying $|V_i|$ is justified.

Justification for un-specifying P and Q: The power balanced equation can be written as:

$$\sum_{i=1}^{N} P_{Gi} - \sum_{i=1}^{N} P_{Di} - \sum P_{loss} = 0 \quad (2.3)$$

$$\sum_{i=1}^{N} Q_{Gi} - \sum_{i=1}^{N} Q_{Di} - \sum Q_{loss} = 0 \quad (2.4)$$

In a power flow study, the generator of active and reactive power cannot be set to the correct values, since the loss in the lines is unknown till the study is complete. Therefore, it is necessary to have one bus as the slack bus at which the complex power generation is not initially set. The generation at the slack bus is such that, it supplies the difference in the total system load plus losses minus the sum of the complex powers specified at the remaining buses. In an N-bus power system, for coding convenience bus 1 is selected as the slack bus.

2.3 Power Flow Solution by Newton Raphson Method

Injected current at i^{th} bus can be represented as:

$$I_i = \sum_{j=1}^{N} Y_{ij} V_j \quad (2.5)$$

The conjugate of injected power at i^{th} bus can be represented as:

$$P_i - jQ_i = V_i^* I_i = V_i^* \sum_{j=1}^{N} Y_{ij} V_j \quad (2.6)$$

Representing the complex voltage and Y-bus element of equation (2.6) in polar form, it can be written as:

$$P_i - jQ_i = \sum_{j=1}^{N} |V_i| \left|V_j\right| \left|Y_{ij}\right| \angle(\theta_{ij} - \delta_{ij}) \ \ where \ \angle\delta_{ij} = \angle\delta_i - \angle\delta_j \qquad (2.7)$$

On simplification of equation (2.7), the expression for the real and reactive power injection at the i^{th} bus for an interconnected power system can be represented as:

$$P_i = \sum_{j=1}^{N} |V_i| \left|V_j\right| \left(G_{ij} cos\delta_{ij} + B_{ij} \sin\delta_{ij}\right) \text{for i} = 1,2, \ldots, \text{N} \qquad (2.8)$$

$$Q_i = \sum_{j=1}^{N} |V_i| \left|V_j\right| \left(G_{ij} sin\delta_{ij} - B_{ij} \cos\delta_{ij}\right) \text{for i} = 1,2, \ldots, \text{N} \qquad (2.9)$$

Where $G_{ij} = \left|Y_{ij}\right| cos\theta_{ij}$ and $B_{ij} = \left|Y_{ij}\right| sin\theta_{ij}$

It can be observed in the above equations (2.8) and (2.9) that the injected power P and Q at each bus in an N bus power system are functions of N bus voltage magnitudes $|V|$ and another N number of phase angles (δ), totalling 2N bus quantities.

Representing real and reactive power balance as the two functional for the system, they are represented as;

$F(\delta, V) = 0$; for real balance power at the buses, which is functions of **δ** and **V**

$F'(\delta, V) = 0$; for reactive power balance at the buses, which is functions of **δ** and **V**

The F (δ, V) and F' (δ, V) for i^{th} bus can be represented as:

$$f_i = P_{Gi} - P_{Di} - \sum_{j=1}^{N} V_i V_j \left(G_{ij} \cos\delta_{ij} + B_{ij} \sin\delta_{ij}\right) \qquad for\ i = 1, \ldots, N \quad (2.10)$$

$$f_i' = Q_{Gi} - Q_{Di} - \sum_{j=1}^{N} V_i V_j \left(G_{ij} \sin\delta_{ij} - B_{ij} \cos\delta_{ij}\right) \qquad for\ i = 1, \ldots, N (2.11)$$

Using Newton Raphson first order interpolation method for solution of non-linear sets of equation, the load flow analysis model can be represented as:

$$\begin{bmatrix} \frac{\partial f_2}{\partial \delta_2} & \cdots & \frac{\partial f_2}{\partial \delta_k} & \frac{\partial f_2}{\partial \delta_m} & \cdots & \frac{\partial f_2}{\partial \delta_N} & \frac{\partial f_2}{\partial V_2} & \cdots & \frac{\partial f_2}{\partial V_k} & \frac{\partial f_2}{\partial V_m} & \cdots & \frac{\partial f_2}{\partial V_N} \\ \cdot & \cdots & \cdot & \cdot & \cdots & \cdot & \cdot & \cdots & \cdot & \cdot & \cdots & \cdot \\ \cdot & \cdots & \cdot & \cdot & \cdots & \cdot & \cdot & \cdots & \cdot & \cdot & \cdots & \cdot \\ \frac{\partial f_k}{\partial \delta_2} & \cdots & \frac{\partial f_k}{\partial \delta_k} & \frac{\partial f_k}{\partial \delta_m} & \cdots & \frac{\partial f_k}{\partial \delta_N} & \frac{\partial f_k}{\partial V_2} & \cdots & \frac{\partial f_k}{\partial V_k} & \frac{\partial f_k}{\partial V_m} & \cdots & \frac{\partial f_k}{\partial V_N} \\ \frac{\partial f_m}{\partial \delta_2} & \cdots & \frac{\partial f_m}{\partial \delta_k} & \frac{\partial f_m}{\partial \delta_m} & \cdots & \frac{\partial f_m}{\partial \delta_N} & \frac{\partial f_m}{\partial V_2} & \cdots & \frac{\partial f_m}{\partial V_k} & \frac{\partial f_m}{\partial V_m} & \cdots & \frac{\partial f_m}{\partial V_N} \\ \cdot & \cdots & \cdot & \cdot & \cdots & \cdot & \cdot & \cdots & \cdot & \cdot & \cdots & \cdot \\ \cdot & \cdots & \cdot & \cdot & \cdots & \cdot & \cdot & \cdots & \cdot & \cdot & \cdots & \cdot \\ \frac{\partial f_N}{\partial \delta_2} & \cdots & \frac{\partial f_N}{\partial \delta_k} & \frac{\partial f_N}{\partial \delta_m} & \cdots & \frac{\partial f_N}{\partial \delta_N} & \frac{\partial f_N}{\partial V_2} & \cdots & \frac{\partial f_N}{\partial V_k} & \frac{\partial f_N}{\partial V_m} & \cdots & \frac{\partial f_N}{\partial V_N} \\ \frac{\partial f'_2}{\partial \delta_2} & \cdots & \frac{\partial f'_2}{\partial \delta_k} & \frac{\partial f'_2}{\partial \delta_m} & \cdots & \frac{\partial f'_2}{\partial \delta_N} & \frac{\partial f'_2}{\partial V_2} & \cdots & \frac{\partial f'_2}{\partial V_k} & \frac{\partial f'_2}{\partial V_m} & \cdots & \frac{\partial f'_2}{\partial V_N} \\ \cdot & \cdots & \cdot & \cdot & \cdots & \cdot & \cdot & \cdots & \cdot & \cdot & \cdots & \cdot \\ \cdot & \cdots & \cdot & \cdot & \cdots & \cdot & \cdot & \cdots & \cdot & \cdot & \cdots & \cdot \\ \frac{\partial f'_k}{\partial \delta_2} & \cdots & \frac{\partial f'_k}{\partial \delta_k} & \frac{\partial f'_k}{\partial \delta_m} & \cdots & \frac{\partial f'Q_k}{\partial \delta_N} & \frac{\partial f'_k}{\partial V_2} & \cdots & \frac{\partial f'_k}{\partial V_k} & \frac{\partial f'_k}{\partial V_m} & \cdots & \frac{\partial f'_k}{\partial V_N} \\ \frac{\partial f'_m}{\partial \delta_2} & \cdots & \frac{\partial f'_m}{\partial V_k} & \frac{\partial f'_m}{\partial \delta_m} & \cdots & \frac{\partial f'_m}{\partial \delta_N} & \frac{\partial f'_m}{\partial V_2} & \cdots & \frac{\partial f'_m}{\partial V_k} & \frac{\partial f'_m}{\partial V_m} & \cdots & \frac{\partial f'_m}{\partial V_N} \\ \cdot & \cdots & \cdot & \cdot & \cdots & \cdot & \cdot & \cdots & \cdot & \cdot & \cdots & \cdot \\ \cdot & \cdots & \cdot & \cdot & \cdots & \cdot & \cdot & \cdots & \cdot & \cdot & \cdots & \cdot \\ \frac{\partial f'_N}{\partial \delta_2} & \cdots & \frac{\partial f'_N}{\partial \delta_k} & \frac{\partial f'_N}{\partial \delta_m} & \cdots & \frac{\partial f'_N}{\partial \delta_N} & \frac{\partial f'_N}{\partial V_2} & \cdots & \frac{\partial f'_N}{\partial V_k} & \frac{\partial f'_N}{\partial V_m} & \cdots & \frac{\partial f'_N}{\partial V_N} \end{bmatrix} \times \begin{bmatrix} \Delta\delta_2 \\ \cdot \\ \cdot \\ \Delta\delta_k \\ \Delta\delta_m \\ \cdot \\ \cdot \\ \Delta\delta_N \\ \Delta V_2 \\ \cdot \\ \cdot \\ \Delta V_k \\ \Delta V_m \\ \cdot \\ \cdot \\ \Delta V_N \end{bmatrix} = \begin{bmatrix} -f_2 \\ \cdot \\ \cdot \\ -f_k \\ -f_m \\ \cdot \\ \cdot \\ -f_N \\ -f'_2 \\ \cdot \\ \cdot \\ -f'_k \\ -f'_m \\ \cdot \\ \cdot \\ -f'_N \end{bmatrix} \quad (2.12)$$

The elements of Jacobian matrix are as follows:

$$\frac{\partial f_i}{\partial \delta_i} = -\sum_{\substack{j=1 \\ j \neq i}}^{N} V_i V_j \left(-G_{ij} \sin\delta_{ij} + B_{ij} \cos\delta_{ij}\right) = -\frac{\partial P_i}{\partial \delta_i} \quad \text{for } i = 2, \ldots, \mathrm{N} \qquad (2.13)$$

$$\frac{\partial f_i}{\partial \delta_j} = -V_i V_j \left(G_{ij} \sin\delta_{ij} - B_{ij} \cos\delta_{ij}\right) = \frac{\partial P_i}{\partial \delta_j} \qquad \text{for } j = 2, \ldots, \mathrm{N};\ i \neq j \qquad (2.14)$$

$$\frac{\partial f_i}{\partial V_i} = -\left[2G_{ii}V_i + \sum_{\substack{j=1 \\ j \neq i}}^{N} V_j \left(G_{ij} \cos\delta_{ij} + B_{ij} \sin\delta_{ij}\right)\right] = -\frac{\partial P_i}{\partial V_i} \quad \text{for } i = 2, \ldots, \mathrm{N} \qquad (2.15)$$

$$\frac{\partial f_i}{\partial V_j} = -V_i \left(G_{ij} \cos\delta_{ij} + B_{ij} \sin\delta_{ij}\right) = -\frac{\partial P_i}{\partial V_j} \qquad \text{for } j = 2, \ldots, \mathrm{N};\ i \neq j \qquad (2.16)$$

$$\frac{\partial f'_i}{\partial \delta_i} = -\sum_{\substack{j=1 \\ j \neq i}}^{N} V_i V_j \left(G_{ij} \cos\delta_{ij} + B_{ij} \sin\delta_{ij}\right) = -\frac{\partial Q_i}{\partial \delta_i} \qquad \text{for } i = 2, \ldots, \mathrm{N} \qquad (2.17)$$

$$\frac{\partial f'_i}{\partial \delta_j} = V_i V_j \left(G_{ij} \sin\delta_{ij} + B_{ij} \cos\delta_{ij}\right) = -\frac{\partial Q_i}{\partial \delta_j} \quad \text{for } j = 2, \ldots, \text{N};\ i \neq j \tag{2.18}$$

$$\frac{\partial f'_i}{\partial V_i} = -[-2B_{ii}V_i + \sum_{\substack{j=1 \\ j\neq i}}^{N} V_j \left(G_{ij} \sin\delta_{ij} - B_{ij} \cos\delta_{ij}\right)] = -\frac{\partial Q_i}{\partial V_i} \text{ for } i = 2, \ldots, \tag{2.19}$$

$$\frac{\partial f'_i}{\partial V_j} = -V_i \left(G_{ij} \sin\delta_{ij} - B_{ij} \cos\delta_{ij}\right) = -\frac{\partial Q_i}{\partial V_j} \quad \text{for } j = 2, \ldots, \text{N};\ i \neq j \tag{2.20}$$

$$f_i = P_{Gi} - P_{Di} - P_i = -\Delta P_i \tag{2.21}$$

$$f'_i = Q_{Gi} - Q_{Di} - Q_i = -\Delta Q_i \tag{2.22}$$

Replacing negative of differentiation of functions f and $f_i^{'}$ of the Jacobian matrix by the differentiation of real and reactive power injections at the buses and negative of functions f and $f_i^{'}$ by ΔP_i and ΔQ_i, the Newton Raphson load flow model can be represented as:

$$\begin{bmatrix}
\frac{\partial P_2}{\partial \delta_2} & \cdots & \frac{\partial P_2}{\partial \delta_k}\frac{\partial P_2}{\partial \delta_m} & \cdots & \frac{\partial P_2}{\partial \delta_N}\frac{\partial P_2}{\partial V_2} & \cdots & \frac{\partial P_2}{\partial V_k}\frac{\partial P_2}{\partial V_m} & \cdots & \frac{\partial P_2}{\partial V_N} \\
\vdots & \cdots & \vdots\ \vdots & \cdots & \vdots\ \vdots & \cdots & \vdots\ \vdots & \cdots & \vdots \\
\vdots & \cdots & \vdots\ \vdots & \cdots & \vdots\ \vdots & \cdots & \vdots\ \vdots & \cdots & \vdots \\
\frac{\partial P_k}{\partial \delta_2} & \cdots & \frac{\partial P_k}{\partial \delta_k}\frac{\partial P_k}{\partial \delta_m} & \cdots & \frac{\partial P_k}{\partial \delta_N}\frac{\partial P_k}{\partial V_2} & \cdots & \frac{\partial P_k}{\partial V_k}\frac{\partial P_k}{\partial V_m} & \cdots & \frac{\partial P_k}{\partial V_N} \\
\frac{\partial P_m}{\partial \delta_2} & \cdots & \frac{\partial P_m}{\partial \delta_k}\frac{\partial P_m}{\partial \delta_m} & \cdots & \frac{\partial P_m}{\partial \delta_N}\frac{\partial P_m}{\partial V_2} & \cdots & \frac{\partial P_m}{\partial V_k}\frac{\partial P_m}{\partial V_m} & \cdots & \frac{\partial P_m}{\partial V_N} \\
\vdots & \cdots & \vdots\ \vdots & \cdots & \vdots\ \vdots & \cdots & \vdots\ \vdots & \cdots & \vdots \\
\vdots & \cdots & \vdots\ \vdots & \cdots & \vdots\ \vdots & \cdots & \vdots\ \vdots & \cdots & \vdots \\
\frac{\partial P_N}{\partial \delta_2} & \cdots & \frac{\partial P_N}{\partial \delta_k}\frac{\partial P_N}{\partial \delta_m} & \cdots & \frac{\partial P_N}{\partial \delta_N}\frac{\partial P_N}{\partial V_2} & \cdots & \frac{\partial P_N}{\partial V_k}\frac{\partial P_N}{\partial V_m} & \cdots & \frac{\partial P_N}{\partial V_N} \\
\frac{\partial Q_2}{\partial \delta_2} & \cdots & \frac{\partial Q_2}{\partial \delta_k}\frac{\partial Q_2}{\partial \delta_m} & \cdots & \frac{\partial Q_2}{\partial \delta_N}\frac{\partial Q_2}{\partial V_2} & \cdots & \frac{\partial Q_2}{\partial V_k}\frac{\partial Q_2}{\partial V_m} & \cdots & \frac{\partial Q_2}{\partial V_N} \\
\vdots & \cdots & \vdots\ \vdots & \cdots & \vdots\ \vdots & \cdots & \vdots\ \vdots & \cdots & \vdots \\
\vdots & \cdots & \vdots\ \vdots & \cdots & \vdots\ \vdots & \cdots & \vdots\ \vdots & \cdots & \vdots \\
\frac{\partial Q_k}{\partial \delta_2} & \cdots & \frac{\partial Q_k}{\partial \delta_k}\frac{\partial Q_k}{\partial \delta_m} & \cdots & \frac{\partial Q_k}{\partial \delta_N}\frac{\partial Q_k}{\partial V_2} & \cdots & \frac{\partial Q_k}{\partial V_k}\frac{\partial Q_k}{\partial V_m} & \cdots & \frac{\partial Q_k}{\partial V_N} \\
\frac{\partial Q_m}{\partial \delta_2} & \cdots & \frac{\partial Q_m}{\partial V_k}\frac{\partial Q_m}{\partial \delta_m} & \cdots & \frac{\partial Q_m}{\partial \delta_N}\frac{\partial Q_m}{\partial V_2} & \cdots & \frac{\partial Q_m}{\partial V_k}\frac{\partial Q_m}{\partial V_m} & \cdots & \frac{\partial Q_m}{\partial V_N} \\
\vdots & \cdots & \vdots\ \vdots & \cdots & \vdots\ \vdots & \cdots & \vdots\ \vdots & \cdots & \vdots \\
\vdots & \cdots & \vdots\ \vdots & \cdots & \vdots\ \vdots & \cdots & \vdots\ \vdots & \cdots & \vdots \\
\frac{\partial Q_N}{\partial \delta_2} & \cdots & \frac{\partial Q_N}{\partial \delta_k}\frac{\partial Q_N}{\partial \delta_m} & \cdots & \frac{\partial Q_N}{\partial \delta_N}\frac{\partial Q_N}{\partial V_2} & \cdots & \frac{\partial Q_N}{\partial V_k}\frac{\partial Q_N}{\partial V_m} & \cdots & \frac{\partial Q_N}{\partial V_N}
\end{bmatrix}
\begin{bmatrix}
\Delta\delta_2 \\ \vdots \\ \vdots \\ \Delta\delta_k \\ \Delta\delta_m \\ \vdots \\ \vdots \\ \Delta\delta_N \\ \Delta V_2 \\ \vdots \\ \vdots \\ \Delta V_k \\ \Delta V_m \\ \vdots \\ \vdots \\ \Delta V_N
\end{bmatrix}
=
\begin{bmatrix}
\Delta P_2 \\ \vdots \\ \vdots \\ \Delta P_k \\ \Delta P_m \\ \vdots \\ \vdots \\ \Delta P_N \\ \Delta Q_2 \\ \vdots \\ \vdots \\ \Delta Q_k \\ \Delta Q_m \\ \vdots \\ \vdots \\ \Delta Q_N
\end{bmatrix} \tag{2.23}$$

The set of equations described above are modified when PV (generator) buses are present. Let x be the number of PV buses.

1. Since the magnitude of voltage is specified for PV buses, their increment $\Delta|V|$ do not exists. Hence, in the increment matrix the elements corresponding to PV buses should be eliminated. With this, the dimension of the increment matrix reduces to$(2N-2-x\times 1)$.
2. In the power mismatch matrix, the reactive power mismatch ΔQ corresponding to the PV buses cannot be calculated, as reactive power for these buses is not specified. Hence the size of the matrix reduces to$(2N-2-x\times 1)$.
3. Due to modification in other matrices the size of the Jacobian now reduces to$(2N-2-x\times 2N-2-x)$.

Representing$|\Delta V|^T=[\Delta V_2,\Delta V_3,\dots..,\Delta V_N],|\Delta\delta|^T=[\Delta\delta_2,\Delta\delta_3,\dots..,\Delta\delta_N]$,
$|\Delta P|^T=[\Delta P_2,\Delta P_3,\dots..,\Delta P_N]$, $|\Delta Q|^T=[\Delta Q_2,\Delta Q_3,\dots..,\Delta Q_N]$ the load flow Jacobian matrix J can be represented as

$$\begin{bmatrix}\Delta P\\ \Delta Q\end{bmatrix}=[J]\begin{bmatrix}\Delta\delta\\ \Delta V\end{bmatrix} \quad (2.24)$$

2.4 Prediction and Correction steps for Continuation load flow analysis

In order to simulate a load change, a load parameter λ is inserted into demand power at k^{th} bus, and then the expression for power demand can be represented as:

$$P_{Dk}=P_{Dok}+\lambda P_{\Delta base}=P_{Dok}+\lambda KLP_k \quad (2.25)$$

$$Q_{Dk}=Q_{Dok}+\lambda Q_{\Delta base}=Q_{Dok}+\lambda KLQ_k \quad 2.26)$$

$$P_{Gk}=P_{Gok}+\lambda P_{\Delta base}=P_{Gok}+\lambda KG_k \quad (2.27)$$

Where, P_{Dok} and Q_{Dok} are original load demands on k^{th} bus whereas $P_{\Delta base}$ and $Q_{\Delta base}$ are given quantities of powers chosen to scale λ appropriately. After substituting new demand powers in Equation 2.25 to Equation 2.27, new set of equations can be represented as:

$F(\delta, V, \lambda) = 0$; for real power balance at the buses, which is functions of **δ,** V and λ.

$F'(\delta, V, \lambda) = 0$; for reactive power balance at the buses, , which is functions of **δ**, **V** and λ.

The base solution for λ=0 is found using NR power flow algorithm. Then, the continuation and parameterization processes are applied

2.4.1 Prediction Step

In this step, a linear approximation is used by taking an appropriately sized step in a direction tangent to the solution path. Therefore, the derivative of both sides of Equations 2.10 and 2.11 are taken.

$$(F_\delta + F'_\delta)'\Delta\delta + (F_V + F'_V)'\Delta V + (F_\lambda + F'_\lambda)'\Delta\lambda = 0$$

$$\text{Or, } [(F_\delta + F'_\delta)' \quad (F_V + F'_V)' \quad (F_\lambda + F'_\lambda)'] \begin{bmatrix} \Delta\delta \\ \Delta V \\ \Delta\lambda \end{bmatrix} = 0 \qquad (2.28)$$

In order to solve Equation (2.28), one more equation is needed since an unknown variable λ is added to load flow equations. This can be satisfied by setting one of the tangent vector components to +1 or -1 which is also called continuation parameter. Setting one of the tangent vector components +1 or -1 imposes a non-zero value on the tangent vector and makes Jacobian non-singular at the critical point. As a result Equation (2.28) becomes:

$$\begin{bmatrix} (F_\delta + F'_\delta)' & (F_V + F'_V)' & (F_\lambda + F'_\lambda)' \\ & e_k & \end{bmatrix} \begin{bmatrix} \Delta\delta \\ \Delta V \\ \Delta\lambda \end{bmatrix} = \begin{bmatrix} 0 \\ \pm 1 \end{bmatrix} \qquad (2.29)$$

Where, e_k is the appropriate row vector with all elements equal to zero except the k^{th} element equals, which is taken as 1. At first step λ is chosen as the continuation parameter. As the process continues, the state variable with the greatest rate of change is selected as continuation parameter

due to nature of parameterization. By solving Equation (2.29), the tangent vector can be found. Then, the prediction can be made as follows:

$$\begin{bmatrix}\delta\\V\\\lambda\end{bmatrix}^{K+1} = \begin{bmatrix}\delta\\V\\\lambda\end{bmatrix}^{K} + \sigma\begin{bmatrix}\Delta\delta\\\Delta V\\\Delta\lambda\end{bmatrix}^{K+1}$$

Where the subscript "K+1" denotes the next predicted solution. The step size σ is chosen so that the predicted solution is within the radius of convergence of the corrector. If it is not satisfied, a smaller step size is chosen.

2.4.2 Correction Step

In correction step, the predicted solution is corrected by using local parameterization. The original set of equation is increased by one equation that specifies the value of state variable chosen and it results in:

$$\begin{bmatrix}\mathrm{F}(\delta,\mathrm{V},\lambda) & \mathrm{F}'(\delta,\mathrm{V},\lambda)\\ x_k - \eta\end{bmatrix} = [0] \qquad (2.30)$$

Where x_k is the state variable chosen as continuation parameter and η is the predicted value of this state variable. Equation 2.30 can be solved by using a slightly modified Newton-Raphson power flow method.

2.4.3 Parameterization:

Selection of continuation parameter is important in continuation power flow. Continuation parameter is the state variable with the greatest rate of change. Initially, λ is selected as

continuation parameter since at first steps there are small changes in bus voltages and angles due to light load. When the load increases after a few steps the solution approaches the critical point and the rate of change of bus voltages and angles increase. Therefore, selection of continuation parameter is checked after each corrector step. The variable with the largest change is chosen as continuation parameter. If the parameter is increasing, then it is taken as + 1 and if it is decreasing, then it is taken as -1 in the tangent vector in equation 2.30.

The continuation power flow is stopped when critical point is reached as it is seen in the flow chart. Critical point is the point where the loading has maximum value. After this point it starts to decrease. The tangent component of λ is zero at the critical point and negative beyond this point. Therefore, the sign of $\Delta\lambda$ shows whether the critical point is reached or not.

2.5 Modification of Newton Raphson Load Flow Model to Incorporate Prediction and Correction steps

Continuation parameter λ is introduced in kth bus, therefore, terms ($\frac{\partial F_\lambda}{\partial \lambda}$ and $\frac{\partial F'_\lambda}{\partial \lambda}$) are to be included in the load flow Jacobian matrix as an addition row corresponding to. Again, e_k is set to 1 (i.e, $e_k = 1$) for the kth element of the row that correspond to $\Delta\lambda$. Further, the terms $\frac{\partial f_k}{\partial \lambda}$ and $\frac{\partial f'_k}{\partial \lambda}$ are represented as:

$$\frac{\partial f_k}{\partial \lambda} = -KG_k + KLP_k \qquad (2.31)$$

$$\frac{\partial f'_k}{\partial \lambda} = KLQ_k \qquad (2.32)$$

Thus the modified load flow model for continuation load flow analysis becomes:

$$\begin{bmatrix} \frac{\partial P_2}{\partial \delta_2} & \cdots & \frac{\partial P_2}{\partial \delta_k}\frac{\partial P_2}{\partial \delta_m} & \cdots & \frac{\partial P_2}{\partial \delta_N}\frac{\partial P_2}{\partial V_2} & \cdots & \frac{\partial P_2}{\partial V_k}\frac{\partial P_2}{\partial V_m} & \cdots & \frac{\partial P_2}{\partial V_N} & 0 \\ \vdots & \cdots & \vdots\ \vdots & \cdots & \vdots\ \vdots & \cdots & \vdots\ \vdots & \cdots & \vdots & 0 \\ \vdots & \cdots & \vdots\ \vdots & \cdots & \vdots\ \vdots & \cdots & \vdots\ \vdots & \cdots & \vdots & 0 \\ \frac{\partial P_k}{\partial \delta_2} & \cdots & \frac{\partial P_k}{\partial \delta_k}\frac{\partial P_k}{\partial \delta_m} & \cdots & \frac{\partial P_k}{\partial \delta_N}\frac{\partial P_k}{\partial V_2} & \cdots & \frac{\partial P_k}{\partial V_k}\frac{\partial P_k}{\partial V_m} & \cdots & \frac{\partial P_k}{\partial V_N} & -KG_k + KLP_k \\ \frac{\partial P_m}{\partial \delta_2} & \cdots & \frac{\partial P_m}{\partial \delta_k}\frac{\partial P_m}{\partial \delta_m} & \cdots & \frac{\partial P_m}{\partial \delta_N}\frac{\partial P_m}{\partial V_2} & \cdots & \frac{\partial P_m}{\partial V_k}\frac{\partial P_m}{\partial V_m} & \cdots & \frac{\partial P_m}{\partial V_N} & 0 \\ \vdots & \cdots & \vdots\ \vdots & \cdots & \vdots\ \vdots & \cdots & \vdots\ \vdots & \cdots & \vdots & 0 \\ \vdots & \cdots & \vdots\ \vdots & \cdots & \vdots\ \vdots & \cdots & \vdots\ \vdots & \cdots & \vdots & 0 \\ \frac{\partial P_N}{\partial \delta_2} & \cdots & \frac{\partial P_N}{\partial \delta_k}\frac{\partial P_N}{\partial \delta_m} & \cdots & \frac{\partial P_N}{\partial \delta_N}\frac{\partial P_N}{\partial V_2} & \cdots & \frac{\partial P_N}{\partial V_k}\frac{\partial P_N}{\partial V_m} & \cdots & \frac{\partial P_N}{\partial V_N} & 0 \\ \frac{\partial Q_2}{\partial \delta_2} & \cdots & \frac{\partial Q_2}{\partial \delta_k}\frac{\partial Q_2}{\partial \delta_m} & \cdots & \frac{\partial Q_2}{\partial \delta_N}\frac{\partial Q_2}{\partial V_2} & \cdots & \frac{\partial Q_2}{\partial V_k}\frac{\partial Q_2}{\partial V_m} & \cdots & \frac{\partial Q_2}{\partial V_N} & 0 \\ \vdots & \cdots & \vdots\ \vdots & \cdots & \vdots\ \vdots & \cdots & \vdots\ \vdots & \cdots & \vdots & \\ \vdots & \cdots & \vdots\ \vdots & \cdots & \vdots\ \vdots & \cdots & \vdots\ \vdots & \cdots & \vdots & 0 \\ \frac{\partial Q_k}{\partial \delta_2} & \cdots & \frac{\partial Q_k}{\partial \delta_k}\frac{\partial Q_k}{\partial \delta_m} & \cdots & \frac{\partial Q_k}{\partial \delta_N}\frac{\partial Q_k}{\partial V_2} & \cdots & \frac{\partial Q_k}{\partial V_k}\frac{\partial Q_k}{\partial V_m} & \cdots & \frac{\partial Q_k}{\partial V_N} & KLQ_k \\ \frac{\partial Q_m}{\partial \delta_2} & \cdots & \frac{\partial Q_m}{\partial V_k}\frac{\partial Q_m}{\partial \delta_m} & \cdots & \frac{\partial Q_m}{\partial \delta_N}\frac{\partial Q_m}{\partial V_2} & \cdots & \frac{\partial Q_m}{\partial V_k}\frac{\partial Q_m}{\partial V_m} & \cdots & \frac{\partial Q_m}{\partial V_N} & 0 \\ \vdots & \cdots & \vdots\ \vdots & \cdots & \vdots\ \vdots & \cdots & \vdots\ \vdots & \cdots & \vdots & 0 \\ \vdots & \cdots & \vdots\ \vdots & \cdots & \vdots\ \vdots & \cdots & \vdots\ \vdots & \cdots & \vdots & 0 \\ \frac{\partial Q_N}{\partial \delta_2} & \cdots & \frac{\partial Q_N}{\partial \delta_k}\frac{\partial Q_N}{\partial \delta_m} & \cdots & \frac{\partial Q_N}{\partial \delta_N}\frac{\partial Q_N}{\partial V_2} & \cdots & \frac{\partial Q_N}{\partial V_k}\frac{\partial Q_N}{\partial V_m} & \cdots & \frac{\partial Q_N}{\partial V_N} & 0 \\ 0 & \cdots\cdots & 0\ 0 & \cdots\cdots & 0\ 0 & \cdots\cdots & 1\ 0 & \cdots\cdots & 0 & 0 \end{bmatrix} \begin{bmatrix} \Delta\delta_2 \\ \vdots \\ \vdots \\ \Delta\delta_k \\ \Delta\delta_m \\ \vdots \\ \vdots \\ \Delta\delta_N \\ \Delta V_2 \\ \vdots \\ \vdots \\ \Delta V_k \\ \Delta V_m \\ \vdots \\ \vdots \\ \Delta V_N \\ \Delta\lambda \end{bmatrix} = \begin{bmatrix} \Delta P_2 \\ \vdots \\ \vdots \\ \Delta P_k \\ \Delta P_m \\ \vdots \\ \vdots \\ \Delta P_N \\ \Delta Q_2 \\ \vdots \\ \vdots \\ \Delta Q_k \\ \Delta Q_m \\ \vdots \\ \vdots \\ \Delta Q_N \\ \eta \end{bmatrix} \quad (2.33)$$

2.6 Solution Algorithm:

The research work presented in this thesis aims at investigating the performance and behaviour of the bus measurements base voltage stability indices as they approach the proximity of voltage collapse. Most of the bus measurement based voltage stability analysis requires voltage and current phasors of a bus for two consecutive time steps. To determine voltage and current phasors of a bus for two consecutive time steps, load at a bus is increased using a continuation load flow analysis. Two consecutive load increment steps of the continuation load flow analysis are considered as the time references t_1 and t_2. The bus variables, such as, real and reactive power injections, voltage and current phasors provided by the continuation load flow analysis for two consecutive steps are treated as the bus measurement for time steps t_1 and t_2. The solution steps of the continuation power flow analysis having provision for generating measurement variables for a bus for two consecutive time steps are presented below:

1. Read bus and line data for the power system.

2. Initialize iteration count K=0, target or select bus k, continuation parameter λ = 0 and step size **σ** = 0.001

3. Carry out power flow solution of the system. The time reference for this step is represented as t_1. The voltage and current phasors and real and reactive power injections are represented as $V_{k(t_1)} \cos \delta_{k(t_1),} + j\, V_{k(t_1)} \sin \delta_{k(t_1),}$, $g_{k(t_1)}$+j $h_{k(t_1)}$, $P_{k(t_1)}$, $Q_{k(t_1)}$

4. Introduce element in power flow Jacobian representing the affect of continuation parameter and carry out prediction step of the continuation power flow analysis to determine predicted states

$$\begin{bmatrix} \delta \\ V \\ \lambda \end{bmatrix}^{K+1} = \begin{bmatrix} \delta \\ V \\ \lambda \end{bmatrix}^{K} + \sigma \begin{bmatrix} \Delta\delta \\ \Delta V \\ \Delta\lambda \end{bmatrix}^{K+1}$$

5. Carryout correction step of the continuation power flow analysis.

6. The time reference for this step is represented as t_2 and corresponding voltage and current phasors and real and reactive power injections are represented as $V_{k(t_2)} \cos \delta_{k(t_2),} + j\, V_{k(t_2)} \sin \delta_{k(t_2),}$, $g_{k(t_2)}$+j $h_{k(t_2)}$, $P_{k(t_2)}$, $Q_{k(t_2)}$

7. Use $V_{k(t_1)} \cos \delta_{k(t_1),} + j\, V_{k(t_1)} \sin \delta_{k(t_1),}$, $g_{k(t_1)}$+j $h_{k(t_1)}$, $P_{k(t_1)}$, $Q_{k(t_1)}$ and $V_{k(t_2)} \cos \delta_{k(t_2),} + j\, V_{k(t_2)} \sin \delta_{k(t_2),}$, $g_{k(t_2)}$+j $h_{k(t_2)}$, $P_{k(t_2)}$, $Q_{k(t_2)}$ as bus measurements values for two consecutive time steps for kth bus for measurement based voltage stability analysis.

8. Replace the bus measurements values of time reference t_1 by the time reference t_2, i.e., $V_{k(t_1)} = V_{k(t_2)}$, $\delta_{k(t_1),} = \delta_{k(t_2),}$ $g_{k(t_1)} = g_{k(t_2)}$, $h_{k(t_1)} = h_{k(t_2)}$, $P_{k(t_1)} = P_{k(t_2)}$ and $Q_{k(t_1)} = Q_{k(t_1)}$

9. Increment K. (K= K+1).

10. Check for $\Delta\lambda > 0.0\ (i.e,.+ve)$, if yes go to step 4

11. Stop.

2.7 Conclusions:

In this chapter, the detailed theoretical background and the computational process of a continuation power flow analysis having provisions for generation of bus phasor variables for two consecutive time references. This continuation load flow analysis model can be used to verify the performance of bus measurement based voltage stability indices of a power system. For this purpose, successive prediction-correction steps provided by continuation parameter λ are used to generate consecutive bus phasor measurements. These two bus measurements are used to verify the nature of variation of measurement based Voltage Stability Indices for a power system in the next chapters.

Chapter- 3

Use of local bus phasor measurements to analyze voltage stability of a power system

3.1 Introduction

Several methods were proposed for indentifying the voltage stability condition of an interconnected power system using the measurements of voltage and current phasors of a bus. For this purpose, phasor measurement units (PMUs) are used. A PMU is a device which measures the electrical waves on an electrical network, using a common time source (reference bus) for synchronization. The phasor measurement technology developed since the end of the 1980s, together with advances in computational facilities, networking infrastructure and communications, have opened new perspectives for designing wide-area monitoring, detection, protection and control systems. The Phasor Measurement Unit (PMU) hardware is now based on proven technology and is considered as the most accurate and advanced time-synchronized technology available to power engineers. This chapter provides the detailed process for investigating performance of measurement based voltage stability indices using the continuous power flow analysis developed in chapter-2 as a tool for generating bus measurement variable. Two indices are considered for this purpose.

3.2 Method for voltage stability analysis of an interconnected power system using voltage and current phasors of a bus

Vu et al. proposed a voltage stability index (VSI) that uses the local voltage and current phasor measurements at a load bus [37]. To determine the voltage stability index of a load bus, two consecutive measurements of voltage and current phasors are needed. The method is simple and it needs the measurements of a local PMU for consecutive two time references.

Another voltage stability index called Equivalent Node Voltage Collapse Index (ENVCI), where Equivalent System Model (ESM) of a load bus with transmission lines connected to it as $\boldsymbol{\pi}$-model is proposed [39]. An Equivalent Local Network Model (ELNM) has been derived by representing transmission lines connected to the bus as an equivalent transmission line. The ELNM requires the parameters of the transmission lines connected to the selected load bus and voltage phasors of the system buses that are connected to the selected load bus. Therefore, this method requires PMUs at all the connecting buses and at the selected node.

The voltage stability indices proposed in the above mentioned two methods are considered for investigating their characteristic behavior along the PV curve and around the proximity of voltage collapse using the continuation load flow analysis described in chapter-2. It is already mentioned that provision is made in continuation load flow analysis described in chapter-2 to generate bus measurements for connected buses of the selected load buses to determine ENVCI. These two indices are considered for investigation due to fact that the theoretical approaches adopted for derivation of voltage stability indices are different for both the methods.

3.2.1. Voltage stability index based on two consecutive measurements of voltage and current phasors of a local bus

Vu K., Begovic M.M., Novosel D., proposed a method for the determination of Thevenin's Equivalent Circuit (TEC) of an interconnected power system [36], using two consecutive measurements of voltage and current phasors of a load bus. TEC of an interconnected power system with respect to a target bus k can be represented as shown in Fig. 3.1.

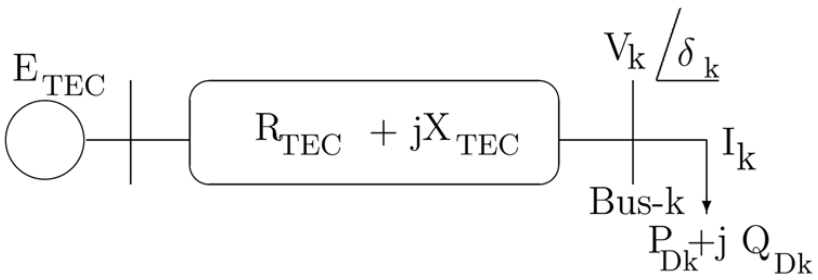

Fig. 3.1 TEC of an interconnected power system with respect to a target bus k

Where, R_{TEC} and X_{TEC} are the equivalent resistance and reactance of the TEC.
The TEC vector source voltage can be expressed as

$$\bar{E}_{TEC} = \overline{V_k} + (R_{TEC} + jX_{TEC}) \overline{I_k}$$

The above equation can be represented in complex form with real and imaginary components of voltages and current $\bar{E}_{TEC}$ $(e_{TEC} + jf_{TEC})$, $\overline{V_k}$ $(e_k + j\ f_k)$ and $\overline{I_k}$ $(g_k + j\ h_k)$ as given below

$$e_{TEC} + jf_{TEC} = e_k + j\ f_k + (R_{TEC} + jX_{TEC})(g_k + j\ h_k) \quad (3.1)$$

Separating real and imaginary parts of equation (3.1), it can be expressed as:

$$e_{TEC} - R_{TEC} g_k + X_{TEC} h_k = e_k \quad (3.2)$$

$$f_{TEC} - R_{TEC} h_k - X_{TEC} g_k = f_k \quad (3.3)$$

Equations (3.2) & (3.3) can be represented in matrix form as given below:

$$\begin{bmatrix} 1 & 0 & -g_k & h_k \\ 0 & 1 & -h_k & -g_k \end{bmatrix} \begin{bmatrix} e_{TEC} \\ f_{TEC} \\ R_{TEC} \\ X_{TEC} \end{bmatrix} = \begin{bmatrix} e_k \\ f_k \end{bmatrix} \quad (3.4)$$

System equation represented by matrices represented in (3.4) has two sets of equations and four unknown variables, namely, the TEC source voltage phasor e_{TEC} and f_{TEC} and source resistance and reactance R_{TEC} and X_{TEC} . To determine these unknown variables, four sets of equations are needed in system equation represented by (3.4). Therefore, it is proposed to use consecutive measurements of voltage and current phasors to determine the TEC source voltage and source impedance. Using two consecutive measurements of bus voltage and current phasors of a bus-k (i.e. for time instances t_1 and t_2), eq. (3.4) can be represented as

$$\begin{bmatrix} 1 & 0 & -g_k(t_1) & h_k(t_1) \\ 0 & 1 & -h_k(t_1) & -g_k(t_1) \\ 1 & 0 & -g_k(t_2) & h_k(t_2) \\ 0 & 1 & -h_k(t_2) & -g_k(t_2) \end{bmatrix} \begin{bmatrix} e_{TEC} \\ f_{TEC} \\ R_{TEC} \\ X_{TEC} \end{bmatrix} = \begin{bmatrix} e_k(t_1) \\ f_k(t_1) \\ e_k(t_2) \\ f_k(t_2) \end{bmatrix} \quad (3.5)$$

Solution of (3.5) provides the values of R_{TEC} and X_{TEC}. The magnitude of the Thevenin's equivalent impedance can be expressed as

$$Z_{TEC} = \sqrt{R_{TEC}^2 + X_{TEC}^2} \quad (3.6)$$

The resistance and reactance of the load can be determined using the voltage and current phasors as follows

$$R_k = \frac{e_k(t_2)g_k(t_2)+f_k(t_2)h_k(t_2)}{g_k^2(t_2)+h_k^2(t_2)} \quad (3.7)$$

$$X_k = \frac{f_k(t_2)g_k(t_2)+f_k(t_2)h_k(t_2)}{g_k^2(t_2)+h_k^2(t_2)} \quad (3.8)$$

The magnitude of load impedance can be expressed as

$$Z_k = \sqrt{R_k^2 + X_k^2} \quad (3.9)$$

The values of Z_k and Z_{TEC} becomes equal at the point of voltage collapse. Using this basis, the voltage stability index for k^{th} bus is represented as:

$$VSI_k = 1 - \frac{Z_{TEC}}{Z_k} \quad (3.10)$$

The value voltage stability index VSI_k decreases as the bus approaches the proximity of voltage collapse and it would be zero at the collapse point as at the point of collapse, where, $Z_k = Z_{TEC}$.

.

3.2.2. Voltage stability index based on two consecutive measurements of voltage phasors of interconnected buses and the selected bus

The voltage stability index called equivalent node voltage collapse index (ENVCI) has been proposed using an equivalent local network model (ELNM) of a load bus of a power system, depicted in figure 3.2 [39].

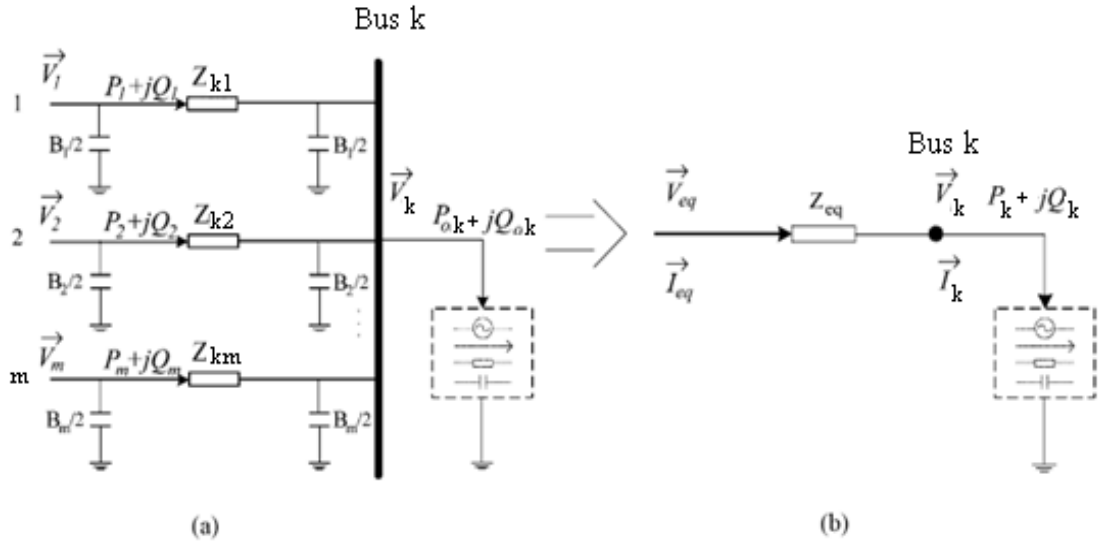

Fig. 3.2. (a) Original local network model; (b) Equivalent local network model(ELNM)

To arrive at ELNM, at first, an equivalent system model (ESM) has been represented as shown in figure 3.3. The ESM is represented using the effect of the transmission lines connected to the selected bus under consideration. Again, the load power delivered at k-bus is represented as P_{on} + jQ_{on}. The $P_n + jQ_n$ is $P_{on} + jQ_{on}$ plus the reactive charging powers at the receiving end of all the

lines at the receiving end.

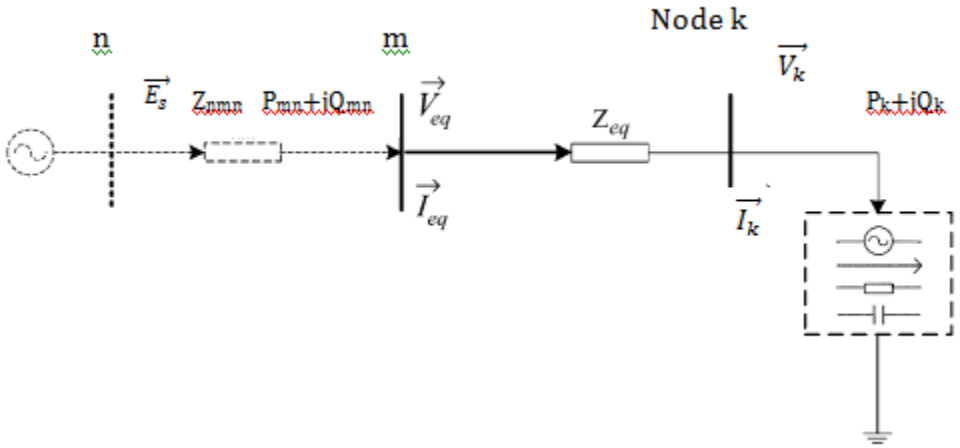

Fig. 3.3 Equivalent system model

The ELNM requires the parameters of the transmission lines connected to the load bus and voltage phasors of the buses that are connected to the load bus. In the figure-3.2 ***k*** represents the bus number of the selected bus, which is connected to other buses of power system through ***m*** number of transmission lines. The equivalent voltage and admittance of the ELNM is represented as [39]

The load power delivered at k-bus is represented as P_{on} + jQ_{on}. The P_n + jQ_n is P_{on} + j Q_{on} plus the reactive charging powers at the receiving end of all the lines at the receiving end.

The equivalent voaltge

$$\overrightarrow{V_{eq}} = V_{eq}\angle\delta_{eq} = \frac{\sum_{i=1}^{m} Y_{ni}\,\vec{V}_i}{\sum_{i=1}^{m} Y_{ni}} \qquad (3.11)$$

Where

$$Y_{ni} = \frac{1}{Z_{ni}} \qquad Y_{eq} = \sum_{i=1}^{m} Y_{ni}$$

here Y_{ni} and Z_{ni} are the admittance and impedance of lines between the nodes i and n respectively; $\overrightarrow{V_i}$and $\overrightarrow{V_k}$ are the voltage phasors at the node i and k; $\overrightarrow{V_k^*}$ is the conjugate phasor of $\overrightarrow{V_k}$; m is the number of lines with power flows entering the node k.

It is obvious that the outgoing current at the node n can be expressed as:

$$\overrightarrow{I_n} = \frac{S_n^*}{\overrightarrow{V_n^*}} = \sum_{i=1}^{m} Y_{ni} \left(\vec{V}_i - \overrightarrow{V_n} \right) = \sum_{i=1}^{m} Y_{ni} \vec{V}_i - \sum_{i=1}^{m} Y_{ni} \overrightarrow{V_n}$$

$$= \sum_{i=1}^{m} Y_{ni} - Y_{eq} \overrightarrow{V_n} \qquad (3.12)$$

S_n^* is the conjugate of complex power at node n

Multiplying the both side of Eq. (3.12) by $\overrightarrow{V_n^*}$, it yields

$$S_n^* = \overrightarrow{V_n^*} \overrightarrow{I_n} = \overrightarrow{V_n^*} \sum_{i=1}^{m} Y_{ni} \vec{V}_i - \overrightarrow{V_n^*} Y_{eq} \overrightarrow{V_n} \qquad (3.13)$$

Representing the equivalent voltage $\overrightarrow{V_{eq}}$ of the ELNM as, we have

$$\overrightarrow{V_{eq}} = \mathrm{V_{eq}} \angle \delta_{eq} = \frac{\sum_{i=1}^{m} Y_{ni} \overrightarrow{V_i}}{\sum_{i=1}^{m} Y_{ni}}$$

Introducing the term $\overrightarrow{V_{eq}}$ in Eq. (3.13), we have

$$S_n^* = (\overrightarrow{V_n^*} \overrightarrow{V_{eq}} - V_n^2) \, Y_{eq} \qquad (3.14)$$

$$\overrightarrow{I_n} = (\overrightarrow{V_{eq}} - \overrightarrow{V_n}) \, Y_{eq} \qquad (3.15)$$

From Eqs. (3.14) and (3.15), an equivalent single line model (i.e., ELNM) which represents the second portion of the local network containing the lines with power
flows entering the node n is obtained as shown in Fig. 3.2(b). In this model, only voltage phasors and line parameters (impedances) of the second portion of the local network are needed. Note that Z_{eq} in the figure is the reciprocal of $Y_{eq.}$

A dummy voltage source $\overrightarrow{E_s}$ with impedance Z_{nm} is added to the ELNM to include the effect of the system outside the local network, as shown in Fig. 3.3. Note that all the grounding branches

representing reactive charging powers at the sending ends of the lines with power flows entering the node k have been assumed to be part of Z_{nm}, which can be estimated later. The $\overrightarrow{E_s}$ and Z_{nm} will have exactly the same effect as the whole system outside the local network as long as they can assure the identical voltage phasors and power flows for the equivalent line. To make this hold, the following equation has to be satisfied:

$$(P_{sn} + JQ_{sn})^* = \overrightarrow{V_{eq}^*} \cdot \frac{\overrightarrow{E_s} - \overrightarrow{V_{eq}}}{Z_{nm}} = \overrightarrow{V_{eq}^*} \cdot \frac{\overrightarrow{V_{eq}} - \overrightarrow{V_k}}{Z_{eq}} \quad (3.16)$$

where, P_{sn} and Q_{sn} are the real and reactive powers flowing into the local network, which corresponds to $\sum_{i=1}^{m}(P_i + JQ_i)$ in Fig. 3.2(a). The Z_{nm} represents the equivalent system impedance that the power flow encountered in the system before it reaches the local network. From Eq. (3.16), the following equations can be derived:

$$V_{eq} \angle -\delta_{eq} \cdot \frac{E_s \angle \delta_s - V_{eq} \angle \delta_{eq}}{Z_{nm}} = V_{eq} \angle -\delta_{eq} \cdot \frac{V_{eq} \angle \delta_{eq} - V_k \angle \delta_k}{Z_{eq}}$$

$$\frac{E_s \angle (\delta_s - \delta_{eq}) - V_{eq}}{Z_{nm}} = \frac{V_{eq} - V_k \angle (\delta_k - \delta_{eq})}{Z_{eq}}$$

$$\frac{Z_{nm}}{Z_{eq}} = \frac{E_s \angle (\delta_s - \delta_{eq}) - V_{eq}}{V_{eq} - V_k \angle (\delta_k - \delta_{eq})}$$

For, $Z_{kn} = Z_{nm} + Z_{eq}$ and a complex coefficient K is represented as

$$K = \frac{Z_{nm} + Z_{eq}}{Z_{eq}} = \frac{Z_{kn}}{Z_{eq}} = \frac{E_s \angle (\delta_s - \delta_{eq}) - V_k \angle (\delta_k - \delta_{eq})}{V_{eq} - V_k \angle (\delta_k - \delta_{eq})} \quad (3.17)$$

Now, $E_s' = E_s' \angle \delta_s' = E_s \angle (\delta_s - \delta_{eq}) \cdot \overrightarrow{V_k'} = V_k' \angle \delta_n' = V_k \angle (\delta_k - \delta_{eq})$ and $V_{eq}' = V_{eq}' \angle 0 = V_{eq}$ in eq.(3.16) , we have

$$E_s' = K \cdot V_{eq}' + (1 - K)\overrightarrow{V_n'} \quad (3.18)$$

It is assumed that the equivalent voltage source $\overrightarrow{E_s'}$ and impedance Z_{nm} are constant between two adjacent system equilibrium states. Therefore, two consecutive measurements having time references t_1 and t_2 Eq. (3.17) can be represented as

$$\overrightarrow{E_s'} = K \cdot V_{eq1}' + (1-K)\overrightarrow{V_{k(t_1)}'} \quad (3.19)$$

$$\overrightarrow{E_s'} = K \cdot V_{eq2}' + (1-K)\overrightarrow{V_{k(t_2)}'} \quad (3.20)$$

Solving Eqs. (3.18) and (3.19), the complex coefficient K can be determined as:

$$K = \frac{1}{1-(V_{eq1}'-V_{eq2}')/\left(\overrightarrow{V_{k(t_1)}'}-\overrightarrow{V_{k(t_2)}'}\right)} \quad (3.21)$$

By substituting K into Eq. (3.18) or (3.19), $\overrightarrow{E_s'}$ can be obtained and then $E_s \angle\theta_s$ can be calculated. With K, it is easy to calculate Z_{kn} from Eq. (3.16):

$$Z_{kn} = \mathrm{K}\, Z_{eq} \quad (3.22)$$

In the above derivation process, a single line ESM is obtained, in which effects of both the local network and the system outside the local network have been established. By using this model, the two key quantities that are needed to calculate the new ENVCI, which is derived in the next subsection, can be either measured or calculated from the node voltage phasors at two ends of the lines in the second portion of the local network. Apparently, the voltage phasor $V_k \angle\theta_k$ at the node N can be directly measured whereas the equivalent source voltage $E_n \angle\theta_n$ can be estimated from the voltage phasors and line parameters through intermediate equivalent voltage phasor $V_{eq} \angle\theta_{eq}$ and equivalent parameter Y_{eq}. It should be emphasized that the ESM derived here is not a single equivalence for the whole system but an equivalence representing the effects of the whole system on a single node (bus) in a specific system state. In other words, each node in a system state corresponds to a different ESM. These ESMs of individual nodes are used to calculate their ENVCI indices

$$ENVCI_k = 2\left(e_{k(t_2)}e_s - f_{k(t_2)}f_s\right) + \left(e_s^2 - f_s^2\right) \quad (3.23)$$

The value of voltage stability index $ENVSI_k$ decreases as the bus approaches the proximity of voltage collapse and it becomes zero at the point of collapse.

3.3 Simulations and results

To examine the performance and characteristic behaviour of the PMU measurement based indices described in section-3.2, simulations were carried out in IEEE 30 and IEEE 118 bus systems. The single line diagram, network data and the base case load flow results for of IEEE 30 and IEEE 118 bus systems are presented in Appendix. Continuation load flow analysis described in chapter-2 is used to determine the two consecutive voltage and current phasors along the PV curve and around the proximity of voltage collapse of the selected load buses of the IEEE systems. Several busses for IEEE 30 and IEEE 118 bus systems were considered for simulations. Buses with different loading capabilities were investigated during simulations.

Several busses of IEEE 30 and IEEE 118 bus systems were considered for simulations. However, results for some of buses of the systems were presented. The buses with different loading bearing capability of the systems were included in thesis to highlight the variation of the indices for buses with different loading bearing capability. The simulations were carried out to verify the nature of change of both VSIs for same load variation using a continuation load flow, where load are increased gradually to drive the systems toward the system collapse.

The simulation results of IEEE 30 and IEEE 118 bus systems are presented in table-3.1 and table-3,2 respectively,

Table 3.1: Phasor measurement based VSI for IEEE 30 bus system

load bus 29 of IEEE 30 bus system		load bus 21 of IEEE 30 bus system		load bus 7 of IEEE 30 bus system

P_{Dk}	VSI_k	$ENVCI_k$	P_{Dk}	VSI_k	$ENVCI_k$	P_{Dk}	VSI_k	$ENVCI_k$
0.063	0.9521	0.9217	0.3224	0.9238	0.9134	0.6138	0.9293	0.9256
0.0843	0.9325	0.894	0.4292	0.8932	0.8811	0.8273	0.9011	0.9002
0.1109	0.9047	0.8567	0.5601	0.8502	0.8372	1.0982	0.8618	0.8653
0.1425	0.865	0.8071	0.7116	0.79	0.7787	1.4276	0.8073	0.818
0.1778	0.8083	0.7424	0.8732	0.7063	0.7025	1.8043	0.7323	0.7549
0.2136	0.7277	0.6608	1.0266	0.592	0.6066	2.1989	0.6312	0.6728
0.2456	0.6153	0.5622	1.1504	0.444	0.4918	2.5644	0.5005	0.57
0.2699	0.4682	0.4502	1.2301	0.2717	0.3642	2.8497	0.3441	0.4485
0.2848	0.2995	0.3331	1.2677	0.1075	0.2366	3.0244	0.1795	0.3163
0.2919	0.1445	0.2234	1.2791	-0.0017	0.127	3.0989	0.0383	0.1884
0.2946	0.0473	0.1343	1.281	-0.0354	0.0519	3.116	-0.0433	0.0843
0.2953	0	0.0707	1.2811	-0.0064	-0.0061	3.1168	-0.0526	0.0188
0.2955	-0.0111	0.0321				3.1169	-0.017	-0.0012
0.2956	-0.1121	-0.118						

Table 3.2: Phasor measurement based VSI for IEEE 118 bus system

load bus 118 of IEEE 118 bus system			load bus 88 of IEEE 118bus system			load bus 45 of IEEE 118bus system		
P_{Dk}	VSI_k	$ENVCI_k$	P_{Dk}	VSI_k	$ENVCI_k$	P_{Dk}	VSI_k	$ENVCI_k$
0.609	0.9461	0.8713	0.8975	0.8845	0.9166	0.7154	0.8997	0.9154
0.8121	0.924	0.8431	1.2079	0.8397	0.8897	0.9692	0.8607	0.8964
1.063	0.8927	0.8051	1.599	0.7787	0.8524	1.2961	0.8076	0.8704

1.3573	0.848	0.7546		2.0681	0.6972	0.8012		1.7031	0.7364	0.835
1.6781	0.7842	0.6891		2.5927	0.5922	0.7323		2.1861	0.644	0.7878
1.994	0.6939	0.6068		3.1234	0.465	0.6421		2.7226	0.5301	0.7261
2.2649	0.57	0.5084		3.591	0.3241	0.5288		3.269	0.4011	0.6477
2.4591	0.4134	0.3983		3.9299	0.1832	0.3954		3.7659	0.2704	0.5523
2.5702	0.2451	0.2863		4.1098	0.0529	0.2509		4.1569	0.1536	0.4418
2.6194	0.1062	0.1855		4.1516	-0.0129	0.0579		4.4103	0.0593	0.3222
2.636	0.0261	0.1073		4.1534	-0.0197	0.0243		4.5322	-0.0118	0.2029
2.6405	-0.003	0.056		4.1537	-0.0083	-0.0016		4.5648	-0.0572	0.0966
2.6414	-0.0071	0.0271						4.5649	-0.0737	0.0091
2.6417	-0.0016	0.0055						4.565	0.0011	0.0021
2.6418	-0.0003	0.0013								
2.6419	0.0766	-0.016								

The nature of variation of VSI and ENVCI for selected buses of IEEE 30 bus and IEEE 118 bus systems are presented in figure-3.4 to figure-3.9.

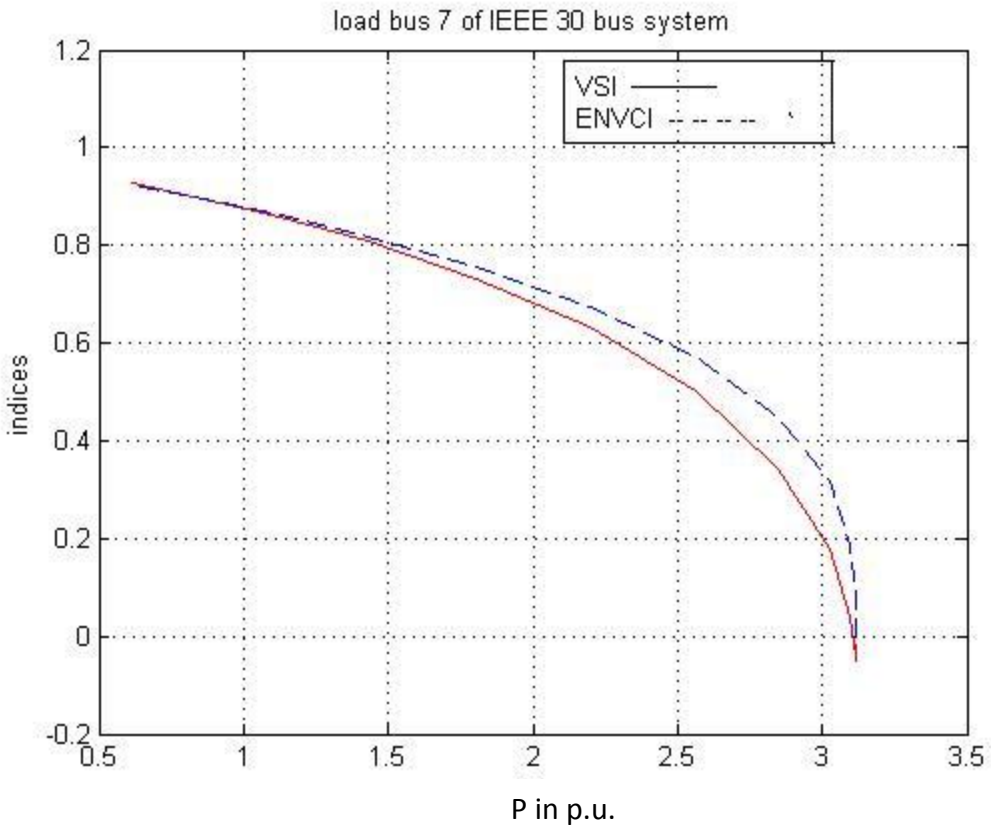

Figure 3.4: Nature of variation of indices VSI and ENVCI of bus-7 of IEEE 30 bus system determined by using two consecutive bus phasors variables provided by the load increment steps of the continuation load flow analysis.

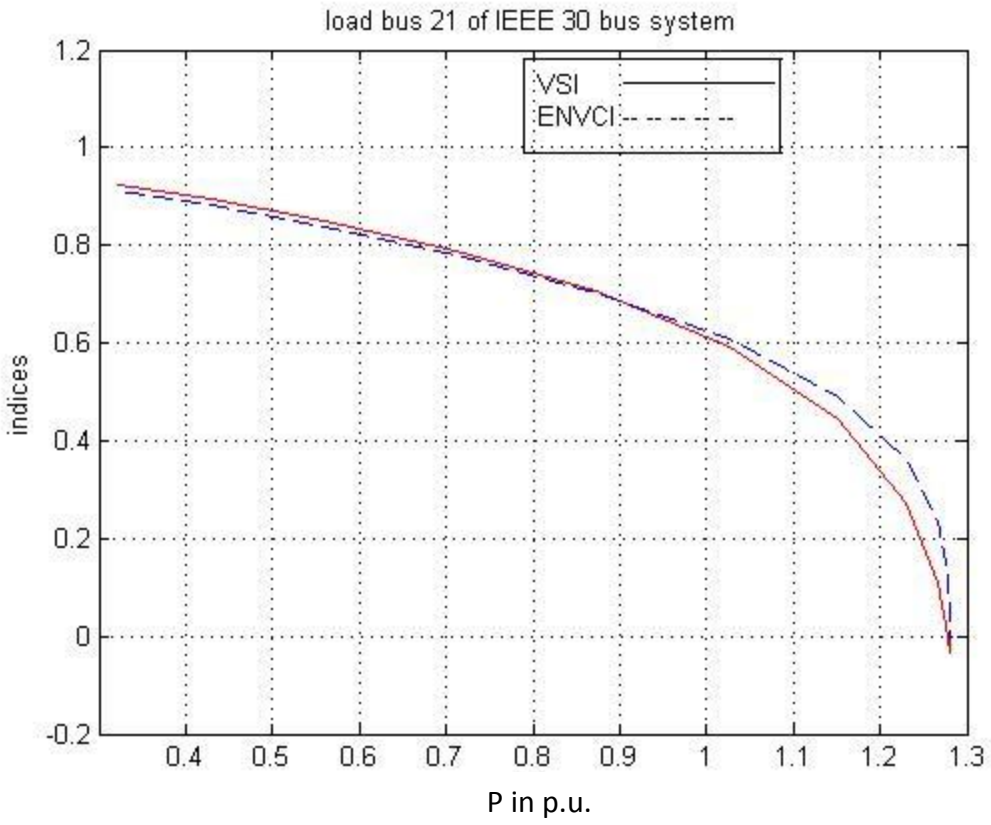

Figure 3.5: Nature of variation of indices VSI and ENVCI of bus-21 of IEEE 30 bus system determined by using two consecutive bus phasors variables provided by the load increment steps of the continuation load flow analysis.

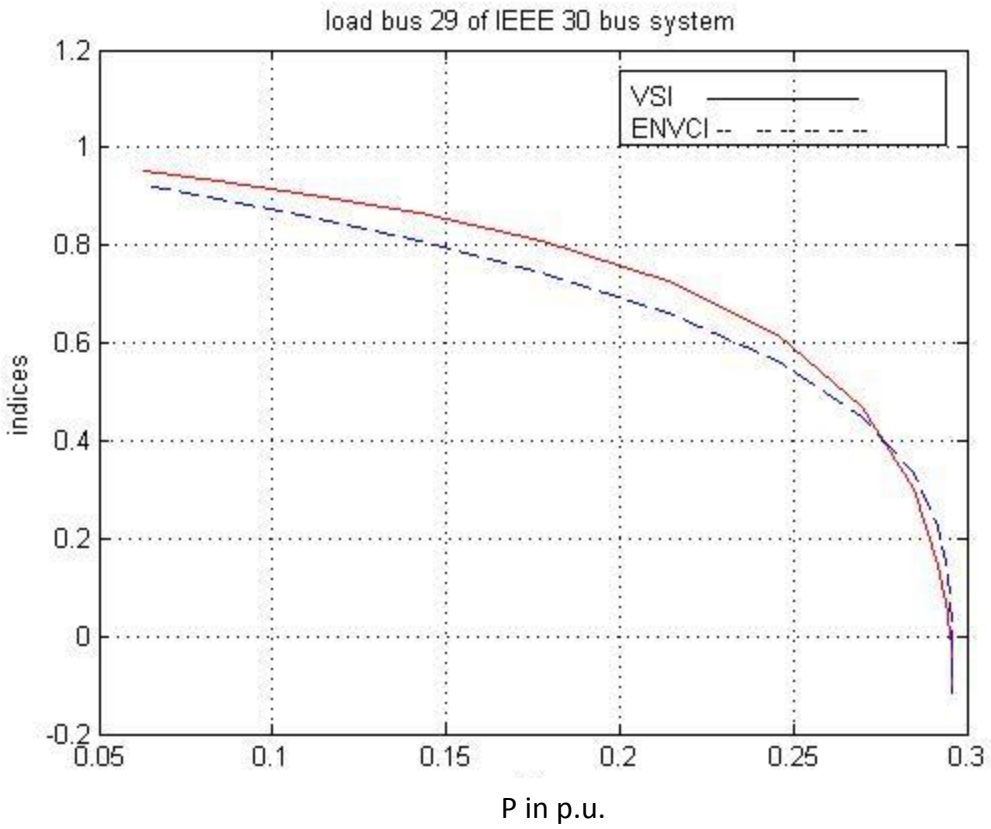

Figure 3.6: Nature of variation of indices VSI and ENVCI of bus-29 of IEEE 30 bus system determined by using two consecutive bus phasors variables provided by the load increment steps of the continuation load flow analysis.

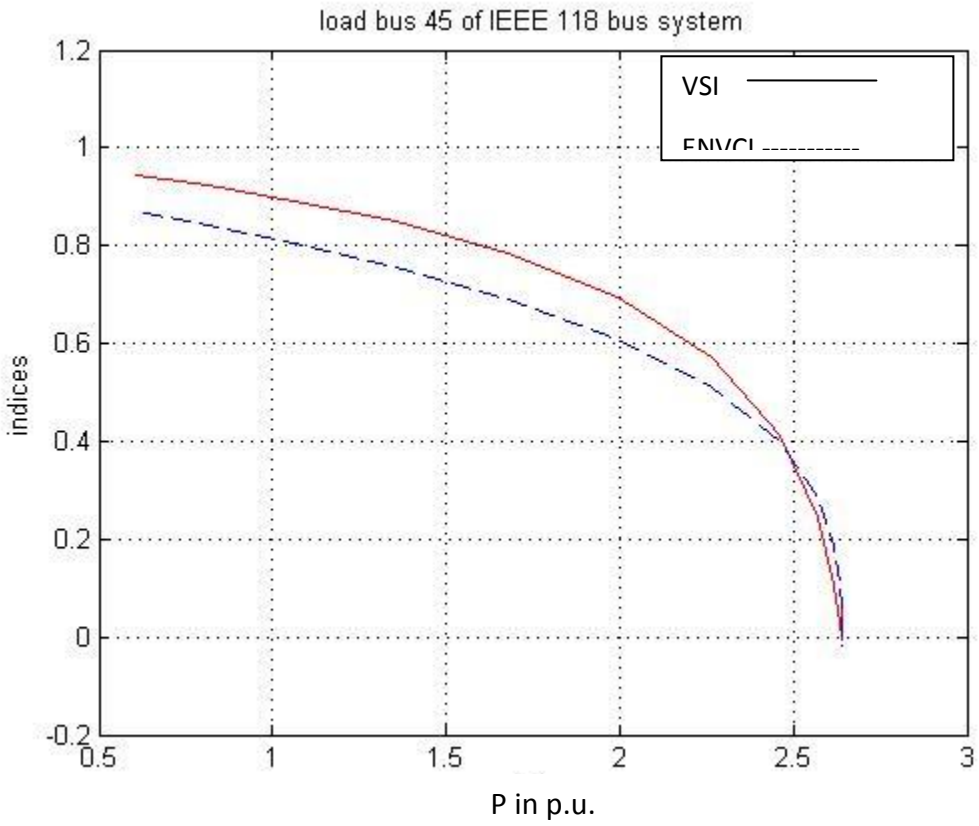

Figure 3.7: Nature of variation of indices VSI and ENVCI of bus-45 of IEEE 118 bus system determined by using two consecutive bus phasors variables provided by the load increment steps of the continuation load flow analysis.

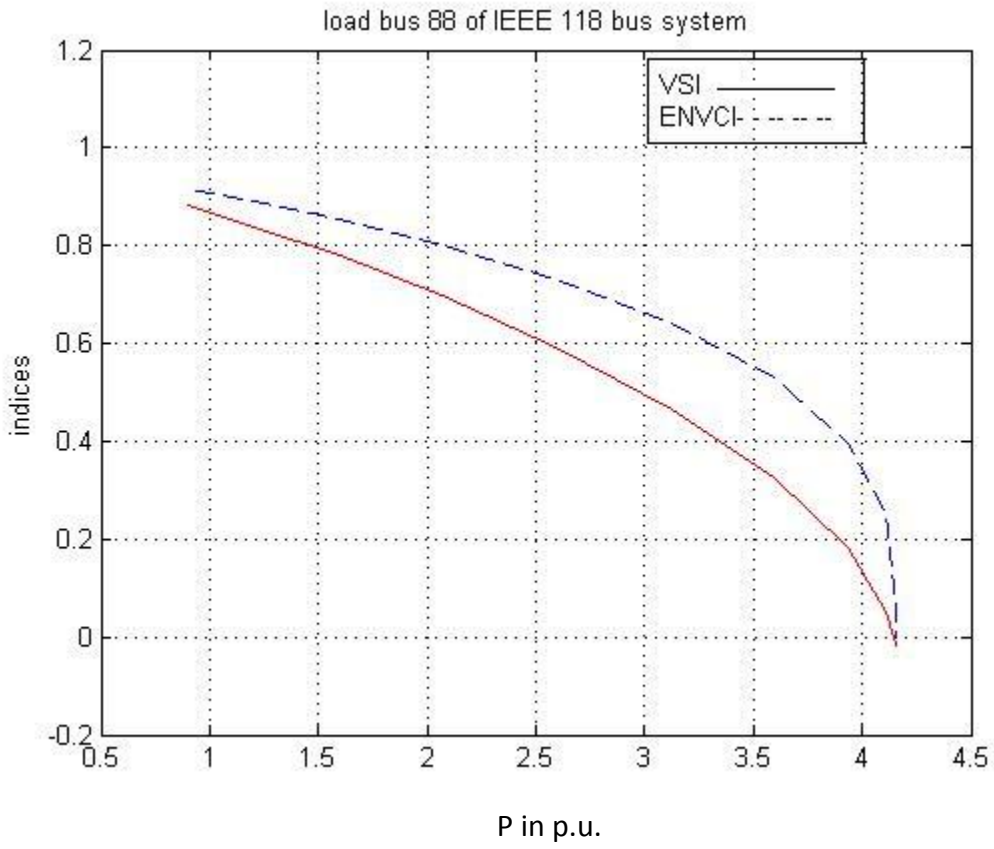

Figure 3.8: Nature of variation of indices VSI and ENVCI of bus-88 of IEEE 118 bus system determined by using two consecutive bus phasors variables provided by the load increment steps of the continuation load flow analysis.

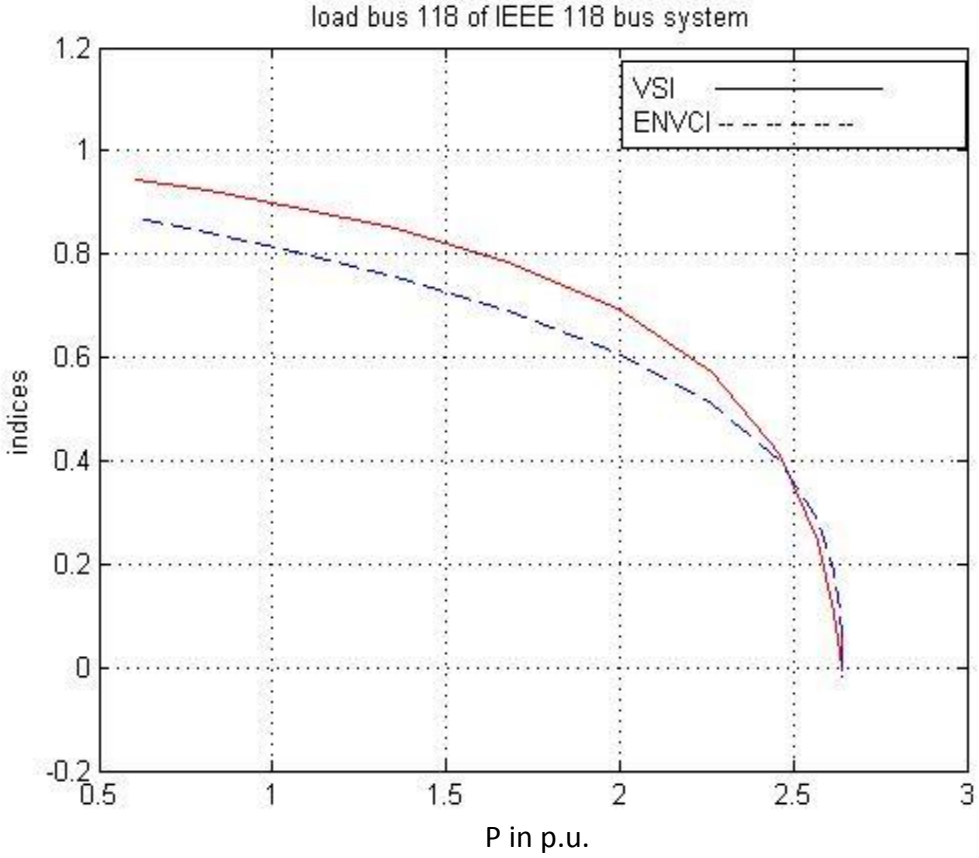

Figure 3.9: Nature of variation of indices VSI and ENVCI of bus-118 of IEEE 118 bus system determined by using two consecutive bus phasors variables provided by the load increment steps of the continuation load flow analysis.

Simulations carried out on IEEE 30 and IEEE 118 bus systems indicated that indices VSI and ENVCI decrease with increase in load and as the bus approaches the proximity of voltage collapse variation of indices becomes sharp. They become 0 at the point of voltage collapse. Further, it has been observed that variation of the indices with respect to change in load exhibit similar trend for all the buses. However, for a bus having higher load around the proximity of voltage collapse, nature of variation of VSI and ENVSI differed. For example, Bus-7 of IEEE 30 bus system and bus-88 of IEEE 118 bus system showed load around the proximity of voltage collapse as 3.1p.u. and 4.1 p.u. respectively. For these two cases, load margin for same value of VSI and ENVCI differs significantly, especially when the bus approaches the proximity of collapse. VSI shows more load margin than ENVCI for these buses.

1.4 Conclusion

It has been observed from simulation results presented in this thesis for IEEE 30 and IEEE 118 bus system that both indices are reliable in offering the measure of voltage stability condition of a bus. The bus becomes vulnerable to voltage instability problem as the indices approach zero. At the point of collapse both indices become zero as claimed by the authors in their papers. However, indices showed different values for same load margin.

Chapter- 4

Use of bus measurements to analyze voltage stability problem of a power system

4.1 Introduction:

The phasor measurement technology has been developing since the end of the 1980s. The advances in embedded system technology, networking infrastructure and communications, have created new perspectives for designing wide-area monitoring, detection, protection and control of power systems. The Phasor Measurement Unit (PMU) hardware is now based on proven technology and is considered as the most accurate and advanced time-synchronized technology available to power engineers. Voltage and current phasors of a bus contain sufficient information to develop mathematical model(s) for analysing its characteristic behaviour or respond to the load change at the bus. PMU is a costly device, for example a low-cost PMU such as SEL-487E PMU cost about $5750.00. In addition to this, time synchronization of the phasor variables invites continuous operating cost and is somehow dependent on remote measurement.

This chapter proposes a method to determine impedance of a Two Bus Equivalent Circuit (TBEC) of an interconnected power system with respect to a target/selected load bus, using two consecutive measurements of real power, reactive power and voltage magnitude of the target/selected bus. The condition of maximum power transfer theorem is used to determine the voltage stability condition of the power system using its TBEC and load parameters [57]. The measurements of real power, reactive power and bus voltage magnitude at a bus could be extracted / captured from a Smart Energy Meter (SEM). SEM is available in the price range of $8.00–$500.00. Again, the proposed method is independent of remote measurement and also does not invite any type of continuous operating cost. Therefore, the financial involvement for

implementation of the proposed method would be significantly lower compared with that of PMU-based method.

4.2 Proposed method for voltage stability analysis of an interconnected power system using real power, reactive power and voltage magnitudes of a bus

It is proposed to use measurements of - (i) real power (ii) reactive power and (iii) bus voltage magnitude of a bus for analysis of voltage stability condition of the bus. Again these variables can be captured by a simple smart energy meter, as they are non-phasor quantities. Since, bus voltage magnitude (without the phase angle associated with the bus voltage) is needed for the proposed method; therefore, the k^{th} bus (under consideration) is treated as a reference bus (i.e. $\delta_k = 0$). The TBEC of an interconnected power system with respect to a target bus k is represented as shown in Fig. 4.1. R_{TBEC} and X_{TBEC} are the equivalent resistance and reactance of the TBEC.

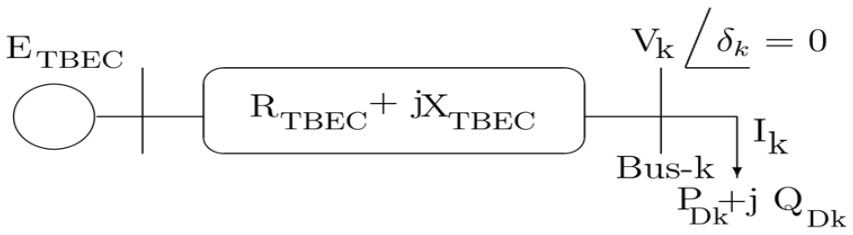

Fig. 4.1: TBEC of an interconnected power system with respect to a target bus k

In the proposed method, the voltage magnitude at the k^{th} bus will be measured,
That is, voltage magnitude at the k^{th} bus would be a known variable. Therefore voltage of the k^{th} bus is taken as reference (i.e. $\delta_k = 0$), where R_{TBEC} and X_{TBEC} are the equivalent resistance and reactance of the TBEC. The equivalent source voltage of TBEC can be expressed as

$$\begin{aligned}\bar{E}_{TBEC} &= e_{TBEC} + j\, f_{TBEC} \\ &= \overline{V_k} + (R_{TBEC} + jX_{TBEC})\, \bar{I}_k \\ &= e_k + j\,0 + (R_{TBEC} + j\,X_{TBEC})\, \bar{I}_k \end{aligned} \quad (4.1)$$

As, the k^{th} bus is considered as the reference bus, the voltage at k^{th} bus can be represented as:

$\overline{V_k} = V_k \angle\delta_k = V_k \angle 0 = V_k$

and $\overline{V_k^*} = V_k$

Applying this condition in equation (4.1), we have

$$\bar{E}_{TBEC} = V_k + (R_{TBEC} + jX_{TBEC}) \bar{I}_k \quad (4.2)$$

Using the measurement variables – real power, reactive power and voltage magnitude at the k^{th} bus for time instant t, the current from the source to load of the TBEC can be expressed as

$$\bar{I}_k(t) = \frac{P_{Dk}(t) - j\, Q_{Dk}(t)}{\overline{V_k}*(t)} \quad (4.3)$$

Since, voltage at the k^{th} bus is the reference voltage; equation (4.3) can be expressed

$$\bar{I}_k(t) = \frac{P_{Dk}(t) - j\, Q_{Dk}(t)}{V_k(t)} = \frac{P_{Dk}(t)}{V_k(t)} - j\frac{Q_{Dk}(t)}{V_k(t)} \quad (4.4)$$

Thus, the expression for the source voltage for the TBEC can be expressed as

$$\bar{E}_{TBEC} = V_k(t) + \bar{Z}_{TBEC}\bar{I}_K(t)$$

$$= V_k(t) + \left(\frac{P_{Dk}(t)}{V_k(t)} - j\frac{Q_{Dk}(t)}{V_k(t)}\right)(R_{TBEC} + jX_{TBEC}) \quad (4.5)$$

Now, using the measurements of real power, reactive power and voltage magnitude at the k^{th} bus for two consecutive time instances t_1 and t_2, (4.5) can be expressed as

$$\bar{E}_{TBEC} = V_k(t_1) + \left(\frac{P_{Dk}(t1)}{V_k(t1)} - j\frac{Q_{Dk}(t1)}{V_k(t1)}\right)(R_{TBEC} + jX_{TBEC}) \quad (4.6)$$

$$\bar{E}_{\text{TBEC}} = V_k\,(t_2) + \left(\frac{P_{Dk}\,(t2)}{V_k(t2)} - j\,\frac{Q_{Dk}\,(t2)}{V_k(t2)}\right)(R_{TBEC} + jX_{TBEC}) \quad (4.7)$$

Equating (4.6) and (4.7) for real and imaginary component of E_{TBEC}, the expressions for resistance (R_{TBEC}) and reactance (X_{TBEC}) of the TBEC can be written as

$$R_{TBEC} = \frac{V_k(t_1) - V_k(t_2)}{\left[\left(\frac{Q_{Dk}(t_2)}{V_k(t_2)} - \frac{Q_{Dk}(t_1)}{V_k(t_1)}\right)^2 / \left(\frac{P_{Dk}(t_2)}{V_k(t_2)} - \frac{(P_{Dk}\,t_1)}{V_k(t_1)}\right] + \left[\frac{Q_{Dk}(t_2)}{V_k(t_2)} - \frac{Q_{Dk}(t_1)}{V_k(t_1)}\right]} \quad (4.8)$$

$$X_{TBEC} = \frac{\frac{Q_{Dk}(t_2)}{V_k(t_2)} - \frac{Q_{Dk}(t_1)}{V_k(t_1)}}{\frac{P_{Dk}(t_2)}{V_k(t_2)} - \frac{P_{Dk}(t_1)}{V_k(t_1)}} R_{TBEC} \quad (4.9)$$

Therefore the magnitude of the impedance of the TBEC is

$$Z_{TBEC} = \sqrt{R_{TBEC}^2 + X_{TBEC}^2} \quad (4.10)$$

Again, using the bus measurement variables – P_{Dk}, Q_{Dk} and V_k, the values of R_k, X_k and Z_k could be determined by the following equations

$$R_k = \frac{V_k^2(t_2)P_{Dk}(t_2)}{P_{Dk}^2(t_2)+Q_{Dk}^2(t_2)} \quad (4.11)$$

$$X_k = \frac{V_k^2(t_2)Q_{Dk}(t_2)}{P_{Dk}^2(t_2)+Q_{Dk}^2(t_2)} \quad (4.12)$$

$$Z_k = \sqrt{R_k^2 + X_k^2} \quad (4.13)$$

4.3 Condition for voltage collapse at kth node of TBEC

The voltage collapse of a power system takes place when the maximum power is transferred by the source of the TBEC to the selected bus. The power delivered to the kth bus can be expressed as

$$P_{Dk} = |I_{Dk}|^2 R_k = |I_K|^2 R_k$$

$$= \left| \frac{E_S}{\sqrt{(R_k+R_{TBEC})2+(X_k+X_{TBEC})2}} \right|^2 R_k$$

$$= \frac{E_S}{(Z_k\, cos\phi_k+R_{TBEC})2+(Z_k \sin\phi_k+X_{TBEC})2} Z_k \cos\phi_k \qquad (4.14)$$

where cos φ_k is the power factor of the load at the kth bus. To deliver maximum power to the kth bus by the TBEC

$$\frac{dP_{Dk}}{dZ_k} = 0 \qquad (4.15)$$

It yields

$$\cos\phi_k[(Z_k\, cos\phi_k + R_{TBEC})2 + (Z_k \sin\phi_k + X_{TBEC})2\,] = Z_k \cos\phi_k\, [2R_{TBEC} \cos\phi_k + 2Z_k \cos\phi_k^2 + [2X_{TBEC} \sin\phi_k + 2Z_k \sin\phi_k^2] \qquad (4.16)$$

$$(R_{TBEC}^2 + X_{TBEC}^2) \cos\phi_k + 2R_{TBEC}\, Z_k \cos\phi_k^2 + Z_k^2 \cos\phi_k^3 + 2X_{TBEC}\, Z_k \sin\phi_k\, cos\phi_k + 2Z_k^2 \sin\phi_k^2\, cos\phi_k$$

$$= 2R_{TBEC}\, Z_k \cos\phi_k^2 + 2Z_k^2 \cos\phi_k^3 + 2\, X_{TBEC}\, Z_k \sin\phi_k + 2Z_k^2 \sin\phi_k^2\, cos\phi_k \qquad (4.17)$$

$$(R_{TBEC}^2 + X_{TBEC}^2) \cos\phi_k = Z_k \cos\phi_k^3 + 2Z_k^2 \sin\phi_k^2 \cos\phi_k \qquad (4.18)$$

$$(R_{TBEC}^2 + X_{TBEC}^2) \cos\phi_k = [(Z_k \cos\phi_k^2) + (Z_k \sin\phi)^2\,]\, cos\phi_k \qquad (4.19)$$

$$R_{TBEC}^2 + X_{TBEC}^2 = (Z_k \cos \phi_k^2) + (Z_k \sin\phi)^2 \quad (4.20)$$

$$R_{TBEC}^2 + X_{TBEC}^2 = R_k^2 + X_k^2 \quad (4.21)$$

Equation (4.21) can be expressed as

$$(R_{TBEC} + jX_{TBEC})(R_{TBEC} - jX_{TBEC}) = (R_k + j X_k)(R_k - j X_k) \quad (4.22)$$

From (4.22) it is found that at the point of collapse

$$R_{TBEC} = R_k \text{ and } X_{TBEC} = X_k$$

Again (4.21) can be represented as

$$Z_{TBEC}^2 = Z_k^2 \quad (4.23)$$

Thus at the point of collapse

$$Z_{TBEC} = Z_k \quad (4.24)$$

Therefore it could be concluded that, at the point of collapse, the load and TBEC parameters would have the relation given below

$$R_{TBEC} = R_k \text{ , } X_{TBEC} = X_k \text{ and } Z_{TBEC} = Z_k \quad (4.25)$$

A VSI could be defined using the ratio of R_k and R_{TBEC} or X_k and X_{TBEC} or Z_k and Z_{TBEC} to monitor voltage stability condition of the k^{th} bus.

Therefore values Z_k and Z_{TBEC} are used to represent the VSI as follows

$$VSI_{TBEC} = 1 - \frac{Z_{TBEC}}{Z_K} \quad (4.26)$$

As the bus approaches to the point of collapse, Z_{TBEC} also closes to Z_K, therefore, the value of VSI_{TBEC} reduces. At the point of collapse $Z_{TBEC} = Z_K$ and VSI_{TBEC} becomes zero.

4.4 Simulation and result

To illustrate the difference between parameters of TBEC and parameters of TEC with respect to a selected or target bus k of a power system, the sample 2-bus system depicted in Fig. 4.2 is adopted.

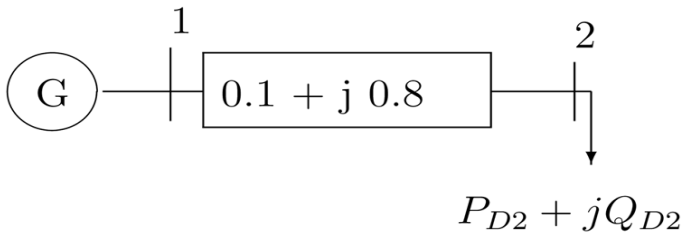

Figure.4.2: A sample two bus test system.

To examine the trend of change of the parameters of the TBEC and TEC for change in load, continuation power flow analysis is used with a step size σ = 0.001. Two consecutive load increment steps of the continuation load flow analysis are taken as the time instances t_1 and t_2, respectively, and accordingly $P_{D2(t1)}$, $Q_{D2(t1)}$, $V_{2(t1)}$, $e_{2(t1)}$, $f_{2(t1)}$, $g_{2(t1)}$, $h_{2(t1)}$, $P_{D2(t2)}$, $Q_{D2(t2)}$, $V_{2(t2)}$), $e_{2(t2)}$), $f_{2(t2)}$), $g_{2(t2)}$ and $h_{2(t2)}$) are determined for the load bus. Using the variables $P_{D2(t1)}$, $Q_{D2(t1)}$, $V_{2(t1)}$, $P_{D2(t2)}$, $Q_{D2(t2)}$ and $V_{2(t2)}$, the parameters R_{TBEC}, X_{TBEC} and Z_{TBEC} of T_{BEC} are calculated using equations 4.8-4.10, also, using the same variables the parameters R_k, X_k and Z_k of load are calculated using Eq.4.11-4.13. Similarly, using the phasor variables $e_2(t_1)$, $f_2(t_1)$, $g_2(t_1)$, $h_2(t_1)$, $e_2(t_2)$, $f_2(t_2)$, $g_2(t_2)$ and $h_2(t_2)$, the parameters R_{TEC}, X_{TEC} and Z_{TEC} of TEC are calculated using Eq.3.5 and 3.6, also, using the same measurement variables, load parameters R_k, X_k and Z_k are calculated using Eq.3.7 -3.9. Fig. 4.3 represents the trend of change of R_{TBEC}, X_{TBEC}, Z_{TBEC}, R_k, X_k and Z_k and Fig.4.4 represents the trend of change of R_{TEC}, X_{TEC}, Z_{TEC}, R_k, X_k and Z_k.

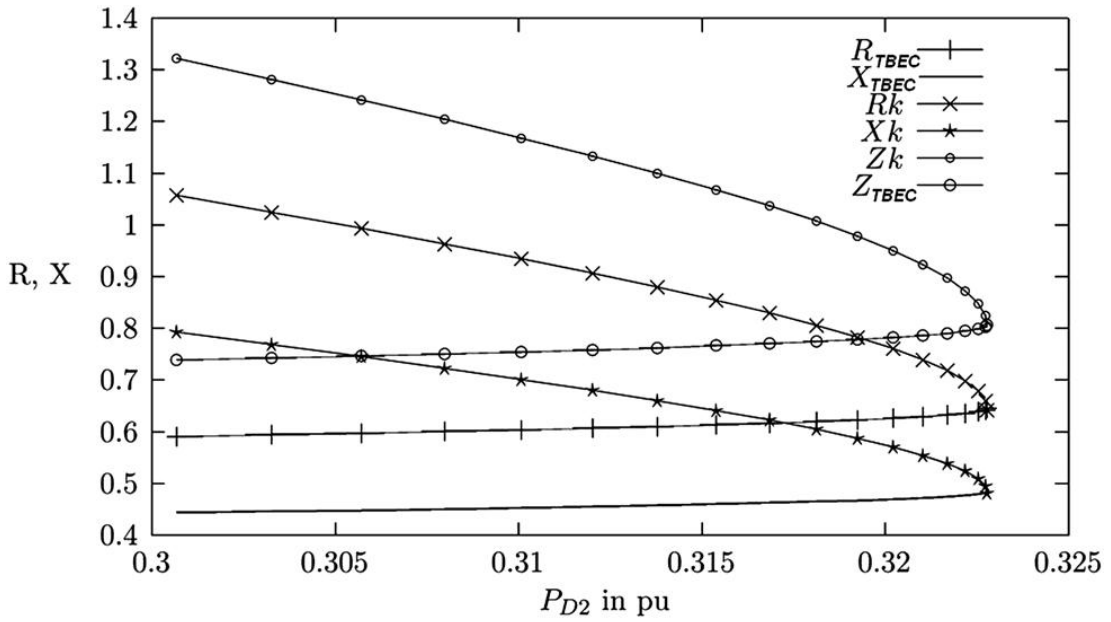

Fig. 4.3 Variation of TBEC parameters for change in load at bus-2 for sample 2-bus system

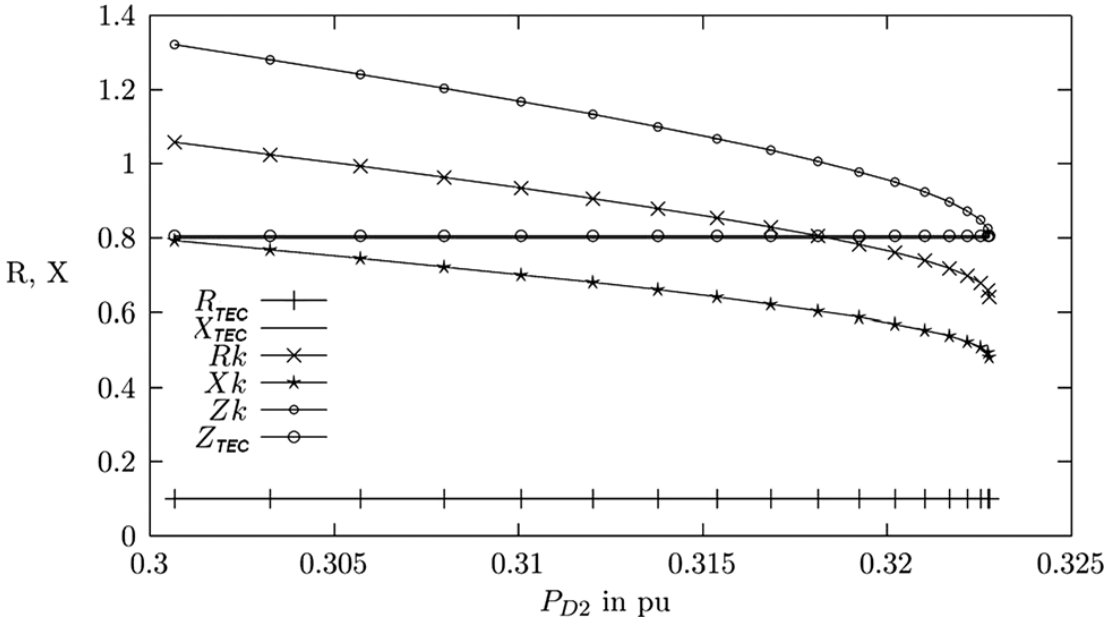

Fig. 4.4 Variation of TEC parameters for change in load at bus-2 for sample 2-bus system

It is observed from Fig. 4.4 that the values of R_{TEC}, X_{TEC} and Z_{TEC} determined using (3.5) and (3.6) with current and voltage phasors for two consecutive time instances t_1 and t_2 remain the same as the R_{TEC} = 0.1, X_{TEC} = 0.8 and Z_{TEC} = $\sqrt{0.1^2 + 0.8^2}$ = 0.80623 during continuation load

flow load increment steps. In fact, according to Thevenin's theorem, $R_{12} = 0.1$, $X_{12} = 0.8$ and $Z_{12} = \sqrt{0.12 + 0.82} = 0.80623$ are the Thevenin's resistance, reactance and impedance of the 2-bus system. Simulation on 2-bus system confirmed that at any loading condition the values of R_{TEC}, X_{TEC} and Z_{TEC} remain same as R_{12}, X_{12} and Z_{12}, respectively. Thus, the phasor measurement method provides the Thevenin's equivalent impedance of the circuit. However, the equivalent resistance, reactance and impedance of the TBEC are different from Thevenin's equivalent resistance, reactance and impedance, respectively. However, at the point of voltage collapse Z_{TEC} becomes equal to Z_k for the TEC, whereas R_{TBEC}, X_{TBEC} and Z_{TBEC} of TBEC circuit become equal to R_k, X_k and Z_k, respectively, as shown in Section 4.3. Therefore, both methods can provide information about the voltage stability condition of a power system.

Simulations were carried out on IEEE 30 and IEEE 118 bus systems. Two consecutive load increment steps of the continuation load flow analysis are taken as the time instances t_1 and t_2, respectively. Using voltage and current phasors for the two instances of continuation load flow analysis, the Thevenin's equivalent parameters and load parameters are determined for the selected buses.

Using voltage magnitude, real and reactive loads for the two instances of continuation load flow analysis, the equivalent parameters for TBEC and load parameters are determined for the selected buses.

Figs. 4.5–4.10 illustrate the variation of R_{TBEC}, X_{TBEC} and Z_{TBEC} of TBEC, R_{TEC}, X_{TEC} and Z_{TEC} of TEC and R_k, X_k and Z_k for the buses 29, 21 and 7 of the IEEE 30 bus system with respect to change in load (P_{Dk}) at 29, 21 and 7 individually with load power factor 0.8. Figs. 4.11 – 4.16 illustrate the variation R_{TBEC}, X_{TBEC} and Z_{TBEC} of TBEC, R_{TEC}, X_{TEC} and Z_{TEC} of TEC and R_k, X_k and Z_k for the buses 118, 88 and 76 of the IEEE 118 bus system with respect to change in load (P_{Dk}) at 118, 88 and 76 individually with load power factor 0.

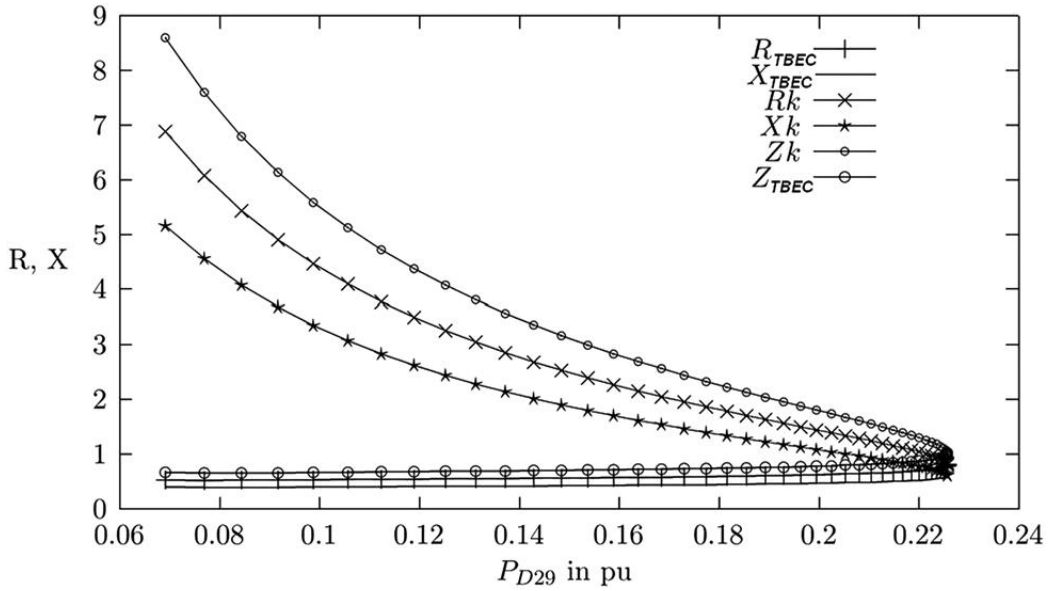

Fig. 4.5 Variation of TBEC parameters for change in load at bus-29 for IEEE30 bus system

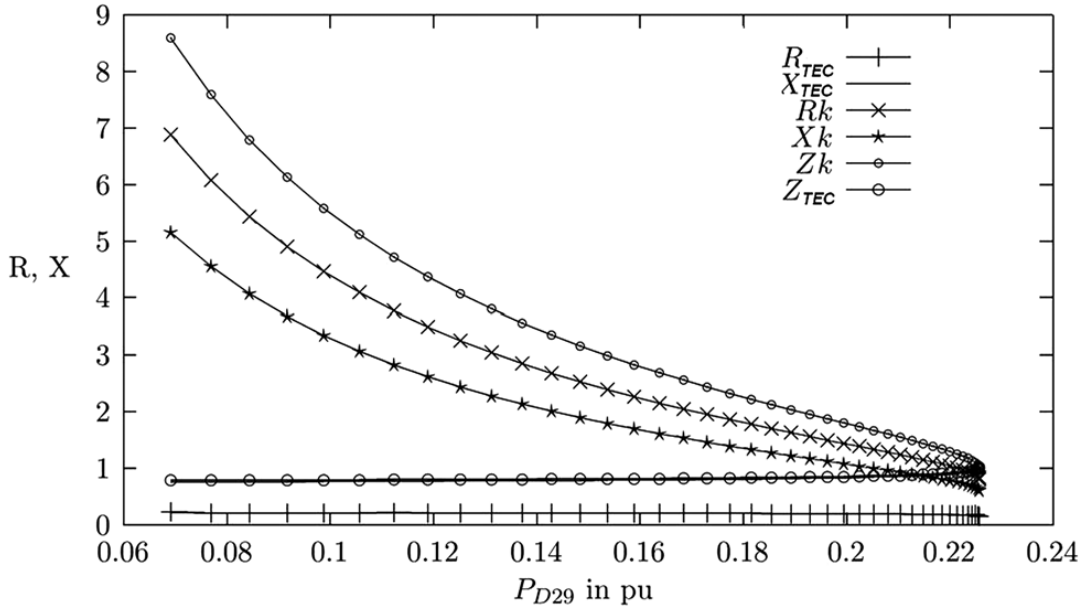

Fig. 4.6 Variation of TEC parameters for change in load at bus-29 for IEEE 30 bus system

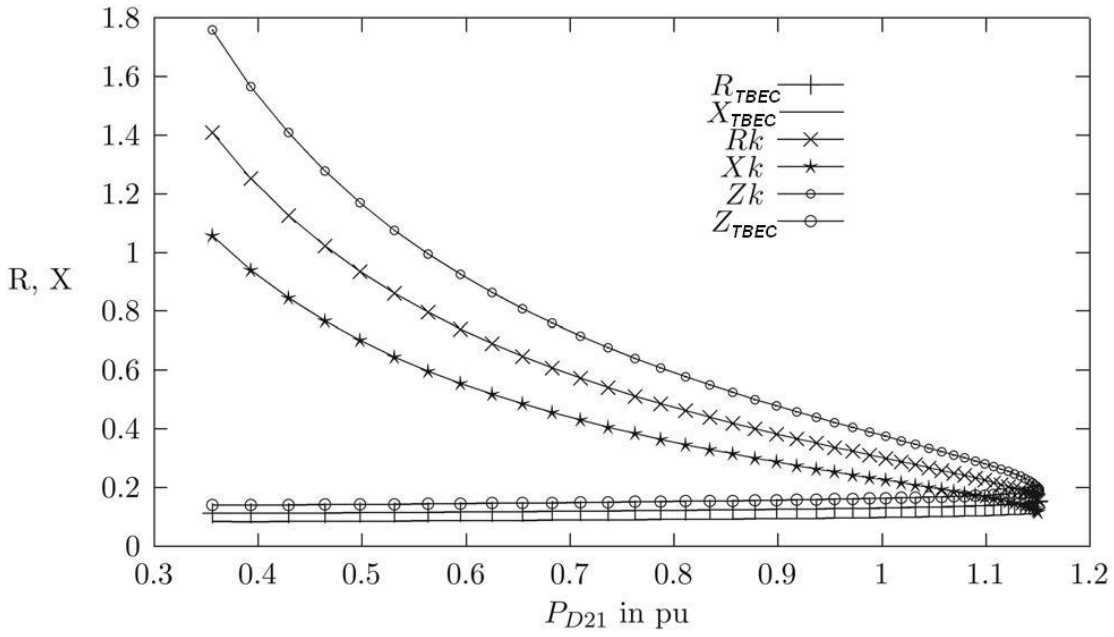

Fig. 4.7

Variation of TBEC parameters for change in load at bus-21 for IEEE30 bus system

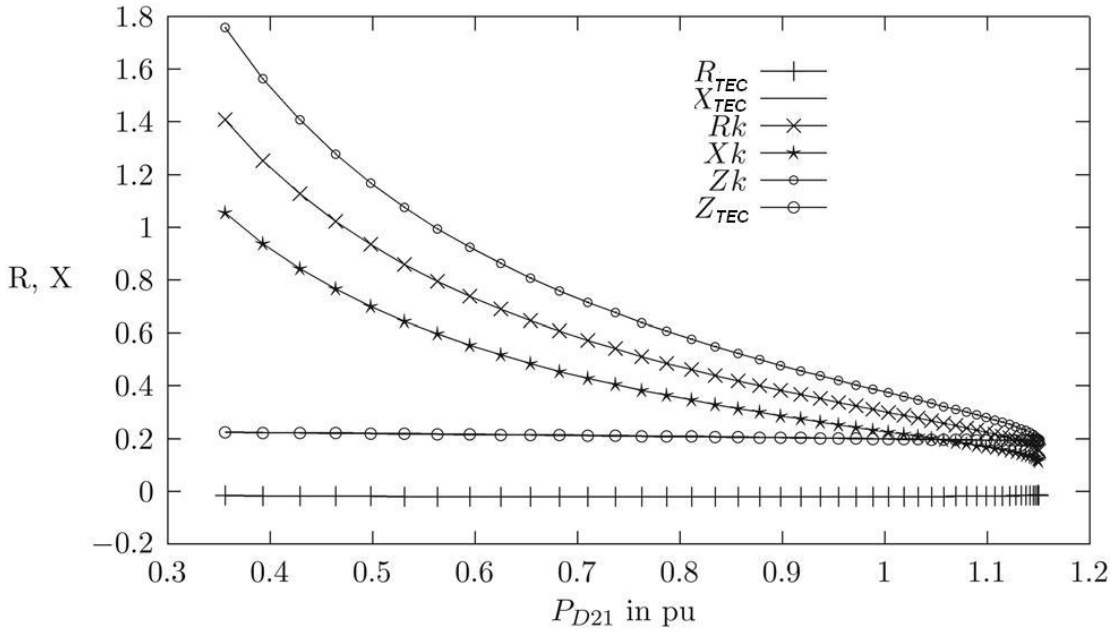

Fig. 4.8

Variation of TEC parameters for change in load at bus-21 for IEEE 30 bus system

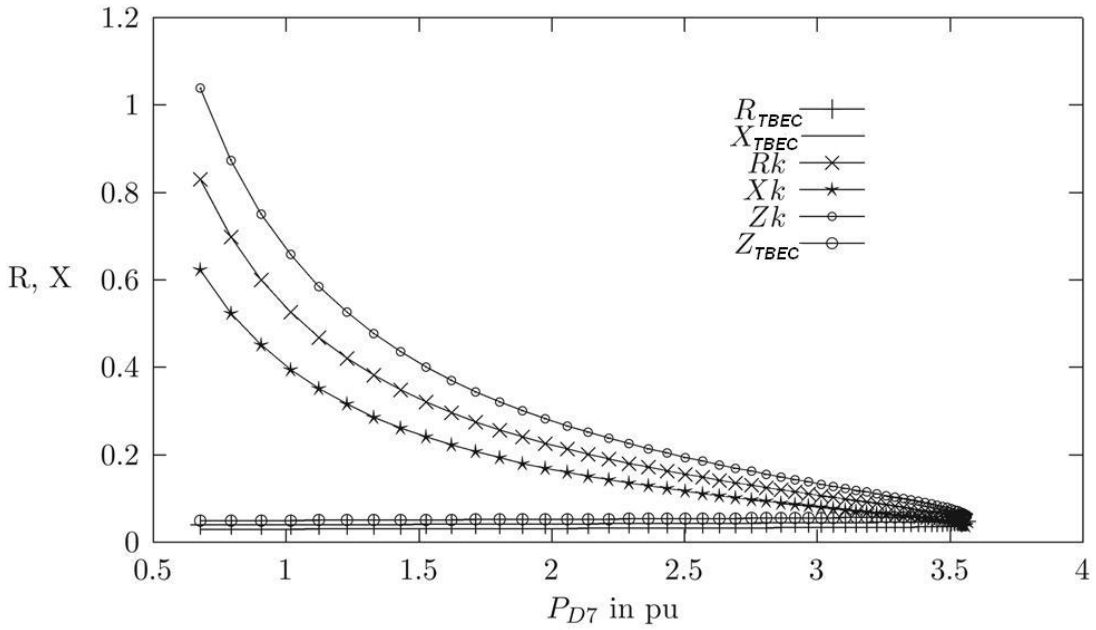

Fig. 4.9 Variation of TBEC parameters for change in load at bus-7 for IEEE30 bus system

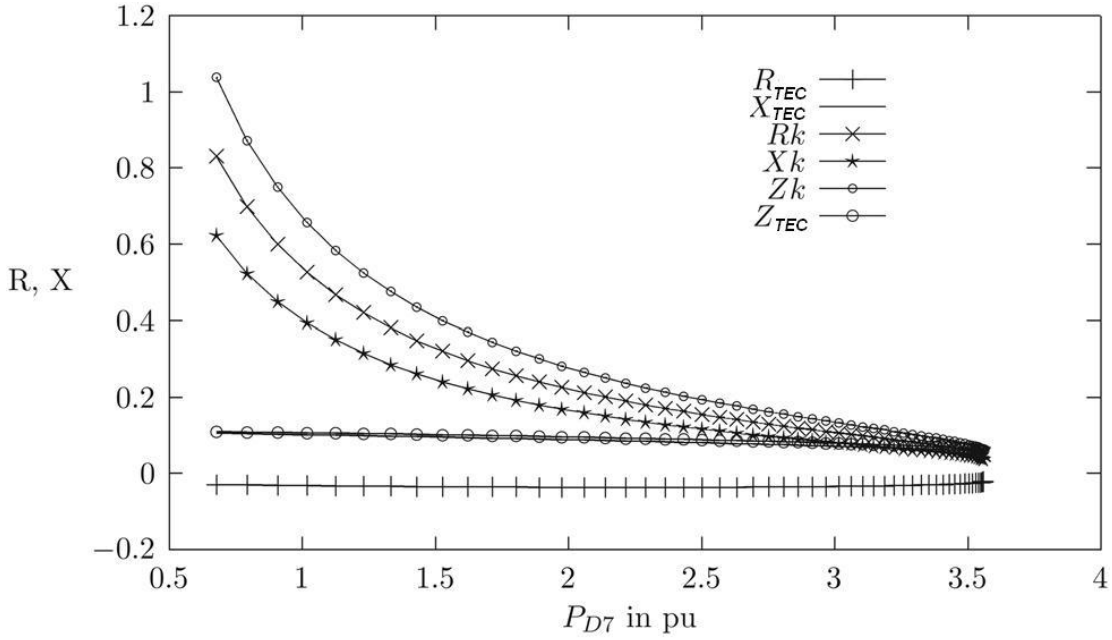

Fig. 4.10 Variation of TEC parameters for change in load at bus-7 for IEEE 30 bus system

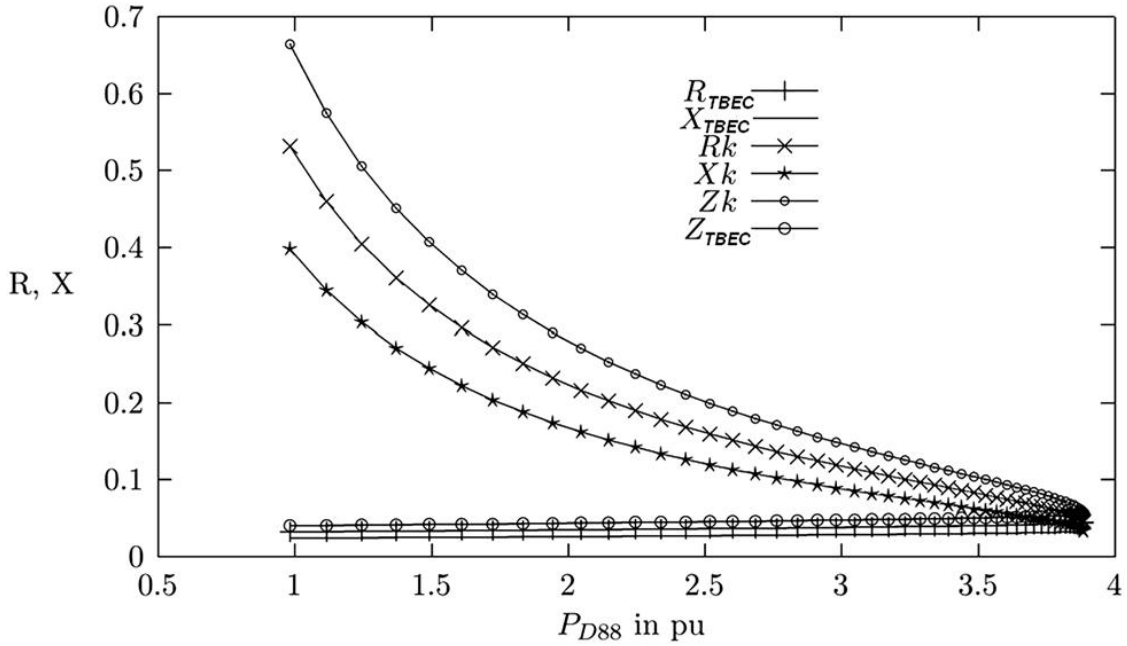

Fig.4.11 Variation of TBEC parameters for change in load at bus-88 for IEEE 118 bus system

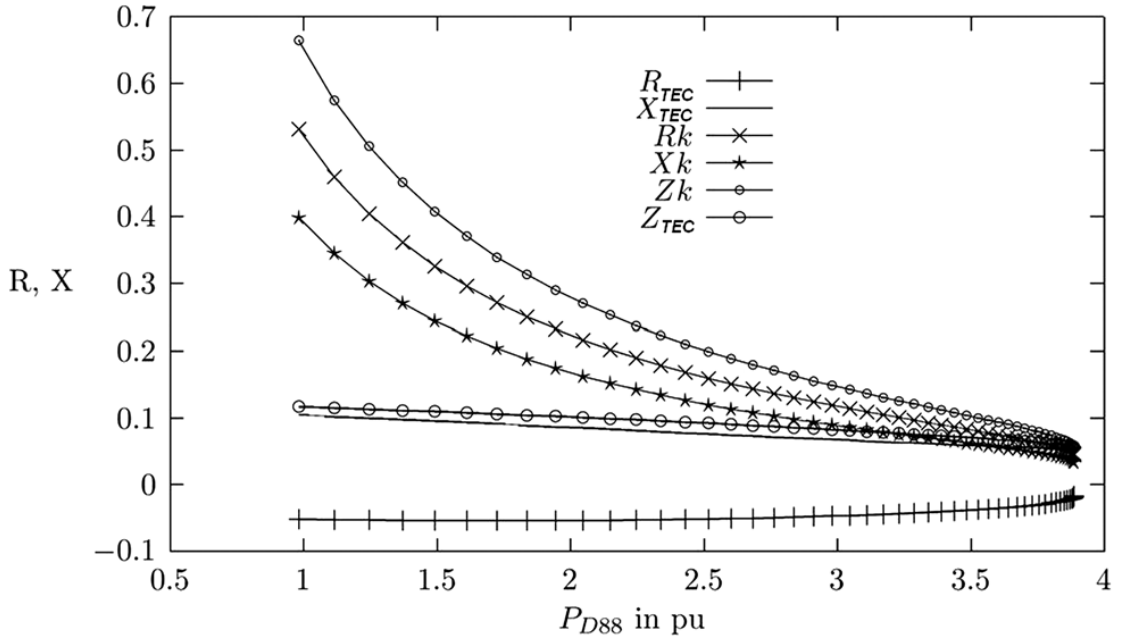

Fig. 4.12 Variation of TEC parameters for change in load at bus-88 for IEEE 118 bus system

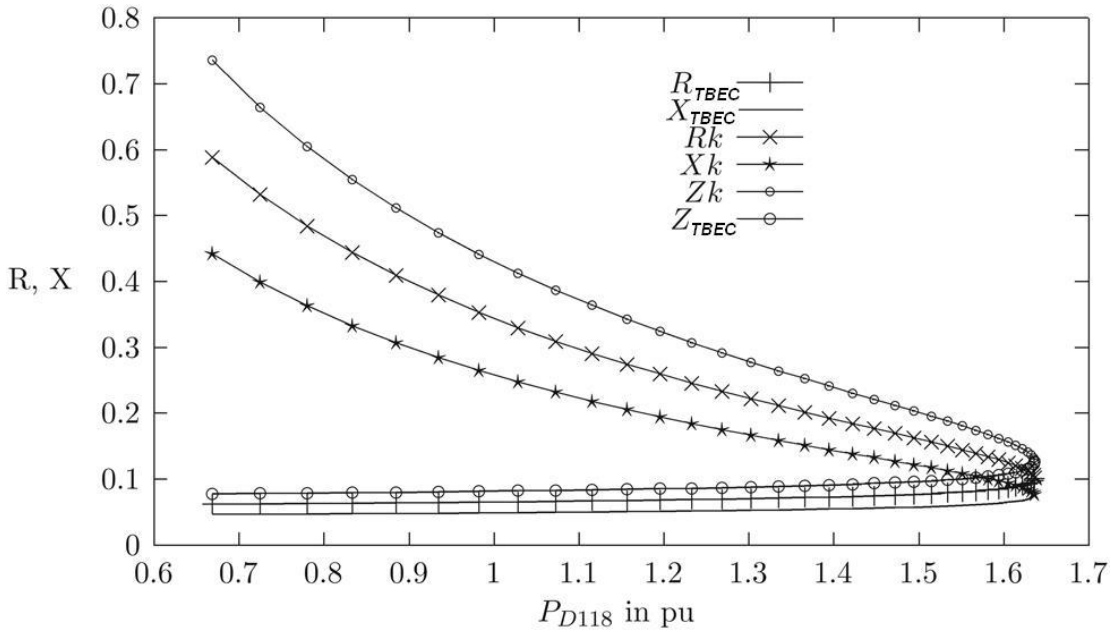

Fig.4.13

Variation of TBEC parameters for change in load at bus-118 for IEEE 118 bus system

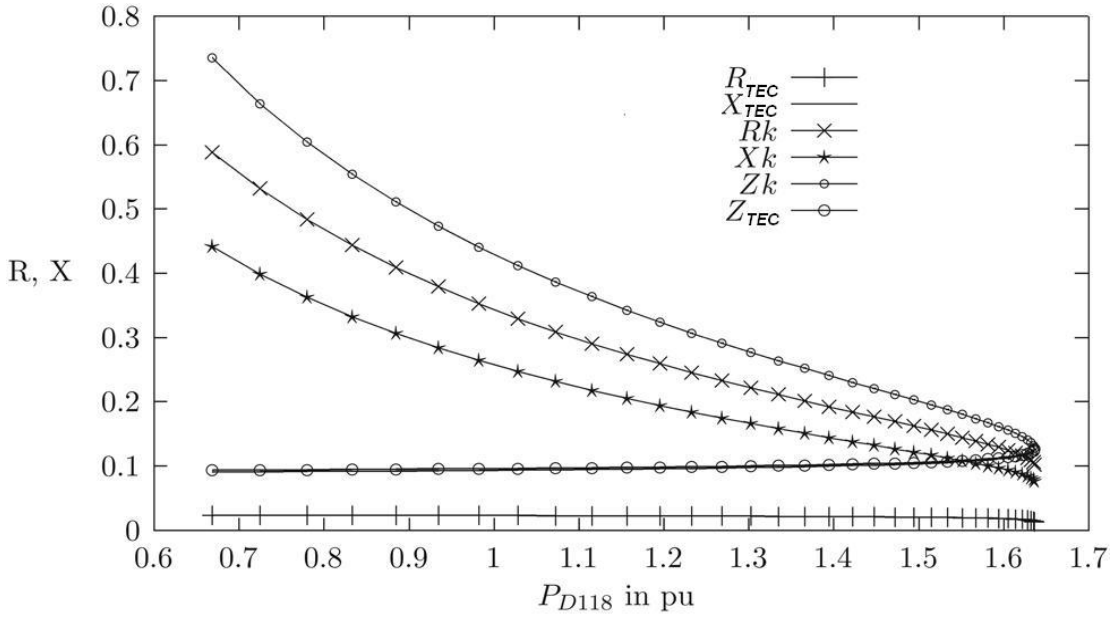

Fig. 4.14

Variation of TEC parameters for change in load at bus-118 for IEEE 118 bus system

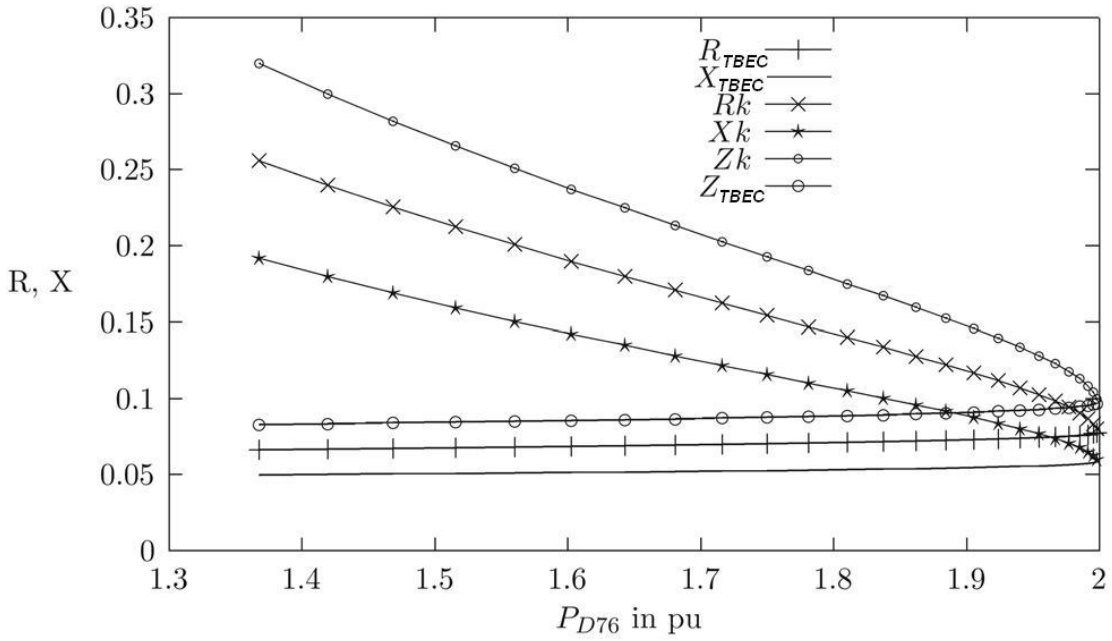

Fig.4.15

Variation of TBEC parameters for change in load at bus-76 for IEEE 118 bus system

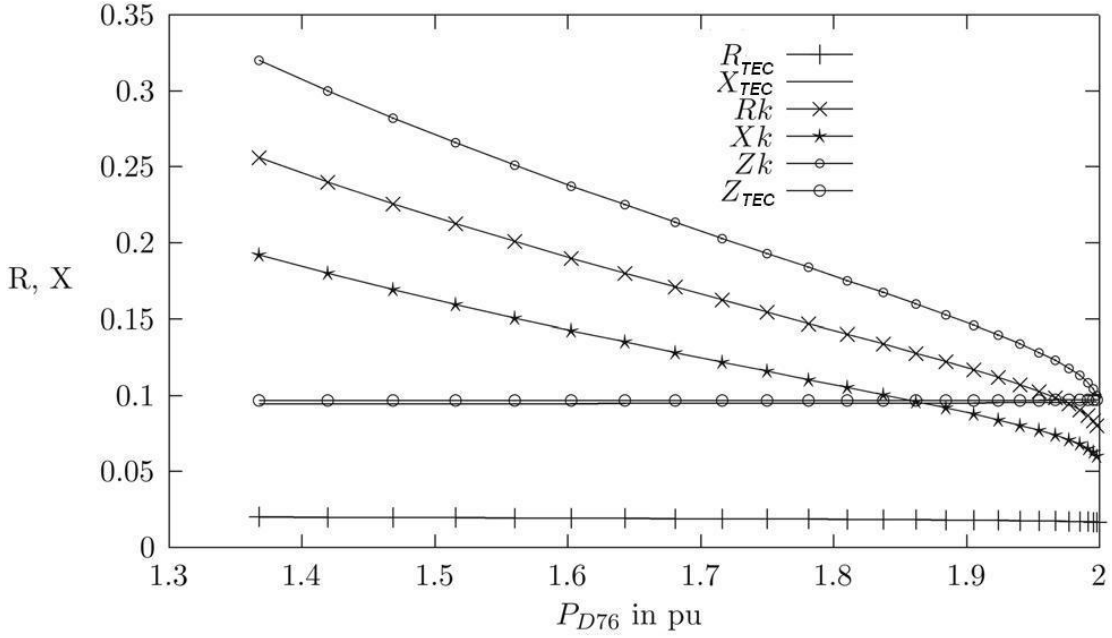

Fig. 4.16

Variation of TEC parameters for change in load at bus-76 for IEEE 118 bus system

Simulation results on IEEE 30 and IEEE 118 bus systems indicated that the phasor measurement method provides the Thevenin's equivalent impedance of the circuit, and values of R_{TEC} and X_{TEC} remain the same for the buses during load variation .Whereas the equivalent resistance, reactance and impedance of the TBEC are different from Thevenin's equivalent resistance, reactance and impedance, respectively. It is evident from the simulation results carried out on IEEE 30 and IEEE 118 bus systems that, for the TEC, the value of Z_{TEC} approaches the value of Z_k as the load P_{Dk} increases and at the point of collapse Z_{TEC} becomes equal to Z_k. In case of TBEC, the values of R_{TBEC}, X_{TBEC} and Z_{TBEC} approach to R_k, X_k and Z_k, respectively, as the load P_{Dk} increases and at the point of collapse R_{TBEC}, X_{TBEC} and Z_{TBEC} become equal to R_k, X_k and Z_k, respectively. Simulations were also carried out to examine the nature of variations of VSI_{TEC} and VSI_{TBEC} because of change in load at the selected buses (P_{Dk}).

Figs. 4.17–4.19 illustrate the variations of VSI_{TEC} and VSI_{TBEC} for the buses 29, 21 and 7 of the IEEE 30 bus system with respect to change in load (P_{Dk}) at 29, 21 and 7 individually with load power factor 0.8. Figs. 4.20–4.22 illustrate the variations of VSI_{TEC} and VSI_{TBEC} for the buses 88, 118 and 76 of the IEEE 118 bus system with respect to change in load (P_{Dk}) at 88, 118 and 76 individually with load power factor 0.8.

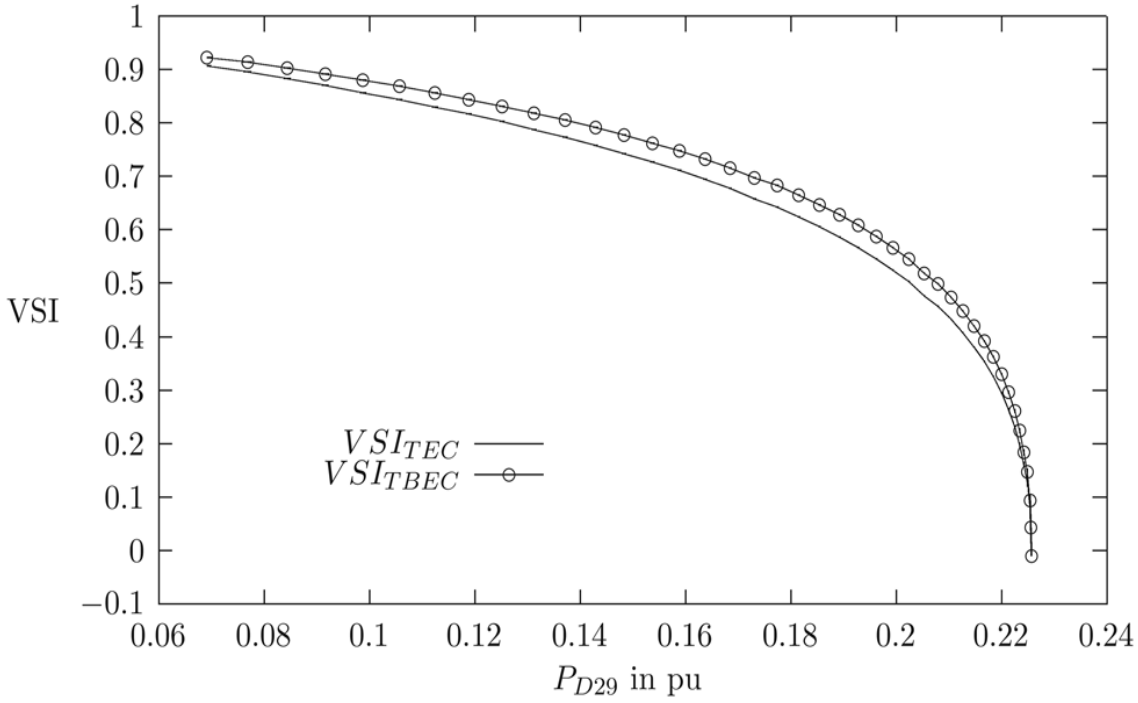

Fig. 4.17 Variation of VSI for change in load at bus-29 for IEEE 30 bus system

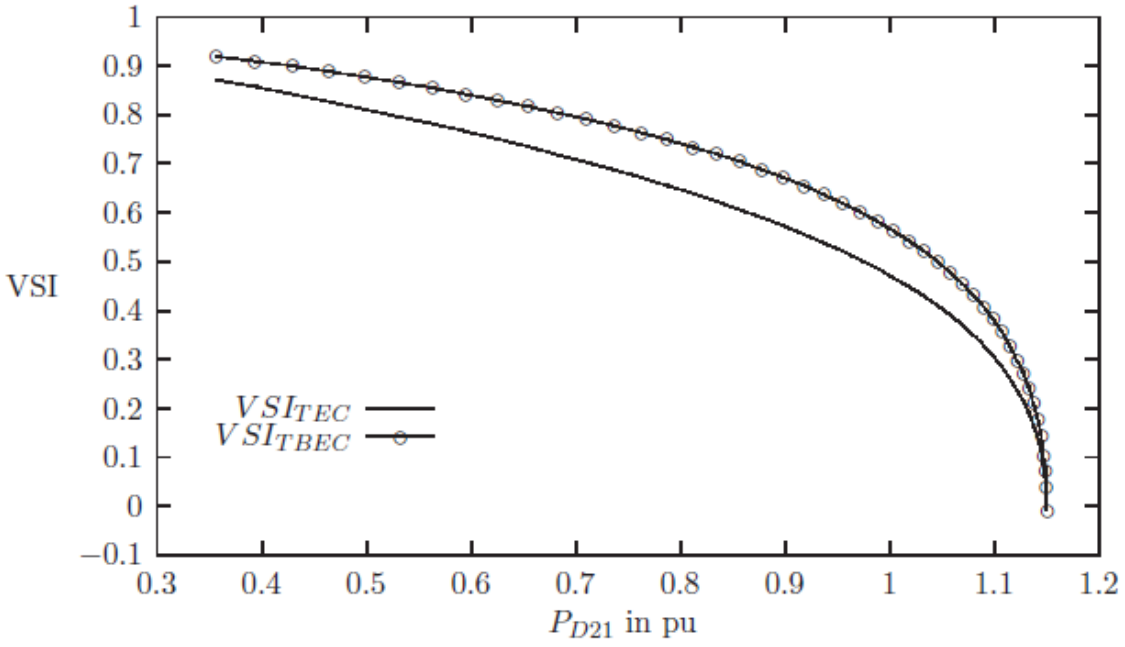

Fig. 4.18Variation of VSI for change in load at bus-21 for IEEE 30 bus system

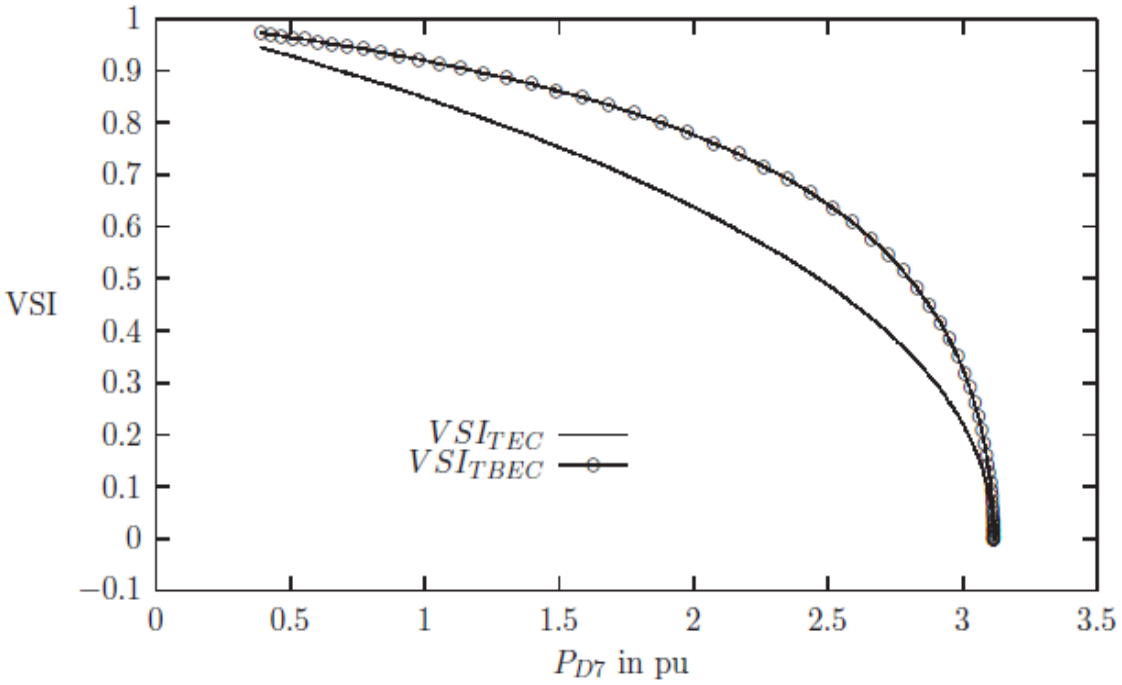

Fig. 4.19 Variation of VSI for change in load at bus-7 for IEEE 30 bus system

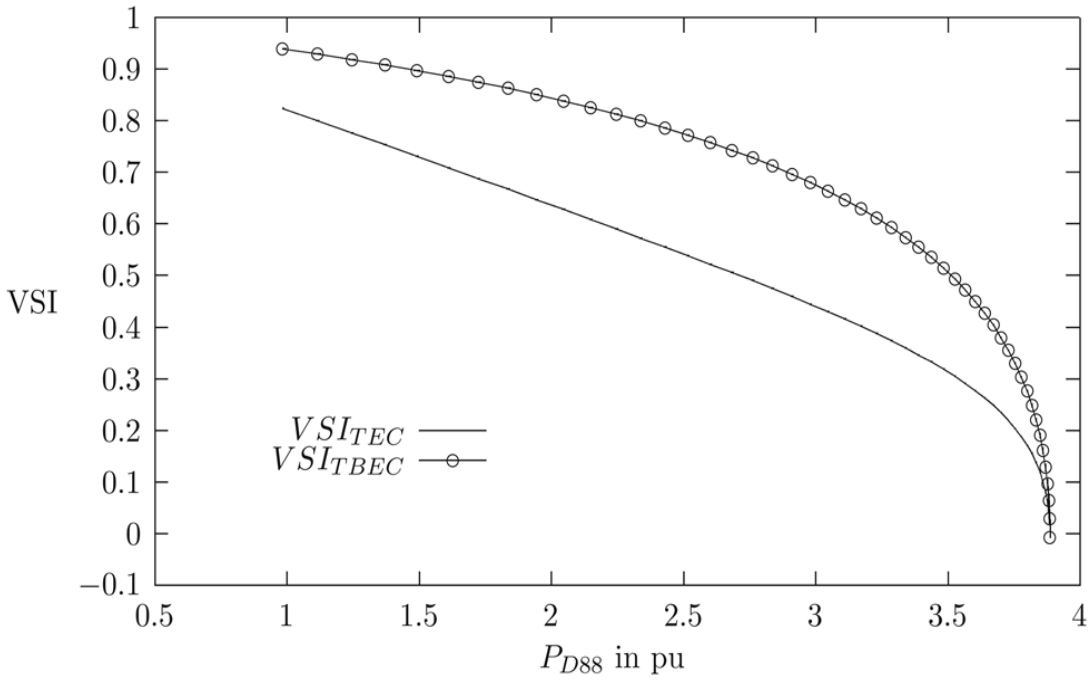

Fig. 4.20 Variation of VSI for change in load at bus-88 for IEEE 118 bus system

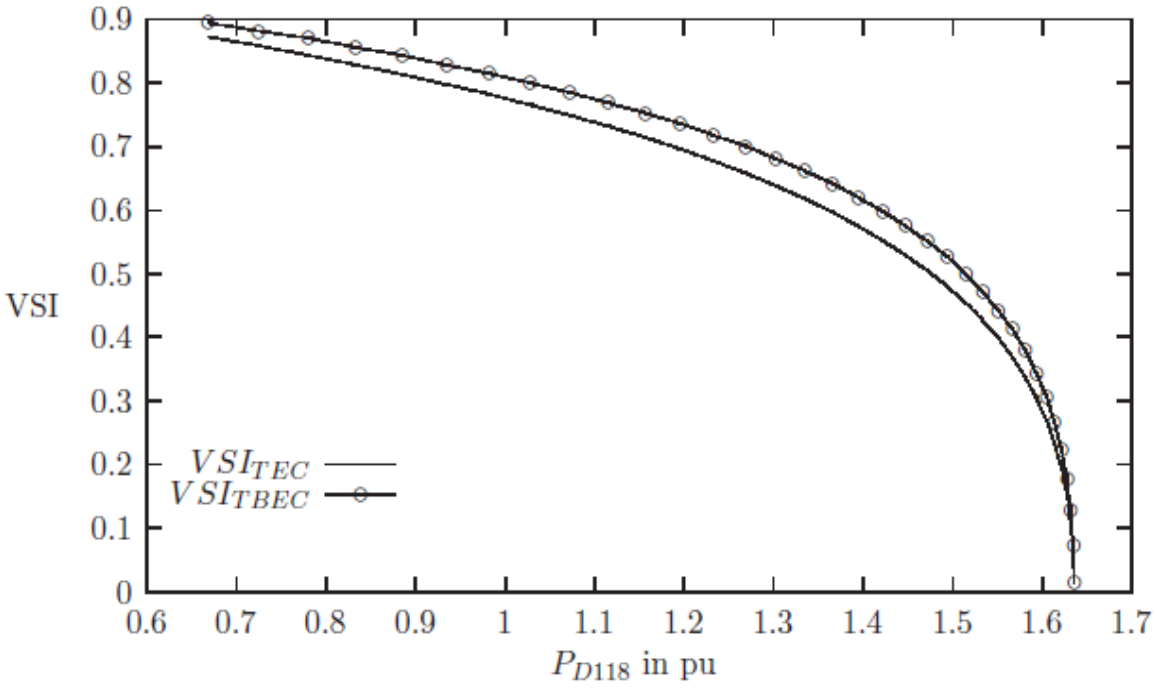

Fig. 4.21 Variation of VSI for change in load at bus-118 for IEEE 118 bus system

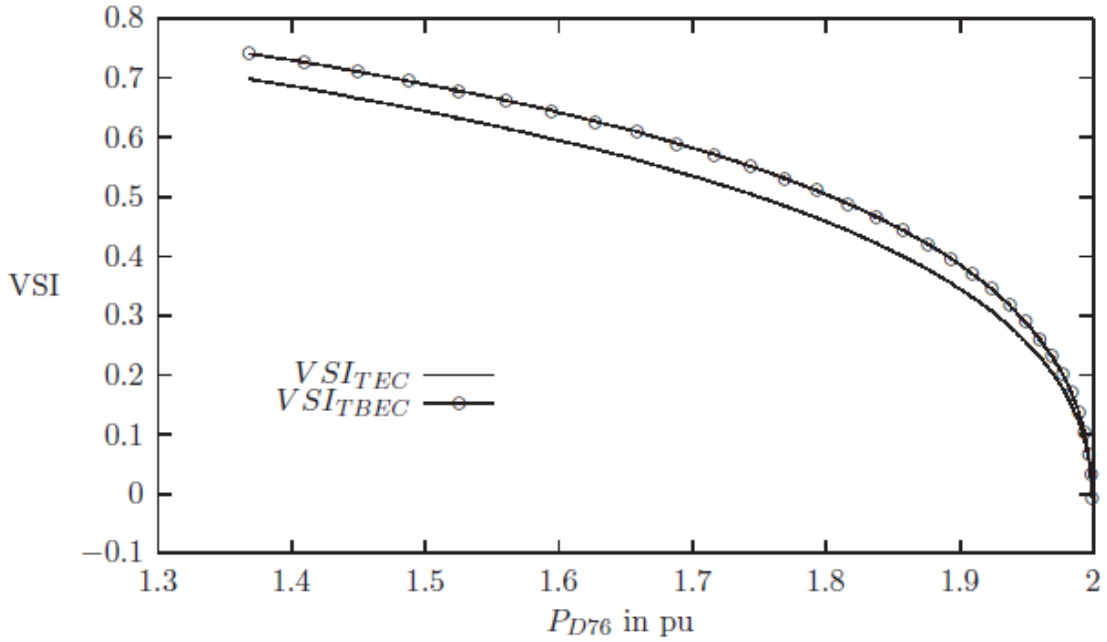

Fig. 4.22 Variation of VSI for change in load at bus-76 for IEEE 118 bus system

Simulation on IEEE 30 and IEEE 118 bus systems indicated that VSI_{TEC} and VSI_{TBEC} values decrease with increase in load, and the change is rapid as the system approaches the proximity of voltage collapse. At the point of voltage collapse, both the indices become zero. However, it has been observed that the buses which having large percentage load margin, the VSI_{TEC} against P_{Dk} curve differs from VSI_{TBEC} = 0.4 for both the test systems, the load margin appeared to be significantly low, whereas for the value VSI_{TEC} = 0.4, the load margin appears to be high for load

buses, bus-7 of IEEE 30 bus system and bus-88 of IEEE 118 bus system. To quantify this effect, percentage load margin PLM_{TECk} and PLM_{TBECk} are defined for the same values of VSI_{TEC} and VSI_{TBEC} as follows;

$$PLM_{TECk} = \frac{P_{Dk}^{crt} - P_{Dk(TEC)}}{P_{Dk}^{crt}} 100\%$$

$$PLM_{TBECk} = \frac{P_{Dk}^{crt} - P_{Dk(TBEC)}}{P_{Dk}^{crt}} 100\%$$

where P_{Dk}^{crt} is the value of load at the point of collapse, which is the same for the VSI_{TEC} against P_{Dk} curve and VSI_{TBEC} against P_{Dk} curve. $P_{Dk(TEC)}$ and $P_{Dk(TBEC)}$ are the values of load for same values of VSI_{TEC} and $VSIT_{BEC}$.

Table 4.1 – 4.4 present values of $P_{Dk(TEC)}$, $P_{Dk(TBEC)}$, P_{Dk}^{crt} , PLM_{TECk} and PLM_{TBECk} for bus numbers 29, 21 and 7 of IEEE 30 bus system and bus numbers 118, 88 and 76 of IEEE 118 bus system for $VSI_{TEC} = VSI_{TBEC} = 0.6$, $VSI_{TEC} = VSI_{TBEC} = 0.5$, $VSI_{TEC} = VSI_{TBEC} = 0.4$ and $VSI_{TEC} = VSI_{TBEC} = 0.3$ respectively.

Table 4.1: Values of $\boldsymbol{P_{Dk(TEC)}}$, $\boldsymbol{P_{Dk(TBEC)}}$, $\boldsymbol{P_{Dk}^{crt}}$, $\boldsymbol{PLM_{TECk}}$ and $\boldsymbol{PLM_{TBECk}}$ for IEEE30 and IEEE118 bus system for $VSI_{TEC} = VSI_{TBEC} = 0.6$

System	K (bus no.)	$P_{Dk(TEC)}$	$P_{Dk(TBEC)}$	P_{Dk}^{crt}	PLM_{TECk}	PLM_{TBECk}
IEEE 30	29	0.184	0.193	0.225	18.22	14.22
IEEE 30	21	0.928	.975	1.15	19.30	15.21
IEEE 30	7	2.20	2.65	3.20	31.25	17.18
IEEE 118	118	1.37	1.43	1.62	15.43	11.72
IEEE 118	88	2.25	3.32	3.9	42.30	14.87
IEEE 118	76	1.59	1.69	2	20.5	15.5

Table 4.2: Values of $\boldsymbol{P_{Dk(TEC)}}$, $\boldsymbol{P_{Dk(TBEC)}}$, $\boldsymbol{P_{Dk}^{crt}}$, $\boldsymbol{PLM_{TECk}}$ and $\boldsymbol{PLM_{TBECk}}$ for IEEE30 and IEEE118 bus system for $VSI_{TEC} = VSI_{TBEC} = 0.5$

System	K (bus no.)	$P_{Dk(TEC)}$	$P_{Dk(TBEC)}$	P_{Dk}^{crt}	PLM_{TECk}	PLM_{TBECk}
IEEE 30	29	0.195	0.209	0.225	13.33	7.11
IEEE 30	21	0.975	1.05	1.15	15.21	8.69
IEEE 30	7	2.70	2.82	3.20	24.06	11.80
IEEE 118	118	1.47	1.53	1.64	10.36	6.70
IEEE 118	88	2.70	3.58	3.9	30.25	8.20
IEEE 118	76	1.76	1.82	2	12	7.50

Table 4.3: Values of $\boldsymbol{P_{Dk(TEC)}}$, $\boldsymbol{P_{Dk(TBEC)}}$, $\boldsymbol{P_{Dk}^{crt}}$, $\boldsymbol{PLM_{TECk}}$ and $\boldsymbol{PLM_{TBECk}}$ for IEEE30 and IEEE118 bus system for $VSI_{TEC} = VSI_{TBEC} = 0.4$.

System	K (bus no.)	$P_{Dk(TEC)}$	$P_{Dk(TBEC)}$	P_{Dk}^{crt}	PLM_{TECk}	PLM_{TBECk}
IEEE 30	29	0.212	0.218	0.225	5.78	3.11
IEEE 30	21	1.04	1.09	1.15	9.56	5.22
IEEE 30	7	2.7	2.95	3.2	15.73	7.80
IEEE 118	118	1.52	1.565	1.64	7.31	4.57
IEEE 118	88	3.2	3.62	3.9	17.95	7.18
IEEE 118	76	1.86	1.89	2	7	5.5

Table 4.4: Values of $\boldsymbol{P_{Dk(TEC)}}$, $\boldsymbol{P_{Dk(TBEC)}}$, $\boldsymbol{P_{Dk}^{crt}}$, $\boldsymbol{PLM_{TECk}}$ and $\boldsymbol{PLM_{TBECk}}$ for IEEE30 and IEEE118 bus system for $VSI_{TEC} = VSI_{TBEC} = 0.3$

System	K (bus no.)	$P_{Dk(TEC)}$	$P_{Dk(TBEC)}$	P_{Dk}^{crt}	PLM_{TECk}	PLM_{TBECk}
IEEE 30	29	0.22	0.221	0.225	2.2	1.7
IEEE 30	21	1.107	1.125	1.15	3.7	2.17
IEEE 30	7	2.91	3.05	3.20	9.06	4.68
IEEE 118	118	1.59	1.61	1.62	3.04	1.82
IEEE 118	88	3.58	3.78	3.9	8.20	3.07
IEEE 118	76	1.92	1.94	2	4	1.55

Table 4.1-4.4 show that for VSI_{TEC} = 0.6, VSI_{TEC} = 0.5,VSI_{TEC} = 0.4 and VSI_{TEC} = 0.3, the percentage load margin PLM_{TECk} (based on phasor measurement method) varies widely for different buses of the IEEE 30 bus and IEEE 118 bus systems.

On the other hand, it is observed that for VSI_{TBEC} = 0.6, VSI_{TBEC} = 0.5, VSI_{TBEC} = 0.4 and VSI_{TBEC} = 0.3, the percentages of load margin PLM_{TBECk} are within a narrow range for all buses of IEEE 30 and IEEE 118 bus systems. The degree of variation of PLM_{TBECk} for VSI_{TBEC} = 0.6, VSI_{TBEC} = 0.5, VSI_{TBEC} = 0.4 and VSI_{TBEC} = 0.3 within the range of 11.72% to 17.18%, 6.7% to 11.8%, 3.11% to 8.0% and 1.55% to 4.6%.

It seems that the PLM_{TBECk} is independent of nature of bus and configuration of a power system. Therefore, the value of VSI_{TBEC} and the value of PLM_{TBECk} corresponding to the VSI_{TBEC} can be used by the power system planner or operator to know the approximate measure of load margin of a load bus.

.

1.5 Conclusion:

This chapter presents a method for online monitoring of voltage stability condition of a power system using measurements of real power, reactive power and voltage magnitude at a bus. Two consecutive measurements of real power, reactive power and voltage magnitude of a target/selected bus are used to determine parameters of a TBEC of target/selected load bus. Simulation on IEEE 30 and IEEE 118 bus systems indicated that VSI_{TBEC} could provide proper indication of proximity of voltage collapse irrespective of nature of buses or systems. The simulations carried out in the IEEE system indicated that the value PLM_{TBECk} is independent of nature of bus and configuration of a power system. Therefore, the value of VSI_{TBEC} and the value of PLM_{TBECk} corresponding to the VSI_{TBEC} can be used by the power system planner or operator to know the approximate measure of load margin of a load bus.

The proposed method is independent of remote measurement and also does not invite any type of continuous operating cost. The financial involvement for implementation of the proposed method would be significantly lower compared with that of PMU-based method.

Chapter- 5

General conclusions and future scope of the research work

Open access concept of power system operation under deregulatory environment allows participations of IPPs (Independent Power Producer) in a modern power system. As a result, to achieve economical objective of power system under the deregulated environment, a power system is forced to operate at its threshold of operating limit(s). Under such situation, the threat of voltage instability becomes a major concern for power system planners and operators. Voltage instability may create voltage collapse, if the issue is not attended properly. A voltage collapse in large system or subsystem may have far reaching consequences, such as system black out. Therefore, it is important for a power system operator/ planner to know the voltage stability condition of the system under steady operating condition. Several computational based Voltage Stability Indices (VSIs) were proposed to indicate voltage stability condition of a power system under steady state operating condition of the system. A VSI normally used to have a defined threshold value to indicate the proximity of voltage collapse. A bus or buses having VSI value(s) near to the threshold value are to be considered as vulnerable buses to voltage collapse. Necessary corrective measure has to be adopted by power system planners and operators to overcome such problem.

In recent years, bus measurements based methods are proposed to indicate the voltage stability condition of a power system. The on-line monitoring of voltage instability of a power system based on the PMU's local measurements has drawn wide attentions in the field of power system research. Most of these works use Thevenin's equivalent source impedance as the basis for monitoring voltage stability condition of a power system using PMU measurements. The work reported in this thesis, proposed a method for online monitoring of voltage stability condition of a bus of a power system using two consecutive measurements of bus variables namely – (i) real power (ii) reactive power and (iii) bus voltage magnitude of a bus. A new voltage stability index is proposed based on these measurements.

To investigate the validity of the measurement based methods for voltage stability analysis, the algorithm for a continuation power flow analysis is modified to generate measurement variables of a bus for two consecutive time references. The characteristic behavior of two PMU measurement based voltage stability indices available in literature have been examined using the modified continuation power flow analysis. It has been observed that both indices are reliable in offering the measure of voltage stability condition of a bus. The bus becomes vulnerable to voltage instability problem at the indices approach zero. At the point of collapse both indices become zero as claimed by the authors in their papers.

A method for online monitoring of voltage stability condition of a bus using two consecutive measurements of bus variables namely – (i) real power, (ii) reactive power and (iii) bus voltage magnitude of a bus has been propped in this thesis. Further, a new voltage stability index is proposed based on these measurements. Continuation power flow analysis described in the thesis is used to examine the performance and behavior of the index along the PV curve and around the proximity of voltage collapse of the bus. It has been observed that the proposed method can provide measure of load margin based on the index value for any bus of a power system, irrespective of different system characteristic. Again, the advantage of the method is that bus measurements required for determining the voltage stability index of a bus could be extracted from a smart energy meter. Therefore financial involvement for implementation of the proposed method would be significantly low compared to the PMU based methods.

The proposed method for voltage stability analysis based on the measurements of (i) real power, (ii) reactive power and (iii) bus voltage magnitude of a bus has been validated using a modified continuation load flow algorithm. The hardware implementation of the proposed method can be taken up as a future research work to examine the performance of the method under working environment of a power system.

References

1 P. Kundur “Power System Stability and Control” McGraw-Hill, NewYork, 1994

2 Prabha Kundur, John Paserba et al “Definition and Classification of Power System Stability” *EEE Transactions* on *Power Systems Volume*: ***19***, Issue: 3, Aug. ***2004***. pp1387 – 1401

3 X.-Z. Duan, Y.-Z He, and D.-S Chen, “To investigate the mechanism of voltage collapse,” J. Electric power system and automation, vol. 13, no. 2 , 1991,pp. 2-5.

4 Clark. H. K., “New challenges: Voltage stability” IEEE Power ENG. Rev (April 1990) pp. 33-37

5 1. P. Kessel and H. Glavitsch, “Estimating the voltage stability of a power system.” IEEE Trans. on Power Delivery, Vol. PWRD-1, No. 3 July/1986, pp. 346-354.

6 A. K. Sinha and D. Hazarika, “Comparative study of voltage stability indices in a power system”.Int. Journal of Electrical Power \& Energy Systems, Vol. 22, No. 8, Nov. 2000 pp. 589-596

7 A. C. Souza and V. H. Quintana, “New technique of network partitioning for voltage collapse margin calculation” IEEE Proceedings Gerer. Transm. Distrib.,vol 141(6), Nov. 1994, pp. 630-636

8 D. Hazarika, K. C. Sarma and Neelanjana Baura, “A method for determining load margin of a bus in terms of its voltage stability limit in an interconnected power system”, Fifteenth National Power Systems Conference (NPSC), IIT Bombay, December 2008, pp. 29-36

9 D. Hazarika, R. Das “An Algorithm for Determining the Load Margin of an Interconnected Power System” International Journal of Energy Science, Oct.

2012, Vol. 2 Issue. 5, PP. 169-174

10 D. Hazarika “A Fast Continuation Load Flow Analysis for an Interconnected Power System” International Journal of Energy Engineering (IJEE), Nov. 2012, Vol. 2 Iss. 4, PP. 126-136

11 Gubina F. and Strmcnk B., “Voltage collapse proximity index determination using voltage phasor approach.” IEEE Trans. Power System, Vol. 10, No. 2, 1995 pp. 788 -793

12 P A. Lof, G. Anderson and D. J. Hill “Voltage stability indices of stressed power system” IEEE Tran. PWRS Vol. 8, No.1 1993, pp. 326-335

13 A. Tiranuchit and R.J.Thomas, “A posturing strategy against voltage instability in electrical power systems” IEEE Tran. PWRS Vol. 3, No.1, 1989, pp. 87-93

14 D.P. Kothari & I. J.Nagrath, "Modern power system analysis", Fourth edition, McGraw-Hill education (India) PVT Ltd 2011

15 L. D. Arya, S. C. Choube, D. P. Kothari “Reactive Power Optimization Using Static Voltage Stability Index” Electric Power Components and systems, Published online: 29 Oct 2010,pp 615-628

16 Durlav Hazarika, Ranjay Das, Brajesh mohan Gupta “Improvement of bus voltage profile of a target bus using doubly fed induction generator-based distributed generator”. Published in IEEE International conference on power and embedded derive control (ICPEDC2017), 17-18 March, pp386-391, Chennai, India.

17 Y. Tamura, H. Mori and S. Lwanoto “Relationship between voltage instability and multiple load flow solutions in electrical system” IEEE Trans. Vol. 102 , No. 5, 1983 pp. 115-1125

18 A. Tiranuchit and R. J. Thomas, “A posturing strategy against voltage instability in electrical power systems” IEEE Tran. PWRS Vol. 3, No.1, 1989, pp. 87-93

19 Crisan and M. Liu, “Voltage collapse prediction using an improved sensitivity approach” Electrical Power System Research, Vol. 28, No. 3, 1984, pp. 181-190

20 B. Gao, Student Member IEEE G.K. Morison P. Kundur. Fellow IEEE 'Voltage stability evaluation using modal analysis' transaction on power Systems, Vol. 7, No. 4. November 1992 pp. 1423-1543

21 A.O.Ekwue, H.B.Wan, D.T.Y.Cheng and Y.H.Song “Singular value decomposition method for voltage stability analysis on the National Grid system (NGC)” International Journal of electrical Power & Energy Systems Volume 21, Issue 6**, August 1999, Pages 425-432**

22 K. Ellithy ; M. Shaheen ; M. Al-Athba ; A. Al-Subaie ; S. Al-Mohannadi ; S. Al-Okkah ; S. Abu-Eidah “Voltage stability evaluation of real power transmission system using singular value decomposition technique” Power and Energy Conference, 2008. PE Con.2008. IEEE 2nd International , **DOI:** 10.1109/PECON.2008.4762751

23 Li-Jun Cai ; Istvan Erlich “Power System Static Voltage Stability Analysis Considering all Active and Reactive Power Controls - Singular Value Approach” Power Tech, 2007 IEEE Lausanne, **DOI:** 10.1109 /PCT.2007 .4 538345

24 Qiu Xiaoyan; Li Xingyuan; Xu Jian; Xia Lili; , "AC/DC Hybrid Transmission System Voltage Stability Analysis Based on Singular Value Decomposition Method," Power and Energy Engineering Conference (APPEEC), 2010 Asia-Pacific , vol.1, no.4, March 2010 pp. 28-31.

25 V. Ajjarapu and C. Christy, “The continuation power flow - a tool for steady state voltage stability analysis”. IEEE Transactions on Power Systems, Vol 7,

No.1, Feb. 1992, pp. 416-423

26 H.D. Chiang, A.J. Flueck, K.S. Shah, N. Balu, "CPFLOW: A Practical Tool for Tracing Power System Steady-State Stationary Behavior due to Load and Generation Variations", IEEE Transactions on Power Systems, 1995. 10(2): pp. 623–634.

27 A. Dukpa, B. Venkatesh and M. El-Hawary, “Application of continuation power flow method in radial distribution systems,” Electric Power Syst. Research, vol. 79, 2009, pp.1503–1510,.

28 Alex Pama, Ghadir Radman “A new approach for estimating voltage collapse point based on quadratic approximation of PV-curves” Electric Power Systems Research 79 ,2009, 653–659

29 D.A. Alves, L.C.P. da Silva, C.A. Castro, and V.F. da Costa, “Continuation Load Flow Method Parameterized by Transmission Line Power Losses” Int. Conf. on Power Syst. Technology, Proc. Power Convol. 2, 2000, pp. 763–768.

30 M. Z. Laton, I. Musirin, “Voltage Stability Assessment via Continuation Power Flow Method” Int. Journal of Electrical and Electronic Systems research, vol.1, June 2008 pp 71-78

31 L. Wu, T.T. Gu, and L.X. Yao, “Static voltage stability analysis based on improved continuation power flow method,” J. Power system technology, vol. 35, no. 10, 2011, pp. 99-103.

32 L.A. Ll. Zarate and C.A. Castro, “Fast computation of security margins to voltage collapse based on sensitivity analysis,” IEE Proc. Gener. Transm. Distrib., vol. 153, no. 1, 2006, pp. 35–43 ,

33 Farid Karbalaei and Shahriar Abasi “Quick and Accurate Computation of Voltage Stability Margin” Journal of Electrical Engineering and Technology. Jan, 11(1), 2016, pp1-8

34 D. Hazarika “New method for monitoring voltage stability condition of a bus of an interconnected power system using measurements of the bus variables” IET Gener. Transm. Distrib., Vol. 6, Iss. 10, 2012, pp. 977–985

35 D. Hazarika and A.K. Sinha, “Power system restoration: Planning and simulation”. Int. Journal of Electrical Power & Energy Systems, Vol. 25, 2003, pp. 209-218

36 D. Hazarika, B K Talukdar and R Das, "Use of local bus measurements for operational planning of a power system", IET Gener. Transm. Distrib., Vol. 7 Issue 11,2013, pp. 1296-1309.

37 K. Vu, M. M. Begovic, D. Novosel and M. M. Saha, "Use of Local Measurements to Estimate Voltage stability Margin," IEEE Trans. Power Syst, vol. 14, no.3, Aug. 1999, pp. 1029-1035

38 I. Smon, G. Verbic and F. Gubina, "Local Voltage-Stability Index Using Tellegen's Theorem," IEEE Trans. On Power Syst, vol. 21, no. 3, Aug.2006 pp.1267-1275.

39 Y. Wang, W. Li, J. Lu. "A new node voltage stability index based on local voltage phasors". Electric Power Systems Research. vol.79, 2009, pp. 265-271.

40 M. H. Haque, "On-line Monitoring of Maximum Permissible Loading of a Power System within Voltage Stability Limits," IEE Proc.-Gener. Transm. Distrib, vol. 150, no. 1, Jan. 2003, pp.109-112.

41 G. Verbiˇc and F. Gubina, “A new concept of voltage-collapse protection based on local phasors,” IEEE Trans. Power Del., vol. 19, no. 2, Apr. 2004, pp. 576–581.

42 Y. Luo, D.-M. Zhao, and X.-L. Pan, “Study on voltage stability based on PMU technology,” J. Modern electric power, vol. 23, no. 2 , 2006, pp. 6-9

43 C. Sandro and G. N. Taranto. "A real-time voltage instability identification algorithm based on local phasor measurements," IEEE trans. On Power syst. vol. 23, no. 3, Aug. 2008, pp.1271-1279

44 Y. Wang, W. Li, J. Lu. "A new node voltage stability index based on local voltage phasors". Electric Power Systems Research. vol.79, 2009, pp. 265-271.

45 M Glavic, T V Cutsem. "Wide-Area Detection of voltage instability from synchronized phsor measurements. Part I: Principle". IEEE trans. On Power systems. Vol. 24, no.3, Aug. 2009, pp.1408-1416

46 M Glavic, T V Cutsem. "Wide-Area Detection of voltage instability from synchronized phsor measurements. Part II: Simulation Results". IEEE trans. On Power syst. vol. 24, no.3, Aug. 2009, pp.1417-1425.

47 R. Diao, K. Sun, V. Vittal, et al. "Decision Tree based on-line voltage security assessment using PMU measurements". IEEE trans. On Power systems. vol. 24, no.2, May. 2009 pp.832-839

48 Le Fu, B C Pal nd J Cory " Phasor Measurement Application for Power System voltage stability Monitoring", General Meeting of the IEEE Power and Energy Society, IEEE pp 4953-4960

49 W. Xu, et al., “A network decoupling transform for phasor data based voltage stability analysis and monitoring,” IEEE Trans. Smart Grid, vol. 3, no. 1, Mar.2012, pp 261–270

50 I. R. Pordanjani, et al, “Identification of critical components for voltage stability assessment using channel components transform,” IEEE Trans. Smart Grid, vol. 4, no. 2, 2013, pp. 1122-1132

51 F. Hu, K. Sun, et al, “An adaptive three-bus power system equivalent for estimating voltage stability margin from synchronized phasor measurements,” IEEE PES General Meeting, 2014

52 S. M. Abdelkader, D. J. Morrow, “Online Thévenin equivalent determi-nation considering system side changes and measurement errors,” IEEE Trans. Power Systems, vol. PP, no. 99, 2014, pp. 1-10

53 L. He, C.-C. Liu, “Parameter identification with PMUs for instability detection in power systems with HVDC integrated offshore wind energy,” IEEE Trans. Power Systems, vol. 29, no. 2 , 2014, pp. 775-784

54 J.-H. Liu, C.-C. Chu, “Wide-area measurement-based voltage stability indicators by modified coupled single-port models,” IEEE Trans. Power Systems, vol. 29, no. 2, 2014, pp. 756-764

55 H.Yuan, F.Li, "Hybrid voltage stability assessment (VSA) for N-1 contingency," Electric Power Systems Research, vol. 122, May. 2015 pp. 65–75

56 Su, H.Y.; Liu, C.W. “Estimating the Voltage Stability Margin Using PMU Measurements.” IEEE Trans. Power Syst. 31, 2016, pp 3221–3229

57 A. G. Phadke, “Synchronized phasor measurements in power systems” ”IEEE Comput. Appl. Power, vol. 6, no. 3, Apr. 1993**,** pp. 10–15

58 Durlav Hazarika, Bani Kanta Talukdar, Brajesh Mohan Gupta[2]“Identification of voltage stability condition of a power system using measurements of bus variables” IET Journal of Engineering, doi: 10.1049/joe.2014.0263. 2014 Vol.2014,issue 12, 2014, pp 658-664:

APPENDIX

The single line diagram of IEEE 30 bus and IEEE 118 bus systems used for the verification of validity of the bus measurements based voltage stability analysis methods are presented in figure A.1 and A.2 respectively

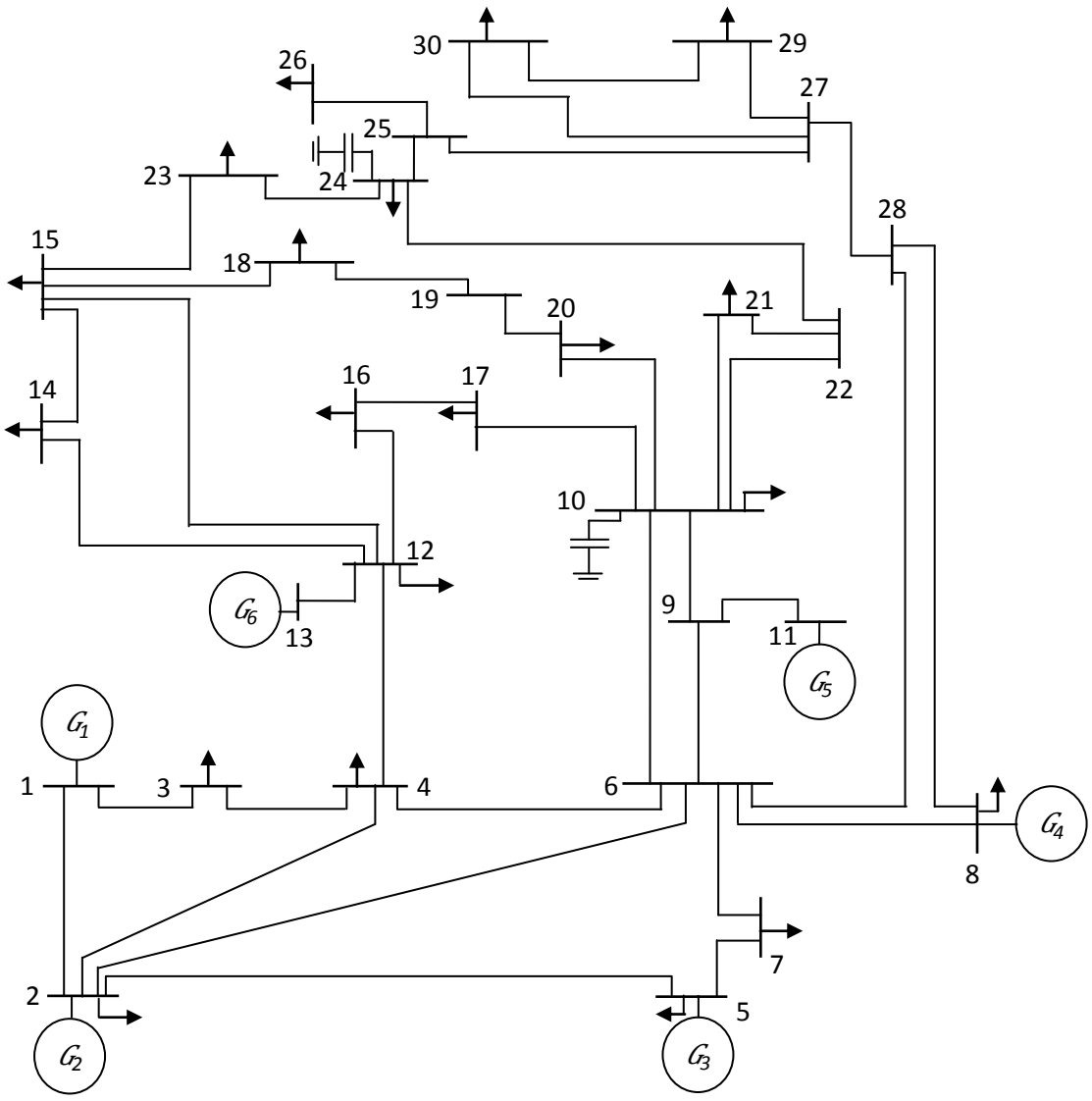

Figure A 1: Single-line diagram of IEEE 30 bus test system

The network transmission lines and transfer data for IEEE 30 bus system are presented in table A-1.1 the information about shunt of this system is providing in table A-1.2.

Table A-1.1: Network transmission line data for IEEE 30 bus system.

From Bus	To Bus	R(pu)	X(pu)	B/2 (pu)	X'merTAP (a)
1	2	0.0192	0.0575	0.0264	1
1	3	0.0452	0.1652	0.0204	1
2	4	0.057	0.1737	0.0184	1
3	4	0.0132	0.0379	0.0042	1
2	5	0.0472	0.1983	0.0209	1
2	6	0.0581	0.1763	0.0187	1
4	6	0.0119	0.0414	0.0045	1
5	7	0.046	0.116	0.0102	1
6	7	0.0267	0.082	0.0085	1
6	8	0.012	0.042	0.0045	1
6	9	0	0.208	0	0.978
6	10	0	0.556	0	0.969
9	11	0	0.208	0	1
9	10	0	0.11	0	1
4	12	0	0.256	0	0.932
12	13	0	0.14	0	1
12	14	0.1231	0.2559	0	1
12	15	0.0662	0.1304	0	1
12	16	0.0945	0.1987	0	1
14	15	0.221	0.1997	0	1
16	17	0.0824	0.1923	0	1
15	18	0.1073	0.2185	0	1
18	19	0.0639	0.1292	0	1

19	20	0.034	0.068	0	1
From Bus	To Bus	R(pu)	X(pu)	B/2 (pu)	X'merTAP (a)
10	20	0.0936	0.209	0	1
10	17	0.0324	0.0845	0	1
10	22	0.0348	0.0749	0	1
10	23	0.0727	0.1499	0	1
21	23	0.0116	0.0236	0	1
15	23	0.1	0.202	0	1
22	24	0.115	0.179	0	1
23	24	0.132	0.27	0	1
24	25	0.1885	0.3292	0	1
25	26	0.2544	0.38	0	1
25	27	0.1093	0.2087	0	1
28	27	0	0.396	0	0.968
27	29	0.2198	0.4153	0	1
27	30	0.3202	0.6027	0	1
29	30	0.2399	0.4533	0	1
8	28	0.0636	0.2	0.0214	1
6	28	0.0169	0.0599	0.065	1

Table A-1.2: Shunt data of IEEE 30 bus system

Bus no.	Shunt Value
10	0.19
24	0.04

The base case load flow results for IEEE 30 bus system with defined loads and generations is provided in table A-1.3

Table A-1.3: Base case load flow results of IEEE 30 bus

Bus No.- i	P_{Gi}	Q_{Gi}	P_{Di}	Q_{Di}	V pu	δ in rad
1	0.5439	0.1200	0.0000	0.0000	1	0.0000
2	0.4127	0.0411	0.1070	0.0370	1.0000	-0.0137
3	0.0000	0.0000	0.2240	0.0520	0.9815	-0.0607
4	0.0000	0.0000	0.1760	0.0460	0.9808	-0.0657
5	0.5879	0.0410	0.1520	0.0700	1.0000	-0.0066
6	0.0000	0.0000	0.0000	0.0000	0.9872	-0.0635
7	0.0000	0.0000	0.3280	0.1090	0.9809	-0.0549
8	0.5588	0.3616	0.3000	0.0900	1.0000	-0.0587
9	0.0000	0.0000	0.0000	0.0000	0.9864	-0.1025
10	0.0000	0.0000	0.0880	0.0200	0.9811	-0.1503
11	0.2200	0.0707	0.0000	0.0000	1.0000	-0.0560
12	0.0000	0.0000	0.1120	0.7050	0.9637	-0.1587
13	0.2200	0.2633	0.0000	0.0000	1.0000	-0.1267
14	0.0000	0.0000	0.0620	0.0160	0.9365	-0.1880
15	0.0000	0.0000	0.3920	0.2250	0.9177	-0.1968
16	0.0000	0.0000	0.0350	0.0180	0.9636	-0.1610
17	0.0000	0.0000	0.0900	0.0580	0.9702	-0.1584
18	0.0000	0.0000	0.0320	0.0090	0.9275	-0.1931
19	0.0000	0.0000	0.0950	0.0240	0.9368	-0.1881
20	0.0000	0.0000	0.0220	0.0070	0.9471	-0.1804
21	0.0000	0.0000	0.0750	0.0120	0.9749	-0.1608
22	0.0000	0.0000	0.0000	0.0000	0.9741	-0.1638
23	0.0000	0.0000	0.1090	0.0530	0.9205	-0.2088
24	0.0000	0.0000	0.1270	0.0370	0.9557	-0.1993
25	0.0000	0.0000	0.0000	0.0000	0.9501	-0.1822
26	0.0000	0.0000	0.0350	0.0130	0.9353	-0.1940

27	0.0000	0.0000	0.0000	0.0000	0.9537	-0.1664
Bus No.- i	P_{Gi}	Q_{Gi}	P_{Di}	Q_{Di}	V pu	δ in rad
28	0.0000	0.0000	0.0000	0.0000	0.9842	-0.0724
29	0.0000	0.0000	0.0640	0.0290	0.9158	-0.1976
30	0.0000	0.0000	0.0960	0.0390	0.9061	-0.2075

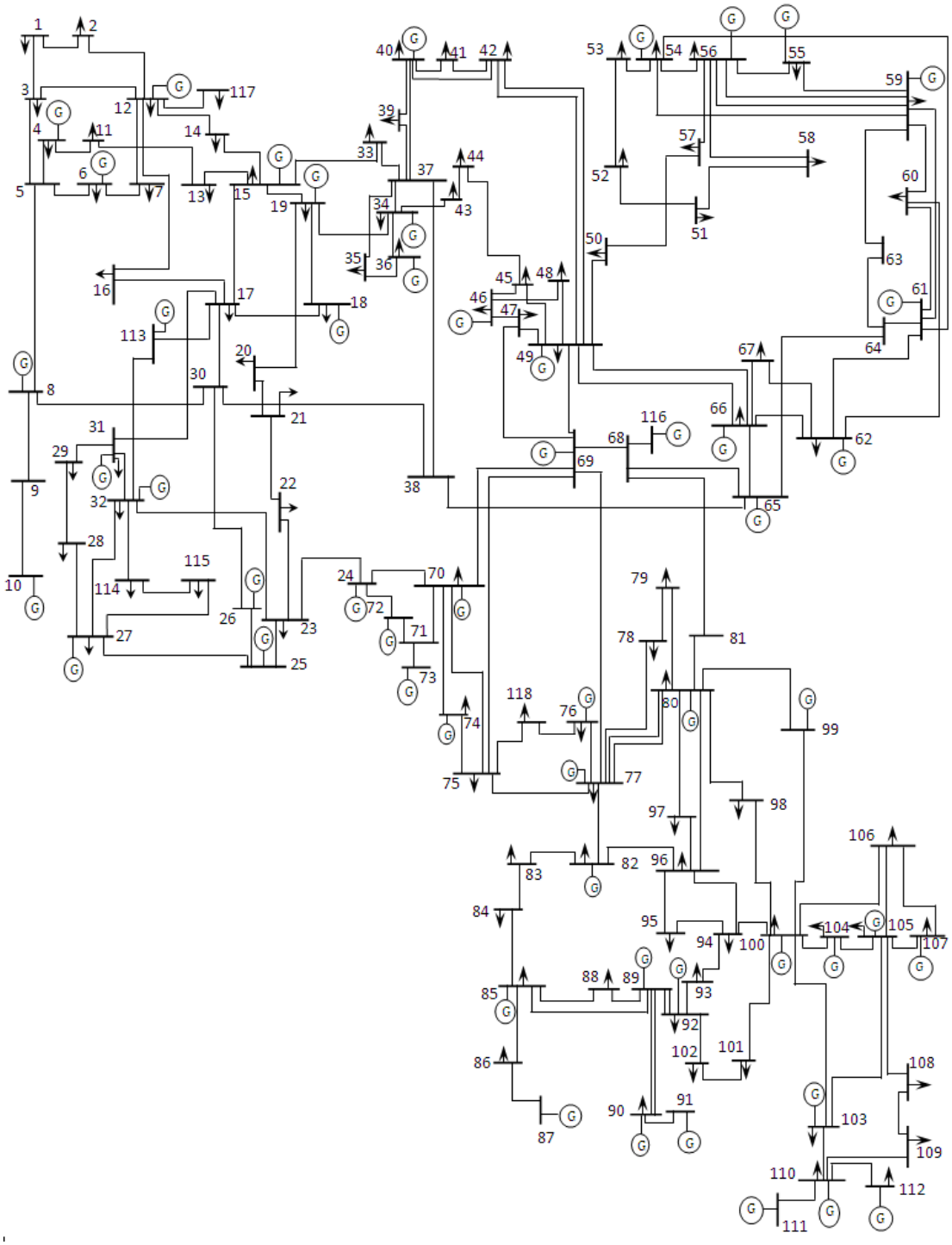

Figure A- 2: Single-line diagram of IEEE 118 bus test system

The network transmission lines and transfer data for IEEE 118 bus system are presented in table A-1.4 and table A-1.5 respectively. The information about shunt of this system are provide in table A.6

Table A-1.4 Network transmission line data for IEEE 118 bus system.

Line No.	From Bus	To Bus	Circuit ID	R (p.u.)	X (p.u.)	B (p.u.)
1	1	2	1	0.0303	0.0999	0.0254
2	1	3	1	0.0129	0.0424	0.01082
3	4	5	1	0.00176	0.00798	0.0021
4	3	5	1	0.0241	0.108	0.0284
5	5	6	1	0.0119	0.054	0.01426
6	6	7	1	0.00459	0.0208	0.0055
7	8	9	1	0.00244	0.0305	1.162
8	9	10	1	0.00258	0.0322	1.23
9	4	11	1	0.0209	0.0688	0.01748
10	5	11	1	0.0203	0.0682	0.01738
11	11	12	1	0.00595	0.0196	0.00502
12	2	12	1	0.0187	0.0616	0.01572
13	3	12	1	0.0484	0.16	0.0406
14	7	12	1	0.00862	0.034	0.00874
15	11	13	1	0.02225	0.0731	0.01876
16	12	14	1	0.0215	0.0707	0.01816
17	13	15	1	0.0744	0.2444	0.06268
18	14	15	1	0.0595	0.195	0.0502
19	12	16	1	0.0212	0.0834	0.0214
20	15	17	1	0.0132	0.0437	0.0444

Line No.	From Bus	To Bus	Circuit ID	R (pu)	X (pu)	B (pu)
21	16	17	1	0.0454	0.1801	0.0466
22	17	18	1	0.0123	0.0505	0.01298
23	18	19	1	0.01119	0.0493	0.01142
24	19	20	1	0.0252	0.117	0.0298
25	15	19	1	0.012	0.0394	0.0101
26	20	21	1	0.0183	0.0849	0.0216
27	21	22	1	0.0209	0.097	0.0246
28	22	23	1	0.0342	0.159	0.0404
29	23	24	1	0.0135	0.0492	0.0498
30	23	25	1	0.0156	0.08	0.0864
31	25	27	1	0.0318	0.163	0.1764
32	27	28	1	0.01913	0.0855	0.0216
33	28	29	1	0.0237	0.0943	0.0238
34	8	30	1	0.00431	0.0504	0.514
35	26	30	1	0.00799	0.086	0.908
36	17	31	1	0.0474	0.1563	0.0399
37	29	31	1	0.0108	0.0331	0.0083
38	23	32	1	0.0317	0.1153	0.1173
39	31	32	1	0.0298	0.0985	0.0251
40	27	32	1	0.0229	0.0755	0.01926
41	15	33	1	0.038	0.1244	0.03194
42	19	34	1	0.0752	0.247	0.0632
43	35	36	1	0.00224	0.0102	0.00268
44	35	37	1	0.011	0.0497	0.01318
45	33	37	1	0.0415	0.142	0.0366
46	34	36	1	0.00871	0.0268	0.00568

Line No.	From Bus	To Bus	Circuit ID	R (pu)	X (pu)	B (pu)
47	34	37	1	0.00256	0.0094	0.00984
48	37	39	1	0.0321	0.106	0.027
49	37	40	1	0.0593	0.168	0.042
50	30	38	1	0.00464	0.054	0.422
51	39	40	1	0.0184	0.0605	0.01552
52	40	41	1	0.0145	0.0487	0.01222
53	40	42	1	0.0555	0.183	0.0466
54	41	42	1	0.041	0.135	0.0344
55	43	44	1	0.0608	0.2454	0.06068
56	34	43	1	0.0413	0.1681	0.04226
57	44	45	1	0.0224	0.0901	0.0224
58	45	46	1	0.04	0.1356	0.0332
59	46	47	1	0.038	0.127	0.0316
60	46	48	1	0.0601	0.189	0.0472
61	47	49	1	0.0191	0.0625	0.01604
62	42	49	1	0.0715	0.323	0.086
63	42	49	2	0.0715	0.323	0.086
64	45	49	1	0.0684	0.186	0.0444
65	48	49	1	0.0179	0.0505	0.01258
66	49	50	1	0.0267	0.0752	0.01874
67	49	51	1	0.0486	0.137	0.0342
68	51	52	1	0.0203	0.0588	0.01396
69	52	53	1	0.0405	0.1635	0.04058
70	53	54	1	0.0263	0.122	0.031

71	49	54	1	0.073	0.289	0.0738
72	49	54	2	0.0869	0.291	0.073
Line No.	From Bus	To Bus	Circuit ID	R (pu)	X (pu)	B (pu)
73	54	55	1	0.0169	0.0707	0.0202
74	54	56	1	0.00275	0.00955	0.00732
75	55	56	1	0.00488	0.0151	0.00374
76	56	57	1	0.0343	0.0966	0.0242
77	50	57	1	0.0474	0.134	0.0332
78	56	58	1	0.0343	0.0966	0.0242
79	51	58	1	0.0255	0.0719	0.01788
80	54	59	1	0.0503	0.2293	0.0598
81	56	59	1	0.0825	0.251	0.0569
82	56	59	2	0.0803	0.239	0.0536
83	55	59	1	0.04739	0.2158	0.05646
84	59	60	1	0.0317	0.145	0.0376
85	59	61	1	0.0328	0.15	0.0388
86	60	61	1	0.00264	0.0135	0.01456
87	60	62	1	0.0123	0.0561	0.01468
88	61	62	1	0.00824	0.0376	0.0098
89	63	64	1	0.00172	0.02	0.216
90	38	65	1	0.00901	0.0986	1.046
91	64	65	1	0.00269	0.0302	0.38
92	49	66	1	0.018	0.0919	0.0248
93	49	66	2	0.018	0.0919	0.0248
94	62	66	1	0.0482	0.218	0.0578
95	62	67	1	0.0258	0.117	0.031
96	66	67	1	0.0224	0.1015	0.02682
97	65	68	1	0.00138	0.016	0.638

98	47	69	1	0.0844	0.2778	0.07092
99	49	69	1	0.0985	0.324	0.0828
100	69	70	1	0.03	0.127	0.122
Line No.	From Bus	To Bus	Circuit ID	R (pu)	X (pu)	B (pu)
101	24	70	1	0.00221	0.4115	0.10198
102	70	71	1	0.00882	0.0355	0.00878
103	24	72	1	0.0488	0.196	0.0488
104	71	72	1	0.0446	0.18	0.04444
105	71	73	1	0.00866	0.0454	0.01178
106	70	74	1	0.0401	0.1323	0.03368
107	70	75	1	0.0428	0.141	0.036
108	69	75	1	0.0405	0.122	0.124
109	74	75	1	0.0123	0.0406	0.01034
110	76	77	1	0.0444	0.148	0.0368
111	69	77	1	0.0309	0.101	0.1038
112	75	77	1	0.0601	0.1999	0.04978
113	77	78	1	0.00376	0.0124	0.01264
114	78	79	1	0.00546	0.0244	0.00648
115	77	80	1	0.017	0.0485	0.0472
116	77	80	2	0.0294	0.105	0.0228
118	79	80	1	0.0156	0.0704	0.0187
119	68	81	1	0.00175	0.0202	0.808
120	77	82	1	0.0298	0.0853	0.08174
121	82	83	1	0.0112	0.03665	0.03796
122	83	84	1	0.0625	0.132	0.0258
123	83	85	1	0.043	0.148	0.0348
124	84	85	1	0.0302	0.0641	0.01234
125	85	86	1	0.035	0.123	0.0276

126	86	87	1	0.02828	0.2074	0.0445
127	85	88	1	0.02	0.102	0.0276
128	85	89	1	0.0239	0.173	0.047
129	88	89	1	0.0139	0.0712	0.01934
Line No.	From Bus	To Bus	Circuit ID	R (pu)	X (pu)	B (pu)
130	89	90	1	0.0518	0.188	0.0528
131	89	90	2	0.0238	0.0997	0.106
132	90	91	1	0.0254	0.0836	0.0214
133	89	92	1	0.0099	0.0505	0.0548
134	89	92	2	0.0393	0.1581	0.0414
135	91	92	1	0.0387	0.1272	0.03268
136	92	93	1	0.0258	0.0848	0.0218
137	92	94	1	0.0481	0.158	0.0406
138	93	94	1	0.0223	0.0732	0.01876
139	94	95	1	0.0132	0.0434	0.0111
140	80	96	1	0.0356	0.182	0.0494
141	82	96	1	0.0162	0.053	0.0544
142	94	96	1	0.0269	0.0869	0.023
143	80	97	1	0.0183	0.0934	0.0254
144	80	98	1	0.0238	0.108	0.0286
145	80	99	1	0.0454	0.206	0.0546
146	92	100	1	0.0648	0.295	0.0472
147	94	100	1	0.0178	0.058	0.0604
148	95	96	1	0.0171	0.0547	0.01474
149	96	97	1	0.0173	0.0885	0.024
150	98	100	1	0.0397	0.179	0.0476
151	99	100	1	0.018	0.0813	0.0216
152	100	101	1	0.0277	0.1262	0.0328

153	92	102	1	0.0123	0.0559	0.01464
154	101	102	1	0.0246	0.112	0.0294
155	100	103	1	0.016	0.0525	0.0536
156	100	104	1	0.0451	0.204	0.0541
Line No.	From Bus	To Bus	Circuit ID	R (pu)	X (pu)	B (pu)
157	103	104	1	0.0466	0.1584	0.0407
158	103	105	1	0.0535	0.1625	0.0408
159	100	106	1	0.0605	0.229	0.062
160	104	105	1	0.00994	0.0378	0.00986
161	105	106	1	0.014	0.0547	0.01434
162	105	107	1	0.053	0.183	0.0472
163	105	108	1	0.0261	0.0703	0.01844
164	106	107	1	0.053	0.183	0.0472
165	108	109	1	0.0105	0.0288	0.0076
166	103	110	1	0.03906	0.1813	0.0461
167	109	110	1	0.0278	0.0762	0.0202
168	110	111	1	0.022	0.0755	0.02
169	110	112	1	0.0247	0.064	0.062
170	17	113	1	0.00913	0.0301	0.00768
171	32	113	1	0.0615	0.203	0.0518
172	32	114	1	0.0135	0.0612	0.01628
173	27	115	1	0.0164	0.0741	0.01972
174	114	115	1	0.0023	0.0104	0.00276
175	68	116	1	0.00034	0.00405	0.164
176	12	117	1	0.0329	0.14	0.0358
177	75	118	1	0.0145	0.0481	0.01198
178	76	118	1	0.0164	0.0544	0.01356

A-1.5 Transformer tap changing data

Transformer No.	From Bus	To Bus	Circuit ID	Tap setting
1	8	5	1	0.985
2	26	25	1	0.96
3	30	17	1	0.96
4	38	37	1	0.935
5	63	59	1	0.96
6	64	61	1	0.985
7	65	66	1	0.935
8	68	69	1	0.935
9	81	80	1	0.935

A-1.6: Shunt data of IEEE 118 bus system

Bus No.	Shunt valu in p.u.
5	-0.400
34	0.140
37	-0.250
44	0.100
45	0.100
46	0.100
48	0.150
74	0.120
79	0.200
82	0.200

83	0.100
105	0.200
107	0.060
110	0.060

The base case load flow results for IEEE 118 bus system with defined loads and generations is provided in table A-1.7

Table A-1.7: Base case load flow results of IEEE 118 bus

Bus No.- i	P_{Gi}	Q_{Gi}	P_{Di}	Q_{Di}	V p.u.	δ in rad.
1	4.589	-0.7535	0.5100	0.2700	0.9550	0.0000
2	0.0000	0.0000	0.2000	0.9000	0.9625	0.1905
3	0.0000	0.0000	0.3900	0.1000	0.9553	0.1229
4	0.0000	0.4760	0.3900	0.1200	0.9980	-0.2695
5	0.0000	0.0000	0.0000	0.0000	0.9971	-0.2620
6	-0.0521	0.0000	0.5200	0.2200	0.9900	-0.2924
7	0.0000	0.0000	0.1900	0.0200	0.9893	-0.2945
8	-0.0521	0.0000	0.2800	0.0000	1.0150	-0.2357
9	0.0000	0.0000	0.0000	0.0000	1.0636	-0.1132
10	4.500	-1.8605	0.0000	0.0000	1.0500	0.0181
11	0.0000	0.0000	0.7000	0.2300	0.9842	-0.3012
12	0.8500	1.4105	0.4700	0.1000	0.9900	-0.2914
13	0.0000	0.0000	0.3400	0.1600	0.9662	-0.3670
14	0.0000	0.0000	0.1400	0.0100	0.9809	-0.3566
15	0.0000	0.1014	0.9000	0.3000	0.9700	-0.5084
16	0.0000	0.0000	0.2500	0.1000	0.9821	-0.3624
17	0.0000	0.0000	0.1100	0.0300	0.9946	-0.4705
18	0.0000	0.2752	0.6000	0.3400	0.9730	-0.5180

19	0.0000	0.0206	0.4500	0.2500	0.963	-0.5350
20	0.0000	0.0000	0.1800	0.0300	0.9606	-0.5447
21	0.0000	0.0000	0.1400	0.0800	0.9609	-0.5349
22	0.0000	0.0000	0.1000	0.0500	0.9683	-0.5100
23	0.0000	0.0000	0.0700	0.0300	0.9844	-0.4530
Bus No.-i	P_{Gi}	Q_{Gi}	P_{Di}	Q_{Di}	V p.u.	δ in rad.
24	0.0000	-0.4836	0.1300	0.0000	0.9920	-0.5073
25	2.2000	1.7042	0.0000	0.0000	1.0500	-0.2910
26	3.1400	-1.9665	0.0000	0.0000	1.0150	-0.2415
27	0.0000	0.0000	0.7100	0.1300	0.9685	-0.5010
28	0.0000	0.0000	0.1700	0.0700	0.9629	-0.5280
29	0.0000	0.0000	0.2400	0.0400	0.9639	-0.5415
30	0.0000	0.0000	0.0000	0.0000	1.0237	-0.3888
31	0.0700	0.9837	0.4300	0.2700	0.9670	-0.5379
32	0.0000	-0.7940	0.5900	0.2300	0.9640	-0.509
33	0.0000	0.0000	0.2300	0.0900	0.9716	-0.5864
34	0.0000	-0.1371	0.5900	0.2600	0.9860	-0.6485
35	0.0000	0.0000	0.3300	0.0900	0.9809	-0.6557
36	0.0000	-0.0418	0.3100	0.1700	0.9800	-0.6557
37	0.0000	0.0000	0.0000	0.0000	0.9928	-0.6401
38	0.0000	0.0000	0.0000	0.0000	1.0214	-0.5277
39	0.0000	0.0000	0.2700	0.1100	0.9689	-0.7575
40	0.0000	0.3589	0.6600	0.2300	0.9700	-0.8100
41	0.0000	0.0000	0.3700	0.1000	0.9672	-0.8436
42	0.0000	0.3871	0.9600	0.2300	0.9850	-0.8853
43	0.0000	0.0000	0.1800	0.0700	0.9773	-0.7439
44	0.0000	0.0000	0.1600	0.1000	0.9790	-0.8361
45	0.0000	0.0000	0.5300	0.2200	0.9850	-0.8548
46	0.1900	0.0115	0.2800	0.1.000	1.0050	-0.8370

47	0.0000	0.0000	0.3400	0.0000	1.0172	-0.8095
48	0.0000	0.0000	0.2000	0.1100	1.0160	-0.8362
49	2.0400	1.2608	0.8700	0.3000	1.0250	-0.8272
50	0.0000	0.0000	0.1700	0.0400	1.0010	-0.8824
51	0.0000	0.0000	0.1700	0.0800	0.9680	-0.9530
Bus No.-i	P_{Gi}	Q_{Gi}	P_{Di}	Q_{Di}	V p.u.	δ in rad.
52	0.0000	0.0000	0.1800	0.0500	0.9591	-0.9761
53	0.0000	0.0000	0.2300	0.1100	0.9490	-1.0097
54	0.4800	0.2511	1.1300	0.3200	0.9550	-1.0053
55	0.0000	0.0827	0.6300	0.2200	0.9520	-1.0161
56	0.0000	-0.0302	0.8400	0.1800	0.9540	-1.0094
57	0.0000	0.0000	0.0200	0.0300	0.971	0.0000
58	0.0000	0.0000	0.1200	0.0300	0.959	0.0000
59	1.5500	-0.0302	0.8400	0.1800	0.9540	-1.0094
60	0.0000	0.0000	0.1200	0.0300	0.9434	-0.9422
61	1.6000	-0.5533	0.0000	0.0000	0.9950	-0.9313
62	0.0000	0.0000	0.7700	0.1400	0.9800	-0.9239
63	0.0000	0.0000	0.0000	0.0000	0.9573	-0.9681
64	0.0000	0.0000	0.0000	0.0000	0.9765	-0.9529
65	3.9100	-2.6903	0.0000	0.0000	1.005	-0.4889
66	3.920	0.6615	0.3900	0.1800	1.0500	-0.7564
67	0.0000	0.0000	0.2800	0.7000	1.0183	-0.8466
68	0.0000	0.0000	0.0000	0.0000	1.0144	-0.5454
69	5.164	1.0696	0.0000	0.0000	1.0350	-0.5717
70	0.0000	0.5839	0.6600	0.2000	0.9840	-0.7237
71	0.0000	0.0000	0.0000	0.0000	0.9871	-0.7104
72	0.0000	-0.1037	0.1200	0.0000	0.9800	-0.6243
73	0.0000	0.0862	0.6000	0.0000	0.9910	-0.7141
74	0.0000	2.4760	0.6800	0.2700	0.9580	-0.8308

75	0.0000	0.0000	0.4700	0.1100	0.8657	-0.8015
76	0.0000	5.3653	0.6800	0.3600	0.9430	-0.9705
77	0.0000	0.7737	0.6100	0.2800	1.0060	-0.6668
78	0.0000	0.0000	0.7100	0.2600	1.0020	-0.6679
79	0.0000	0.0000	0.3900	0.3200	1.0044	-0.6548
Bus No.-i	P_{Gi}	Q_{Gi}	P_{Di}	Q_{Di}	V p.u.	δ in rad.
80	4.7700	1.6183	1.300	0.2300	1.0400	-0.5962
81	0.0000	0.0000	0.0000	0.0000	1.0331	-0.5647
82	0.0000	0.0000	0.5400	0.2700	0.9862	-0.6423
83	0.0000	0.0000	0.2000	0.1000	0.9815	-0.6202
84	0.0000	0.0000	0.110	0.0700	0.9796	-0.5752
85	0.0000	-0.1399	0.2400	0.1500	0.9850	-0.5472
86	0.0000	0.0000	0.2100	0.1000	0.9895	-0.5718
87	0.0400	0.0737	0.0000	0.0000	1.0150	-0.5669
88	0.0000	0.0000	0.4800	0.1000	0.9884	-0.4913
89	6.0700	-0.0749	0.0000	0.0000	1.0050	-0.4193
90	0.0000	0.7003	1.6300	0.4800	0.9850	-0.5307
91	0.0000	-0.1800	0.1000	0.0000	0.9800	-0.5301
92	0.0000	-0.1228	0.6500	0.1000	0.9930	-0.5212
93	0.0000	0.0000	0.1200	0.0700	0.9870	-0.5738
94	0.0000	0.0000	0.3000	0.1600	0.9910	-0.6110
95	0.0000	0.0000	0.4200	0.3100	0.98100	-0.6283
96	0.0000	0.0000	0.3800	0.1500	0.9930	-0.6316
97	0.0000	0.0000	0.1500	0.0900	1.0110	-0.6202
98	0.0000	0.0000	0.3400	0.0800	1.0240	-0.6262
99	0.0000	-0.2138	0.4222	0.0000	1.0100	-0.6343
100	2.5200	0.6183	0.3700	0.1800	1.0170	-0.6188
101	0.0000	0.0000	0.2200	0.1500	0.9930	-0.5932
102	0.0000	0.0000	0.0500	0.0300	0.9910	-0.5472

103	0.4000	0.6617	0.2300	0.1600	1.0100	-0.6841
104	0.0000	-0.0255	0.3800	0.2500	0.9710	-0.7289
105	0.0000	-0.1084	0.3100	0.2600	0.9650	-0.7482
106	0.0000	0.0000	0.4300	0.1600	0.9620	-0.7533
107	0.0000	0.0659	0.5200	0.1200	0.9520	-0.7533
Bus No.-i	P_{Gi}	Q_{Gi}	P_{Di}	Q_{Di}	V p.u.	δ in rad.
108	0.0000	0.0000	0.0200	0.0100	0.9670	-0.7695
109	0.0000	0.0000	0.0800	0.0300	0.9670	-0.7774
110	0.0000	-0.0230	0.3900	0.3000	0.9730	-0.7918
111	0.3600	-0.0280	0.0000	0.0000	0.9800	-0.7631
112	0.0000	0.3856	0.6800	0.1300	0.9750	-0.8459
113	0.0000	0.0532	0.0600	0.0000	0.9930	-0.4779
114	0.0000	0.0000	0.0800	0.0300	0.9600	-0.5160
115	0.0000	0.0000	0.2200	0.7000	0.9600	0.0000
116	0.0000	0.0000	1.8400	0.0000	1.0050	-0.5519
117	0.0000	0.0000	0.2000	0.0800	0.9763	-0.3188
118	0.0000	0.0000	3.0000	5.2800	0.6573	-0.9455

List of Publications/Presentation

Research Publications

1. Durlav Hazarika, Bani Kanta Talukdar, Brajesh Mohan Gupta "Identification of voltage stability condition of a power system using measurements of bus variables" IET Journal of Engineering, doi: 10.1049/joe.2014.0263. 2014,Vol.2014, issue12, pp 658- 664:

2. Durlav Hazarika, Ranjay Das, Brajesh Mohan Gupta "Improvement of bus voltage profile of a target bus using doubly fed induction generator-based distributed generator". Published in IEEE International conference on power and embedded derive control (ICPEDC2017) Chennai, India, 17-18 March, pp386-391.